

THE TWO-DIMENSIONAL THEORY OF  
ELECTROMAGNETIC INDUCTION IN THIN SHEETS  
WITH APPLICATIONS TO THE EARTH

by

VICTOR RICHARD GREEN

B.Sc., University of Victoria, 1971

A THESIS SUBMITTED IN PARTIAL FULFILLMENT  
OF THE REQUIREMENTS FOR THE DEGREE OF

MASTER OF SCIENCE

in the Department

of

Physics

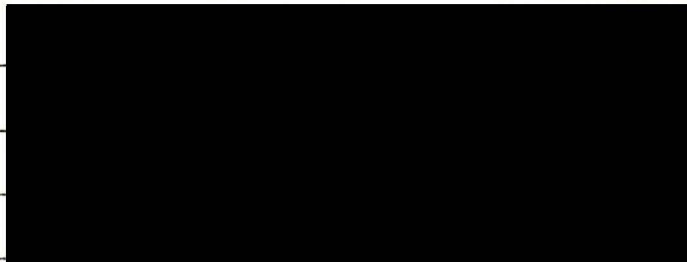
ACCEPTED  
FACULTY OF GRADUATE STUDIES

DEAN

DATE

12 June 1978

We accept this thesis as conforming  
to the required standard



© VICTOR RICHARD GREEN

UNIVERSITY OF VICTORIA

April, 1978

All rights reserved. This thesis may not be reproduced in whole or in part, by mimeograph or other means, without the permission of the author.

ABSTRACT

Supervisor: Professor J.T. Weaver

In this thesis, a method for studying problems of electromagnetic induction in local regions of the Earth where the principal conductivity anomalies are confined to a thin surface layer has been developed using the thin sheet approximation. A two-dimensional model is used in which the Earth is represented by a uniformly conducting half-space covered by an infinitely thin sheet of variable integrated conductivity. A quasi-static magnetic source field, in both E-polarization and B-polarization, is considered.

With the aid of the well-known boundary conditions for thin sheets, the horizontal electric field at the surface of the Earth is shown to satisfy a simple one-dimensional integral equation in both E- and B-polarizations. The method of reducing these integral equations to a linear system of algebraic equations for numerical solution is discussed in detail. The final (discrete) expressions for the fields are presented in a form suitable for programming. (A complete listing of the Fortran program is included in the appendix.)

Results obtained by this method agree well with those obtained analytically by Nicoll and Weaver (1977)

(B-polarization case). When comparing results with those obtained numerically by Fischer et al. (1978a, 1978b) (E-polarization), some differences do occur. However, the similarity of our results and those obtained from an analytical solution of Weidelt (1971) and from the finite-difference formulation of Brewitt-Taylor and Weaver (1976) indicates that our results are indeed accurate.

To illustrate the method, field values are calculated for two simple models in which the integrated conductivity changes (i) abruptly and (ii) gradually from one value to another. A more complex model depicting a cross-section through Vancouver Island is also considered.

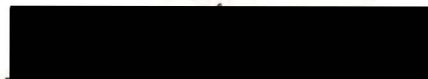


TABLE OF CONTENTS

	<u>Page</u>
ABSTRACT .....	ii
LIST OF TABLES .....	vi
LIST OF FIGURES .....	vii
ACKNOWLEDGEMENTS .....	xi
Dedication .....	xii
CHAPTER 1 INTRODUCTION .....	1
1.1 Historical review .....	1
1.2 Summary of work in this thesis ...	8
CHAPTER 2 EQUATIONS OF ELECTROMAGNETIC INDUCTION .	10
2.1 Maxwell's equations .....	10
2.2 Two-dimensional form of Maxwell's . equations .....	20
CHAPTER 3 THEORY .....	24
3.1 The model .....	24
3.2 Limitations on Price's technique ..	27
3.3 Normal field .....	32
3.4 Anomalous fields in E-polarization	41
3.5 Anomalous fields in B-polarization	56
CHAPTER 4 NUMERICAL METHOD .....	65
4.1 Introduction .....	65
4.2 Numerical form of E-polarization equations .....	71
4.3 Numerical form of B-polarization equations .....	86
4.4 Improved boundary conditions for E-polarization .....	92

	<u>Page</u>
CHAPTER 5 RESULTS AND DISCUSSION .....	99
5.1 Introductory remarks .....	99
5.2 Demonstration of effectiveness of the improved boundary condition for E-polarization problems .....	101
5.3 Comparison with other work .....	104
5.4 Comparison of abrupt and gradual changes in integrated conductivity .	114
5.5 Vancouver Island Model .....	123
5.6 Summary and future work .....	126
REFERENCES .....	129
APPENDIX A EVALUATION OF INTEGRAL COEFFICIENTS CONTAINING BESSEL FUNCTIONS .....	133
APPENDIX B VERIFICATION THAT $J_2(+0)$ EXISTS .....	144
APPENDIX C LISTING OF THE FORTRAN PROGRAM .....	150

LIST OF TABLES

<u>Table</u>	<u>Page</u>
2.1 Typical values of conductivity in the Earth's crust.....	13
5.1 A comparison of field values, showing the effect of the improved boundary conditions for E-polarization problems.....	102
A.1 Coefficients used to determine $A(z)$ to the desired accuracy.....	136

LIST OF FIGURES

<u>Figure</u>		<u>Page</u>
3.1	The mathematical model comprising an infinitely thin surface layer of variable integrated conductivity $\tau(y)$ covering a half-space of uniform conductivity $\sigma$ .....	26
3.2	Attenuation of the horizontal electric field in the top layer of a three-layer model (i.e. ocean, crust, mantle) as a function of the depth (in skin depths) of the top layer.....	30
3.3	Attenuation of the horizontal electric field in the top layer of a two-layer model (overburden, basement rock) as a function of the depth (in skin depths) of the top layer.....	31
3.4	A circuit C enclosing a surface S, as $d \rightarrow 0$ ....	34
4.1	The set of grid points and the limited region of varying integrated conductivity ( $l^- < y < l^+$ ).....	69
5.1	The real and imaginary parts of the horizontal electric field ( $z = 0$ ) for a perfectly conducting thin sheet ( $z = 0, y < 0$ ) covering a conducting half-space shown in the diagram (E-polarization). (Results are compared with those of Fischer et al. (1978b)).....	106

<u>Figure</u>		<u>Page</u>
5.2	The real and imaginary parts of the horizontal magnetic field ( $z = -0$ ) for the model shown in Figure 5.1 (E-polarization). (Results are compared with those of Fischer et al. (1978b)).....	107
5.3	The real and imaginary parts of the vertical magnetic field ( $z = 0$ ) for the model shown in Figure 5.1 (E-polarization). (Results are compared with those of Fischer et al. (1978b)).....	108
5.4	The real and imaginary parts of the horizontal electric field ( $z = 0$ ) for a perfectly conducting thin sheet ( $z = 0, y < 0$ ) covering a conducting half-space shown in the diagram (B-polarization). (Results are compared with those of Nicoll and Weaver (1977)).....	111
5.5	The real and imaginary parts of the vertical electric field ( $z = +0$ ) for the model shown in Figure 5.4 (B-polarization). (Results are compared with those of Nicoll and Weaver (1977)).....	112
5.6	The real and imaginary parts of the horizontal magnetic field ( $z = +0$ ) for the model shown in Figure 5.4 (B-polarization). (Results are compared with those of Nicoll and Weaver (1977)).....	113

<u>Figure</u>		<u>Page</u>
5.7	The effect of abrupt and gradual changes in integrated conductivity on the horizontal electric field at the surface (E-polarization)	115
5.8	The effect of abrupt and gradual changes in integrated conductivity on the horizontal magnetic field at the surface (E-polarization)	116
5.9	The effect of abrupt and gradual changes in integrated conductivity on the horizontal magnetic field just below the infinitely thin sheet (E-polarization).....	117
5.10	The effect of abrupt and gradual changes in integrated conductivity on the vertical magnetic field at the surface (E-polarization).....	118
5.11	The effect of abrupt and gradual changes in integrated conductivity on the horizontal electric field at the surface (B-polarization)	119
5.12	The effect of abrupt and gradual changes in integrated conductivity on the vertical electric field just below the infinitely thin sheet (B-polarization).....	120
5.13	The effect of abrupt and gradual changes in integrated conductivity on the horizontal magnetic field just below the infinitely thin sheet (B-polarization).....	121

Figure

Page

5.14 Amplitudes of the horizontal magnetic field  
at the surface and below the ocean and the  
vertical magnetic field at the surface for  
the model of Vancouver Island (E-polarization) 124

ACKNOWLEDGEMENTS

I would like to thank my supervisor, Dr. J.T. Weaver, for his guidance and support throughout this study.

I would also like to express my appreciation for the many helpful discussions with members of the Geophysics group, especially W. Nienaber, D.J. Thomson, and R.D. Hibbs.

I wish to thank Daphne Greig for her careful typing of this thesis.

I am grateful for financial support provided from funds in Dr. Weaver's National Research Council operating grant A3830.

DEDICATION

I wish to dedicate this thesis to my mother and father for their encouragement and support during my educational career.

## CHAPTER 1

### INTRODUCTION

#### 1.1 Historical review

The electromagnetic field recorded at the surface of the Earth due to sources in the ionosphere has been studied for many years with the aim of inferring information about the Earth's conductivity structure. This study may be divided into problems of a global nature and those of a local nature. Global studies are concerned with the gross features of the conductivity structure of the Earth to great depths (i.e.  $\sim 1000$  km) whereas local studies are concerned with the finer details of the conductivity structure of the crust and upper mantle (i.e.  $\sim 100$  km) over small regions of the Earth which may be considered flat. In recent years, there has been considerable interest in electromagnetic induction problems of a local nature in which lateral conductivity inhomogeneities occur. Problems of this last type are studied in this thesis. Problems of a global nature, which have recently been reviewed by Rikitake (1973), will not be discussed further.

A general treatment of electromagnetic induction in a flat Earth, using a conducting half-space to represent the Earth, was described in a classic paper by Price (1950).

In this paper, a complete analysis of the problem of electromagnetic induction due to an arbitrary known source field acting above a homogeneous conducting half-space, was made. His discussion included physical interpretations of his 'elementary' solutions. By a systematic application of integral transforms and the use of electric and magnetic Hertz vectors aligned normal to the surface of the conducting half-space, Weaver (1971) simplified and consolidated Price's theory. Following Weaver's procedure, Summers and Weaver (1973) generalized the analysis to include the case of an n-layered conducting half-space. Weaver (1973) has reviewed the principal features of electromagnetic induction in a multi-layered Earth.

Lateral variations in conductivity have been investigated using a variety of techniques. Several authors (D'Erceville and Kunetz, 1962; Weaver, 1963; Weaver and Thomson, 1972, and others) have used analytical approaches to the problem of a vertical discontinuity in conductivity. Analytical techniques are usually capable of treating only special problems of simple geometry but they provide valuable checks on other techniques and often give information not attainable by other methods. Numerical techniques are used to solve problems involving more complex structures. In particular, finite difference numerical methods provide one of the most general

mathematical methods for studying electromagnetic induction problems. A disadvantage of this method, though, is that considerable computer time and computer storage space is often required to solve problems involving reasonably complex structures. For some types of problems, numerical and analytical techniques may be combined to lessen this disadvantage. Analogue models, having complex conductivity structures, have also been used to study various interesting problems, such as the 'coast effect' near Japan (Roden, 1964), and the effect of channelling around Vancouver Island (Nienaber et al., 1978), which are not easily studied by mathematical techniques (see review by Dosso, 1973).

Price (1949) described another approach to the problem of conductivity anomalies confined to near the surface in which the Earth is mathematically represented by an infinitely thin sheet of variable integrated conductivity underlain by a non-conducting medium. Since then, considerable extensions to this method have been made. For example, Rikitake (1966) included a conducting half-space which was separated from the non-uniform thin sheet by a non-conducting region, in order to take into account the effect of a highly conducting mantle. In another paper by Rikitake (1968), the conducting half-space, mentioned above, was replaced by one with an undulating

surface to study the effect of upwellings of a deep mantle. In these models, the integrated conductivity varied periodically in one direction.

Many authors have used thin sheet models with discontinuities in the integrated conductivity to study the 'coast effect'. In particular, Roden (1964) studied the 'coast effect' near Japan by mathematically representing the Earth by a thin strip of width,  $a$ , and finite thickness,  $s$ , ( $s \ll a$ ), separated from a perfectly conducting half-space by a non-conducting region. The results obtained from this model were used as a check on the validity of his analogue model measurements, mentioned earlier. A similar model (with  $s \rightarrow 0$  and without the perfectly conducting half-space) was analysed by Parker (1968). Using an analytical technique, he found that the vertical magnetic field tends logarithmically to infinity in the vicinity of the edge and pointed out that previous numerical methods had not permitted this detailed investigation and thus that care should be taken in the numerical analysis to obtain accuracy despite the singular nature of the solution. Weidelt (1971), again using an analytical technique considered a model consisting of two infinitely thin half-sheets of different (finite) integrated conductivities. He also found that the vertical magnetic field tends logarithmically to

infinity near the interface between the two sheets. Furthermore, he showed that the horizontal magnetic field changed discontinuously at the interface. Both Parker and Weidelt noted the need for analytical techniques to serve as checks on numerical procedures for the modelling of arbitrary distributions of integrated conductivity.

Ashour (1971) described a more realistic model to study the 'coast effect' in which the integrated conductivity reduces quickly to zero instead of abruptly changing to zero. The field components are then continuous and finite at the coastline. An important conclusion to be drawn from this investigation is that the induced horizontal magnetic field is enhanced just off the coast and zero or very small at the coast and inland, and also that the vertical magnetic field is enhanced at the boundary even though the integrated conductivity is zero there. Ashour also mentions the importance of observing the field values, not only in the vicinity of the coastline, but also at the continental shelf.

The method of thin sheets has been applied to the study of coastal anomalies in the Southwestern United States by Schmucker (1970). In his mathematical model, a non-conducting region again separates the conducting mantle from the anomalies near the surface. An important

point discussed in his work is the limitations to Price's technique. These limitations are presented in chapter 3 of this thesis.

The thin sheet models discussed in this thesis are two-dimensional, that is, it is assumed that there is no variation in the integrated conductivity in one horizontal direction. It should be pointed out, though, that geometrically simple three-dimensional models of a circular and elliptical region of uniform integrated conductivity in an otherwise uniform thin sheet of different integrated conductivity has been studied (Ashour and Chapman, 1965). Also, many thin hemispherical cap models have been used to investigate global effects.

It is well known that two-dimensional problems may be separated into E-polarization and B-polarization cases. (The horizontal magnetic field of the source is perpendicular to the strike of the anomaly in the E-polarization case and parallel to the strike in the B-polarization case.) For the thin sheets presented so far, only the E-polarization case has been of interest since all the thin sheets have been underlain by a non-conducting region (see review by Ashour, 1973). Schmucker (1971) included, in his model, a conducting (n-layered) half-space immediately below a thin sheet having a strip of different integrated conductivity. He only investigated the E-polarization case, but with this type of model it is possible to study the B-

polarization case since electric currents may flow into the Earth. To study the B-polarization case, Bailey (1977) used a model which consisted of a uniformly conducting half-space in contact with and screened by a perfectly conducting half-plane. Nicoll and Weaver (1977) extended Bailey's problem by adding a perfectly conducting plane at a depth  $D$ , to the model, to represent the highly conducting mantle. These problems were both solved analytically using the Wiener-Hopf technique. Brewitt-Taylor (1975) used a model similar to Nicoll and Weaver but with a perfectly conducting infinitely thin strip of width,  $2a$ , at the surface. His analytical solution was obtained by neglecting self-induction, and was therefore only approximate. He then compared his results with those obtained by applying the finite difference technique to the same model but with a more realistic strip of finite depth and conductivity (Brewitt-Taylor, 1976). Finally, Fischer, Schnegg, and Usadel (1978a, 1978b) considered the E-polarization case using Bailey's model and obtained an integral equation for the field which they solved numerically.

## 1.2 Summary of work in this thesis

In this thesis, the problem of electromagnetic induction in local regions of the Earth where the principal conductivity anomalies are confined to a thin surface layer, is investigated. A two-dimensional model is used in which the Earth is represented by a uniformly conducting half-space covered by an infinitely thin layer of variable integrated conductivity. This model is ideally suited to study 'coast effect' problems since the near-surface conductivity structure perpendicular to the coast changes rapidly over short distances while, parallel to the coast, the near-surface conductivity structure often does not vary significantly over great distances.

The purpose of this thesis is to present the theory (see chapter 3) for a more general thin sheet model in which both E-polarization and B-polarization cases may be discussed. Furthermore, the theory has been developed with the idea of providing boundary values for more complex three-dimensional problems.

An important feature of this model is that the variations of the conductivity with depth are eliminated from the problem so that, with the aid of the well-known boundary conditions for thin sheets, it becomes possible to express the surface horizontal electric field (in both the E-polarization and the B-polarization cases) as the solution

of a simple one-dimensional integral equation. In the E-polarization case, an improved method of accounting for the contribution of the electric field, far from the region of varying conductivity, is included in the numerical evaluation of the integral equation (see section 4.4). Also of importance is the fact that the values of the integrated conductivity at the extreme ends of the model need not be the same, which is desirable when studying realistic 'coast effect' problems. Moreover, the theory allows for a variable integrated conductivity so that the sloping continental shelf may be modelled more closely than in analytical methods. Also, a grid of variable step-size has been incorporated into the numerical method (see chapter 4) so that the edge effect due to abrupt changes in integrated conductivity may be accurately determined.

In chapter 5, some results are presented to illustrate the theory and then briefly discussed.

CHAPTER 2

EQUATIONS OF ELECTROMAGNETIC INDUCTION

2.1 Maxwell's equations

Maxwell's equations mathematically express the relationship between time-varying electric and magnetic fields. These equations can be considerably simplified, when applied to problems dealing with electromagnetic induction in the Earth, if certain assumptions are made regarding the source field and the region of interest. The appropriate differential equations, required to determine the field vectors, can then be found by using Maxwell's equations on this simplified form.

Maxwell's equations, in M.K.S. units, are

$$\bar{\nabla} \times \bar{E} = - \frac{\partial \bar{B}}{\partial t} \quad , \quad (2.1.1)$$

$$\bar{\nabla} \times \bar{H} = \bar{J} + \frac{\partial \bar{D}}{\partial t} \quad , \quad (2.1.2)$$

$$\bar{\nabla} \cdot \bar{D} = \rho \quad , \quad (2.1.3)$$

and  $\bar{\nabla} \cdot \bar{B} = 0 \quad (2.1.4)$

where  $\bar{E}$  is the electric field intensity,  $\bar{D}$  is the electric flux density,  $\bar{B}$  is the magnetic flux density,

$\bar{H}$  is the magnetic field intensity,  $\bar{J}$  is the volume current density, and  $\rho$  is the volume charge density. The term  $\frac{\partial \bar{D}}{\partial t}$  is known as the displacement current density. ( $\bar{E}$  and  $\bar{B}$  will be referred to, loosely, as the electric and magnetic fields, respectively.)

As an immediate simplification, we assume that the time dependence of the electric and magnetic fields in the region of interest can be expressed as

$$\bar{P}(x,y,z,t) = \bar{P}(x,y,z)e^{i\omega t} \quad (2.1.5)$$

where  $\omega$  is the angular frequency of the source and  $\bar{P}$  is any of the field vectors. In this representation, the time derivatives,  $\frac{\partial \bar{P}}{\partial t}$ , can be replaced by  $i\omega\bar{P}$  in Maxwell's equations.

We also assume that the Earth's interior is free of primary source currents and acts as a conductor (i.e. is isotropic and obeys Ohm's law). In such a region,  $\bar{B}$  and  $\bar{H}$ ,  $\bar{E}$  and  $\bar{D}$ , and  $\bar{J}$  and  $\bar{E}$  may be related as follows:

$$\bar{B} = \mu\bar{H} \quad , \quad (2.1.6)$$

$$\bar{D} = \epsilon\bar{E} \quad , \quad (2.1.7)$$

$$\text{and} \quad \bar{J} = \sigma\bar{E} \quad (2.1.8)$$

where  $\mu$  is the permeability,  $\epsilon$  is the permittivity

and  $\sigma$  is the conductivity. In air, the conductivity is approximately zero. In the Earth's crust, the conductivity ranges from approximately  $10^{-6}$  mho/m to  $10^4$  mho/m (see Table 2.1) with the mean conductivity being approximately  $5 \times 10^{-3}$  mho/m. The conductivity in the underlying mantle increases with depth from the mean crustal value (see Rikitake, 1973). Thus the crust is underlain by a region of higher conductivity. This point is of importance, later in this thesis, when considering the validity of representing a layer of the crust by an infinitely thin surface sheet. In air and for most materials in the Earth, the permeability and permittivity are of the order of their free-space values,  $\mu_0$  and  $\epsilon_0$  respectively ( $\mu_0 = 4\pi \times 10^{-7}$  H/m ;  $\epsilon_0 = 8.85 \times 10^{-12}$  F/m). Exceptions to this are some ferromagnetic minerals which have permeabilities up to three times the free-space value and water which has a permittivity about 80 times the free-space value. Materials with values very much higher than these are not expected in significant quantities in the Earth. In order to simplify the computations, the permeability is assumed to be equal to its free-space value everywhere.

Furthermore, we assume that the conductivity structure in the Earth can be approximated by a number of homogeneous conducting regions. In such regions, the volume charge density can be taken as zero, since any volume charge distribution will decay quickly away to the surface of each

TABLE 2.1

Typical Values of Conductivity in the Earth's Crust

	<u><math>\sigma</math> (mho/m)</u>	<u><math>\sigma/\epsilon</math> (Hz)</u>
snow	$10^{-6}$	$10^4$
fresh water	$10^{-4}$	$10^5$
dry rock	$10^{-4}$	$10^6$
earth (moist)	$10^{-2}$	$10^7$
sea water	4	$10^9$
minerals	$10^4$	$10^{14}$

homogeneous conducting region, independent of any applied field (see, for example, Jones, 1964). In free-space, the volume charge density is also assumed to be zero.

By substituting equations (2.1.6) through (2.1.8), with  $\mu = \mu_0$ , into Maxwell's equations and assuming an exponential time dependence as in equation (2.1.5), we find that, in each region of homogeneous conductivity (including  $\sigma = 0$ ), the four Maxwell's equations reduce to two equations in two unknowns, being

$$\bar{\nabla} \times \bar{B} = (\mu_0 \sigma + i\omega\mu_0 \epsilon) \bar{E} \quad , \quad (2.1.9)$$

and 
$$\bar{\nabla} \times \bar{E} = -i\omega\bar{B} \quad . \quad (2.1.10)$$

The redundancy of equation (2.1.3) with  $\rho = 0$  and equation (2.1.4) follows from the general vector identity

$$\bar{\nabla} \cdot (\bar{\nabla} \times \bar{P}) = 0 \quad . \quad (2.1.11)$$

where  $\bar{P}$  represents  $\bar{E}$  or  $\bar{B}$ .

It is well-known that the displacement current term in equation (2.1.9), (i.e.  $i\omega\mu_0 \epsilon$ ), may be neglected in geomagnetic induction studies. For this to be true in the Earth, we must have

$$\omega \ll \frac{\sigma}{\epsilon} \quad (2.1.12)$$

which is easily satisfied for values of  $\sigma$  in the Earth (see Table 2.1) for  $\omega < 1$  kHz . To determine the frequency range in which displacement currents may be neglected in the free-space region, where  $\sigma = 0$  , it is convenient to express equations (2.1.9) and (2.1.10) in dimensionless form. In doing this, we define two dimensionless terms (indicated by primes) as

$$\bar{r}' = \frac{\bar{r}}{\ell} \quad (\text{i.e. } \nabla' = \ell \nabla) \quad (2.1.13)$$

and 
$$\bar{B}' = \frac{\bar{B}}{B_0} \quad (2.1.14)$$

where  $\bar{r}$  is the position vector,  $\ell$  is a characteristic length in the region and  $B_0$  is a characteristic magnetic field. By substituting equations (2.1.13) and (2.1.14) into equation (2.1.10), we find that we are restricted to defining the dimensionless electric field as

$$\bar{E}' = \frac{\bar{E}}{\omega \ell B_0} \quad (2.1.15)$$

The dimensionless forms of equations (2.1.9) and (2.1.10) then become

$$\bar{\nabla}' \times \bar{B}' = i\kappa \bar{E}' \quad (2.1.16)$$

and 
$$\bar{\nabla}' \times \bar{E}' = -i\bar{B}' \quad (2.1.17)$$

where  $\kappa = \omega^2 \ell^2 \mu_0 \epsilon$ .

Now, by substituting equation (2.1.16) into (2.1.17) or vice versa, and then using the vector identity

$$\bar{\nabla} \times (\bar{\nabla} \times \bar{P}) = \bar{\nabla}(\bar{\nabla} \cdot \bar{P}) - \nabla^2 \bar{P} \quad (2.1.18)$$

where  $\bar{P}$  may be any vector (in this case,  $\bar{E}'$  or  $\bar{B}'$ ), we obtain

$$\nabla^2 \bar{P} = -\kappa \bar{P} \quad (2.1.19)$$

Since  $\bar{E}'$  and  $\bar{B}'$  are scaled so that they are of reasonable magnitudes, the right hand side of this equation will be very small if  $\kappa \ll 1$ , or in terms of frequency, if

$$\omega^2 \ll \frac{1}{\ell^2 \epsilon \mu_0} \quad (2.1.20)$$

In this case, we may approximate equation (2.1.19) by

$$\nabla^2 \bar{P} = 0 \quad (2.1.21)$$

which is the same conclusion we would have obtained had we initially neglected the displacement current term (i.e.  $i\kappa \bar{E}'$ ) in equation (2.1.16). Thus the frequency range over which the displacement current term may be

neglected in the free-space region (in the primed or unprimed system) is given by the inequality (2.1.20). For global studies,  $\ell$  is of the order of the radius of the Earth ( $\sim 6400$  km) so that the inequality (2.1.20) is valid for  $\omega < 10\text{Hz}$ . For local studies, where the Earth is approximately flat,  $\ell$  is considerably smaller so that the allowable values of  $\omega$  are correspondingly higher. In particular, if  $\ell$  is of the order of the height of the source ( $\sim 100$  km), then the inequality (2.1.20) is valid for  $\omega < 1$  kHz. In geomagnetic induction studies, we are generally interested in  $\omega < 1$  Hz so that the neglect of displacement currents is well justified.

With the neglect of displacement currents, then, the appropriate form (non-dimensionless) of Maxwell's equations becomes

$$\bar{\nabla} \times \bar{E} = -i\omega\bar{B} \quad (2.1.22)$$

and 
$$\bar{\nabla} \times \bar{B} = \mu_0\sigma\bar{E} \quad (2.1.23)$$

By taking the curl of equation (2.1.22) and (2.1.23), and using the vector identity given by equation (2.1.18), with  $\bar{P}$  representing  $\bar{E}$  or  $\bar{B}$ , the differential equation to be satisfied by the field vectors in each homogeneous conducting region, subject to specified boundary conditions,

is found to be

$$\nabla^2 \bar{P} = i\alpha^2 \bar{P} \quad (2.1.24)$$

where  $\alpha^2 = \omega\mu_0\sigma$  (2.1.25)

In the free-space region, equation (2.1.24) reduces to Laplace's equation,

$$\nabla^2 \bar{P} = 0 \quad (2.1.26)$$

In the non-conducting region, equations (2.1.22) and (2.1.23) can be simplified to

$$\bar{B} = -\bar{\nabla}\Omega \quad (2.1.27)$$

and  $\bar{\nabla} \times \bar{E} = i\omega\bar{\nabla}\Omega$  (2.1.28)

since  $\bar{\nabla} \times \bar{\nabla}a = 0$  (2.1.29)

where  $a$  is any scalar quantity. Here  $\Omega$  is defined as the scalar magnetic potential. Furthermore, by taking the divergence of equation (2.1.28) and using (2.1.11), equation (2.1.26) can be replaced by

$$\nabla^2 \Omega = 0 \quad (2.1.30)$$

In solving equations (2.1.24), (2.1.26) and (2.1.30), we require that the solutions and their first and second derivatives be continuous and finite in any source-free region of homogeneous conductivity and vanish when infinitely far from the source.

## 2.2 Two-dimensional form of Maxwell's equations

Consider the surface of the Earth to be represented by the plane  $z = 0$  with the  $z$ -axis positive downward in a Cartesian coordinate system and with all sources restricted to the region  $z < -h$  ( $h > 0$ ) above the surface.

Many interesting geomagnetic induction problems may be simplified into a two-dimensional form if  $\sigma$ ,  $\bar{E}$  and  $\bar{B}$  are independent of one of the coordinates (say,  $x$ ).

In this case, Maxwell's equations become

$$G_1(y, z) - F_2(y, z) = -i\omega X(y, z) \quad (2.2.1)$$

$$E_2(y, z) = -i\omega Y(y, z) \quad (2.2.2)$$

$$E_1(y, z) = i\omega Z(y, z) \quad , \quad (2.2.3)$$

and  $Z_1(y, z) - Y_2(y, z) = \mu_0 \sigma E(y, z) \quad (2.2.4)$

$$X_2(y, z) = \mu_0 \sigma F(y, z) \quad (2.2.5)$$

$$X_1(y, z) = -\mu_0 \sigma G(y, z) \quad (2.2.6)$$

where  $\bar{B} = (X, Y, Z)$  and  $\bar{E} = (E, F, G)$ . Here the Landau notation for partial derivatives has been used in which the differentiation with respect to the first and second ordered variables is indicated by the subscript 1 and 2, respectively.

In the source-free region, these equations fall into two independent groups which can be discussed separately as the E-polarization problem, governed by equations (2.2.2), (2.2.3) and (2.2.4), and the B-polarization problem, governed by equations (2.2.1), (2.2.5) and (2.2.6). Substituting equations (2.2.2) and (2.2.3) into (2.2.4) gives

$$E_{11}(y,z) + E_{22}(y,z) = i\alpha^2 E(y,z) \quad (2.2.7)$$

in the conducting region, and

$$E_{11}(y,z) + E_{22}(y,z) = 0 \quad (2.2.8)$$

or, in terms of magnetic potential,

$$\Omega_{11}(y,z) + \Omega_{22}(y,z) = 0 \quad (2.2.9)$$

in the non-conducting region. Thus the E-polarization field can be written as

$$\bar{E} = (E, 0, 0) \quad \text{and} \quad \bar{B} = (0, Y, Z) \quad (2.2.10)$$

with 
$$Y(y,z) = \frac{i}{\omega} E_2(y,z) \quad (2.2.11)$$

and 
$$Z(y, z) = \frac{-i}{\omega} E_1(y, z) \quad (2.2.12)$$

where  $E$  must satisfy (2.2.7) or (2.2.8) subject to specified boundary conditions. From equation (2.1.27), it immediately follows that

$$Y(y, z) = \frac{i}{\omega} E_2(y, z) = -\Omega_1(y, z) \quad (2.2.13)$$

and 
$$Z(y, z) = \frac{-i}{\omega} E_1(y, z) = -\Omega_2(y, z) \quad (2.2.14)$$

in  $z < 0$ .

Similarly the B-polarization field in the conducting region is given by

$$\bar{B} = (X, 0, 0) \quad \text{and} \quad \bar{E} = (0, F, G) \quad (2.2.15)$$

with 
$$F(y, z) = \frac{1}{\mu_0 \sigma} X_2(y, z) \quad (2.2.16)$$

and 
$$G(y, z) = \frac{-1}{\mu_0 \sigma} X_1(y, z) \quad (2.2.17)$$

where  $X(y, z)$  must satisfy

$$X_{11}(y, z) + X_{22}(y, z) = i\alpha^2 X(y, z) \quad (2.2.18)$$

again subject to the given boundary conditions. Further-

more, from equation (2.1.24), we know that

$$F_{11}(y,z) + F_{22}(y,z) = i\alpha^2 F(y,z) \quad (2.2.19)$$

and  $G_{11}(y,z) + G_{22}(y,z) = i\alpha^2 G(y,z)$  . (2.2.20)

In the non-conducting region, equations (2.2.5) and (2.2.6) become

$$X_1(y,z) = 0 \quad \text{and} \quad X_2(y,z) = 0 \quad (2.2.21)$$

which implies that,

$$X(y,z) = X_0, \text{ a constant} \quad (2.2.22)$$

Then from equation (2.2.1),  $F(y,z)$  and  $G(y,z)$  must satisfy

$$G_1(y,z) - F_2(y,z) = -i\omega X_0 \quad (2.2.23)$$

CHAPTER 3

THEORY

3.1 The model

A simple two-dimensional model is used to study the resulting geomagnetic field at the surface due to currents in the ionosphere fluctuating above a small section of the Earth having near-surface inhomogeneities in conductivity. In this model, a quasi-static magnetic field located at a height  $h$ , represents the source field. The flat Earth occupies the region  $z > 0$  in a right-handed Cartesian coordinate system while the region  $-h < z < 0$  is assumed to be free space. The actual surface conductivity structure to be studied is contained in an integrated conductivity  $\tau(y)$  given by

$$\tau(y) = \int_0^{d(y)} \bar{\sigma}(y,z) dz \quad (3.1.1)$$

where  $\bar{\sigma}(y,z)$  is the conductivity of the surface layer and  $d(y)$  is the thickness of the surface layer. The technique, originally discussed by Price (1949), is now employed. In this technique, it is assumed that the actual surface conductivity structure can be represented by an infinitely thin layer of equivalent total integrated conductivity,

occupying the  $z = 0$  plane. In this case, equation (3.1.1) becomes

$$\tau(y) = \lim_{d(y) \rightarrow 0} \int_0^{d(y)} \bar{\sigma}(y, z) dz \quad (3.1.2)$$

where  $\bar{\sigma}(y, z)$  mathematically becomes infinite, as  $d(y) \rightarrow 0$ , in such a way that  $\tau(y)$  remains finite. The variations in the integrated conductivity are restricted to a limited range in  $y$  ( $l^- < y < l^+$ ), being constant outside this region, so that

$$\tau(y) = \tau^- + \tau_a(y) \quad (3.1.3)$$

where  $\tau^- = \tau(-\infty)$  and  $\tau^+ = \tau(+\infty)$

with

$$\tau_a(y) = \begin{cases} 0 & (y \leq l^-) \\ \tau_a(y) & (l^- < y < l^+) \\ \tau^+ - \tau^- & (l^+ \leq y) \end{cases}$$

The conductivity of the lower crust is represented by an infinite half-space of uniform conductivity  $\sigma$ , occupying the region  $z > 0$  (see figure 3.1).

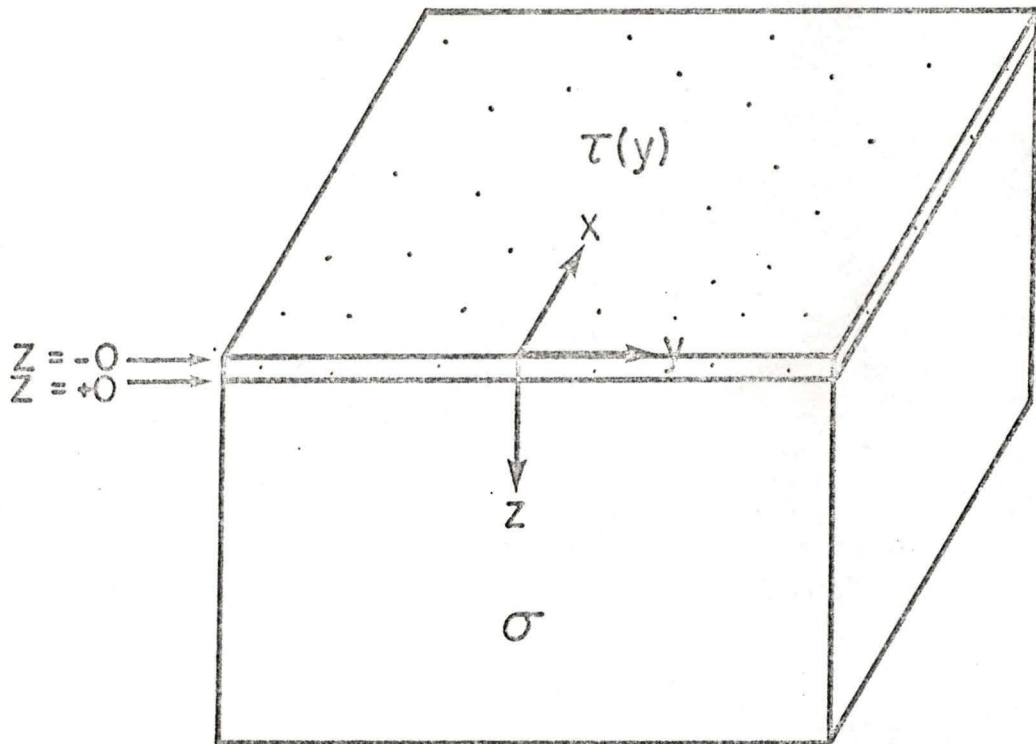


Figure 3.1 The mathematical model comprising an infinitely thin surface layer of variable integrated conductivity  $\tau(y)$  covering a half-space of uniform conductivity  $\sigma$ .

### 3.2 Limitations in Price's technique

We shall see, in the next section, that the horizontal electric field must be continuous across the infinitely thin sheet if we are to use Price's technique. Thus, in the 'real' problem with a finite depth  $d$ , we require that the horizontal electric field remain approximately constant over this depth. Schmucker (1970) discussed the general restrictions on the use of Price's thin sheet approximation which this requirement imposes. He considered a three-layer model consisting of a top layer of thickness  $d$ , (terrestrial surface layers) and a poorly conducting intermediate layer of thickness  $h$ , (crust and upper mantle) overlying a highly conducting substratum. In addition, he assumed that  $\delta_2 \gg h$  and  $\delta_3 \ll h$  where  $\delta_2$  and  $\delta_3$  are the skin depths in the second and third layers, respectively. Using this model, Schmucker found that the horizontal electric field was approximately constant over the depth  $d$ , if the following conditions held:

$$(i) \quad \delta_1 > 3d \quad , \quad (ii) \quad h \gg d \quad ,$$

where  $\delta_1$  is the skin depth of the surface layer. This second condition implies that there should not be a good conductor at shallow depth if we are to use Price's method.

Schmucker's assumptions (i.e.  $\delta_2 \gg h$  and  $\delta_3 \ll h$ ) imply that an extreme conductivity contrast exists between the conductivities of the crust ( $\sigma_2$ ) and mantle ( $\sigma_3$ ). For example, when  $h = 100$  km and  $3d < \delta_1 < \infty$  in his model, we find that  $\sigma_2$  must be much less than  $10^{-10}$  mho/m and  $\sigma_3$  must be infinite. By using a three-layer model similar to Schmucker's (1970), the attenuation of the tangential electric field over a surface layer of depth  $d$ , can be determined for more realistic conductivities of the crust and mantle. From the theory for  $n$ -layered structures described in a review paper by Weaver (1973), we find that

$$\frac{E(d)}{E(0)} = \frac{U_1}{V_1 + V_2 - \frac{U_2^2}{V_2 + \frac{\sqrt{2i}}{\delta_3}}} \quad (3.2.1)$$

where 
$$U_n = \frac{\text{csch}(\sqrt{2i}d_n/\delta_n)}{\delta_n}$$

and 
$$V_n = \frac{\text{coth}(\sqrt{2i}d_n/\delta_n)}{\delta_n} \quad (n = 1, 2)$$

with  $d = d_1$  and  $h = d_2$ .

Using this equation, we can determine the order of attenuation to be expected over a surface layer in coastal regions ( $\sigma_1 \approx 4$  mho/m) where the depth of the

ocean is not likely to be more than 5 km. The results, illustrated in figure 3.2, show the limitations of Price's method. We see that, for a mantle at shallow depth ( $\sim 50$  km), the attenuation is particularly sensitive to the conductivity of the mantle ( $10^{-1}$  mho/m  $< \sigma_2 < \infty$ ) whereas for a mantle at greater depth (500 km), the attenuation is affected very little by the conductivity of the mantle, being somewhat more sensitive to the conductivity of the crustal region ( $0 < \sigma_2 < 10^{-2}$  mho/m). Furthermore, as the depth of the surface layer nears or becomes greater than its skin depth, the attenuation becomes large. In particular, for coastal anomalies, we see that the attenuation tends to increase rapidly for frequencies greater than about 0.25 mHz ( $\sim 1$  cycle per hour) which is in rough agreement with Schmucker (1970, 1971).

As a further example, we consider a typical model, in prospecting geophysics, consisting of a layer of overburden covering more resistive bedrock. From figure 3.3, we find that Price's approximation is valid for frequencies up to about 1 kHz, for a 50 m layer of overburden of conductivity  $10^{-2}$  mho/m lying on a basement of conductivity  $10^{-4}$  mho/m.

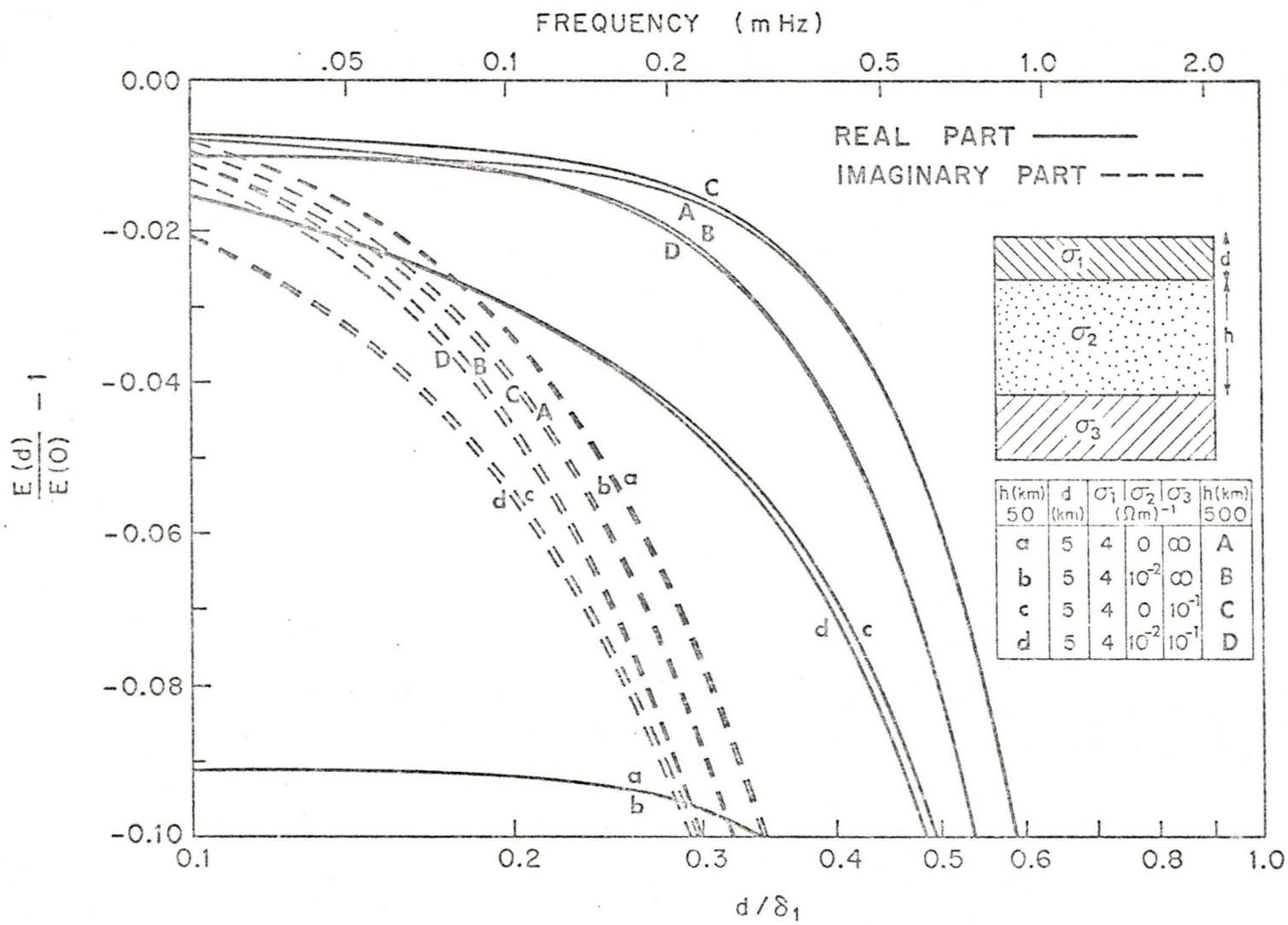


Figure 3.2 Attenuation of the horizontal electric field in the top layer of a three-layer model (i.e. ocean, crust, mantle) as a function of the depth (in skin depths) of the top layer.

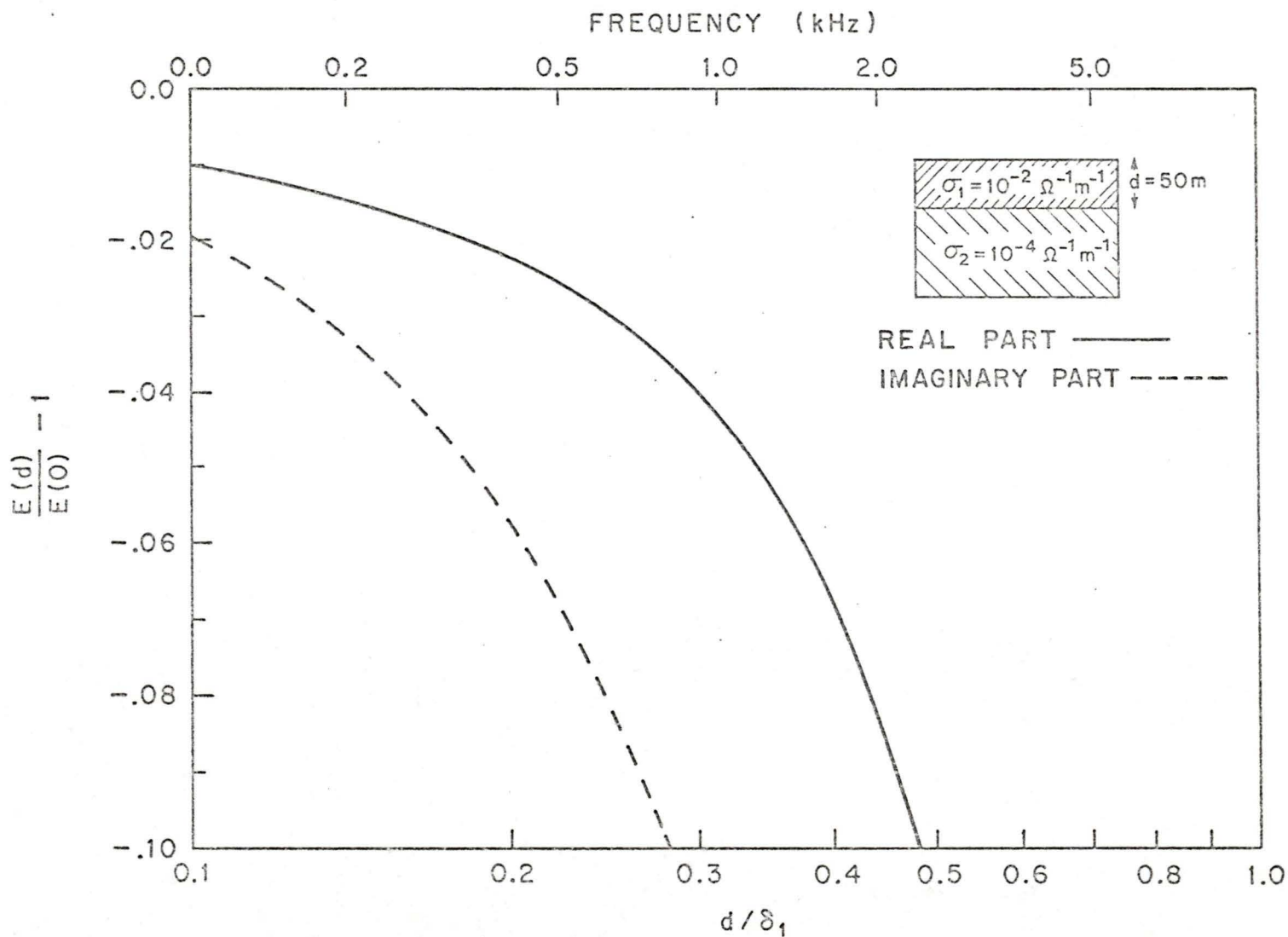


Figure 3.3 Attenuation of the horizontal electric field in the top layer of a two-layer model (overburden, basement rock) as a function of the depth (in skin depths) of the top layer.

### 3.3 Normal field

It is convenient to begin the study of this problem by considering the whole surface layer to be of uniform integrated conductivity  $\tau_n$ , thus reducing the problem to one variable  $z$ . The resulting field, defined as the normal field and denoted by the subscript  $n$ , can be used to form the boundary values for the more complex problem of a surface layer of variable integrated conductivity. The problem is further simplified by first considering the E-polarization field for one variable,

$$\bar{E}_n(z) = (E_n(z), 0, 0) \quad \text{and} \quad \bar{B}_n = (0, Y_n(z), 0) \quad (3.3.1)$$

$$\text{with} \quad Y_n(z) = \frac{i}{\omega} E_n'(z) \quad (3.3.2)$$

$$\text{and} \quad Y_n'(z) = -\mu_0 \sigma E_n(z) \quad (3.3.3)$$

where  $E_n(z)$  must now satisfy

$$E_n''(z) = i\alpha^2 E_n(z) \quad \text{in} \quad z > 0 \quad (3.3.4)$$

$$\text{and} \quad E_n''(z) = 0 \quad \text{in} \quad z < 0 \quad (3.3.5)$$

Here the primes (') indicate differentiation.

The relationship between the electric and magnetic field just above and just below the infinitely thin sheet,

which is required to solve equations (3.3.4) and (3.3.5), can easily be determined by considering a uniform cover of finite depth  $d$ , and then letting  $d \rightarrow 0$ . The integral form of equation (2.1.23),

$$\oint_c \bar{E} \cdot d\bar{\ell} = -i\omega \int_s \bar{B} \cdot d\bar{A} \quad (3.3.6)$$

obtained by using Stoke's theorem, can be employed to show that the horizontal electric field must be continuous across the infinitely thin sheet. Let  $c$  be a rectangular circuit enclosing the surface  $S$ , having two sides parallel and arbitrarily close to the upper and lower boundaries of the surface cover, as in figure 3.4a. As the uniform surface layer becomes infinitely thin (see figure 3.4b), the right-hand side of equation (3.3.6) goes to zero, since

$$\lim_{d \rightarrow 0} \left| \int_s \bar{B} \cdot d\bar{A} \right| = \lim_{d \rightarrow 0} \left| \int_{-0}^{d+0} \int_0^{\ell} Y_n(z) dx dz \right| \leq \lim_{d \rightarrow 0} |M\ell d| = 0 \quad (3.3.7)$$

where  $M$  is the maximum value of  $|Y_n(z)|$  in  $-0 < z < d+0$  which must be finite for any real problem. For this one-dimensional problem, the horizontal electric field is constant and in the  $x$ -direction so equation (3.3.6) becomes

$$E_n(-0)\ell - E_n(+0)\ell = 0 \quad (3.3.8)$$

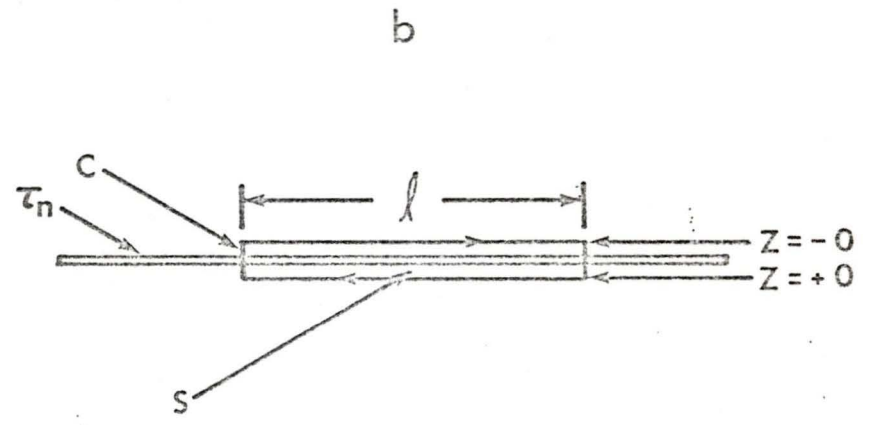
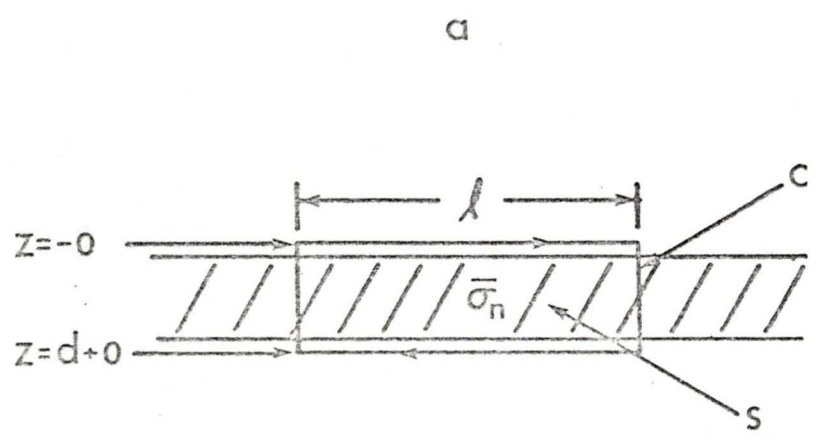


Figure 3.4 A circuit  $C$  enclosing a surface  $S$ , as  $d \rightarrow 0$ .

which implies that

$$E_n(-0) = E_n(+0) = E_n \quad . \quad (3.3.9)$$

Similarly the horizontal magnetic field can be shown to be discontinuous across the infinitely thin sheet by considering the integration of equation (3.3.3) from just above the upper boundary ( $z = -0$ ) to just below the lower boundary ( $z = d+0$ ) of the surface, giving

$$- \int_{-0}^{d+0} Y_n'(z) dz = \mu_0 \int_{-0}^{d+0} E_n(z) \overline{\sigma_n}(z) dz \quad . \quad (3.3.10)$$

Using the mean-value theorem,  $E_n(z)$  can be expressed as

$$E_n(z) = E_n(-0) + zE_n'(a) \quad (3.3.11)$$

where  $(-0 \leq a \leq z)$  .

If this expression for  $E_n(z)$  is substituted into equation (3.3.10) and the surface layer made infinitely thin, then the right-hand side of equation (3.3.10) becomes

$$\begin{aligned}
 \lim_{d \rightarrow 0} \mu_0 \int_{-0}^{d+0} E_n(z) \overline{\sigma}_n(z) dz &= \mu_0 E_n(-0) \lim_{d \rightarrow 0} \int_{-0}^{d+0} \overline{\sigma}_n(z) dz \\
 &+ \mu_0 E_n'(-0) \lim_{d \rightarrow 0} \int_{-0}^{d+0} z \overline{\sigma}_n(z) dz \\
 &= \mu_0 \tau_n E_n
 \end{aligned} \tag{3.3.12}$$

since

$$\lim_{d \rightarrow 0} \left| \int_{-0}^{d+0} z \overline{\sigma}_n(z) dz \right| \leq \tau_n \lim_{d \rightarrow 0} |d| = 0 \tag{3.3.13}$$

while the left-hand side is just

$$\begin{aligned}
 -\lim_{d \rightarrow 0} \int_{-0}^{d+0} Y_n'(z) dz &= -\lim_{d \rightarrow 0} \left[ Y_n(d+0) - Y_n(-0) \right] \\
 &= Y_n(-0) - Y_n(+0)
 \end{aligned} \tag{3.3.14}$$

which implies that

$$Y_n(-0) - Y_n(+0) = \mu_0 \tau_n E_n \tag{3.3.15}$$

Equations (3.3.9) and (3.3.15) give the surface boundary conditions for the normal field. The argument used here to determine these conditions has only relied

on the requirement that the fields be finite (i.e. an  $M$  may be found) and continuous (i.e. an  $\ell$  may be found) and that an integrated conductivity may be defined in the manner described. Thus, under these conditions, the surface boundary conditions we have derived apply also to an infinitely thin layer with varying integrated conductivity.

The continuity conditions can be used to express the surface electric field in terms of the surface magnetic field. The solution of equation (3.3.4), which vanishes as  $z \rightarrow +\infty$ , is

$$E_n(z) = E_n(+0)e^{-\sqrt{i}\alpha z} = E_n e^{-\sqrt{i}\alpha z} \quad (3.3.16)$$

so that equation (3.3.2) then yields

$$Y_n(z) = \frac{-i}{\omega} \sqrt{i}\alpha E_n(z) \quad (3.3.17)$$

Thus, the horizontal magnetic field just below the surface layer is

$$Y_n(+0) = \frac{-i}{\omega} \sqrt{i}\alpha E_n \quad (3.3.18)$$

It follows from equation (3.3.3) that the horizontal magnetic field must be constant in the non-conducting

region, so that in  $z < 0$ ,

$$Y_n(z) = Y_n(-0) = Y_0, \text{ a constant.} \quad (3.3.19)$$

Hence, by integrating equation (3.3.2), we obtain the electric field in the region  $z < 0$  as

$$E_n(z) = E_n - i\omega z Y_0. \quad (3.3.20)$$

Finally, we obtain

$$E_n = \frac{i\omega}{\sqrt{i}\alpha} \left( \frac{Y_0}{1 + \frac{\sqrt{i}\alpha\tau_n}{\sigma}} \right) \quad (3.3.21)$$

by substituting equation (3.3.18) into (3.3.15), and

$$Y_n(+0) = \frac{Y_0}{1 + \frac{\sqrt{i}\alpha\tau_n}{\sigma}} \quad (3.3.22)$$

by substituting equation (3.3.21) back into (3.3.18).

At this point, it is convenient to define the term 'skin depth' which is used often in this thesis. By taking the modulus of equation (3.3.16),

$$\left| E_n(z) \right| = \left| E_n e^{-(1+i)\alpha z/\sqrt{2}} \right| = |E_n| e^{-\alpha z/\sqrt{2}} \quad (3.3.23)$$

it can easily be seen that the amplitude of the field is attenuated with depth by the factor  $e^{-\alpha z/\sqrt{2}}$ . The depth at which the field is attenuated to  $e^{-1}$  of its surface value is defined as the skin depth  $\delta$ , and is given by

$$\delta = \sqrt{\frac{2}{\omega\mu_0\sigma}} = \frac{\sqrt{2}}{\alpha} \quad (3.3.24)$$

The B-polarization fields, in one dimension, are

$$\bar{B}_n(z) = (X_n(z), 0, 0) \quad \text{and} \quad \bar{E}_n(z) = (0, F_n(z), 0) \quad (3.3.25)$$

with  $F_n'(z) = i\omega X_n(z)$  (3.3.26)

and  $X_n'(z) = \mu_0 \sigma F_n(z)$  (3.3.27)

where  $X_n(z)$  must satisfy

$$X_n''(z) = i\alpha^2 X_n(z) \quad (z > 0) \quad (3.3.28)$$

and  $X_n''(z) = 0 \quad (z < 0) \quad . \quad (3.3.29)$

For a surface layer of uniform integrated conductivity, the B-polarization problem is identical to the E-polarization problem, except for a rotation of the source field through 90 degrees in the horizontal plane. Thus, by replacing  $E_n(z)$  by  $F_n(z)$ , and  $Y_n(z)$  by  $-X_n(z)$  in any of the E-polarization equations, we obtain the corresponding B-polarization equations. In particular, the boundary conditions across the infinitely thin sheet are

$$F_n(-0) = F_n(+0) = F_n \quad (3.3.30)$$

and  $X_n(-0) - X_n(+0) = -\mu_0 \tau_n F_n \quad . \quad (3.3.31)$

Furthermore, at the surface, the B-polarization fields are given by

$$X_n(-0) = X_0 \quad , \quad \text{a constant} \quad , \quad (3.3.32)$$

$$X_n(+0) = \frac{X_0}{1 + \frac{\sqrt{i\alpha}\tau_n}{\sigma}} \quad , \quad (3.3.33)$$

and  $F_n = \frac{-i\omega}{\sqrt{i\alpha}} \left( \frac{X_0}{1 + \frac{\sqrt{i\alpha}\tau_n}{\sigma}} \right) \quad . \quad (3.3.34)$

### 3.4 Anomalous fields in E-polarization

We now consider the more complex E-polarization problem of an integrated conductivity which varies as in equation (3.1.3). In this case, the total electric field is found by solving the differential equation

$$\frac{\partial^2}{\partial y^2} E_t(y, z) + \frac{\partial^2}{\partial z^2} E_t(y, z) = i\alpha^2 E_t(y, z) \quad (3.4.1)$$

$$(\alpha = 0 \quad \text{in} \quad z < 0)$$

with the corresponding magnetic fields being

$$Y_t(y, z) = \frac{i}{\omega} \frac{\partial}{\partial z} E_t(y, z) \quad , \quad (3.4.2)$$

and 
$$Z_t(y, z) = \frac{-i}{\omega} \frac{\partial}{\partial y} E_t(y, z) \quad (3.4.3)$$

where the subscript  $t$  denotes the total fields. The boundary conditions for the total fields across the infinitely thin surface layer immediately follow from the normal fields by simply replacing the one-dimensional normal fields by the two-dimensional total fields and

noting that

$$\lim_{d \rightarrow 0} \left| \int_{-0}^{d+0} \frac{\partial}{\partial y} z_t(y, z) dz \right| \leq M \lim_{d \rightarrow 0} |d| = 0 \quad (3.4.4)$$

where  $M$  is the maximum value of  $\left| \frac{\partial}{\partial y} z_t(y, z) \right|$  between  $z = -0$  and  $z = d+0$ . Of course, the normal integrated conductivity,  $\tau_n$ , must be replaced by the varying integrated conductivity  $\tau(y)$ , as given in equation (3.1.3). The surface boundary conditions for the total fields, then, are

$$E_t(y, +0) = E_t(y, -0) = E_t(y, 0) \quad , \quad (3.4.5)$$

$$Y_t(y, -0) - Y_t(y, +0) = \mu_0 \tau(y) E_t(y, 0) \quad , \quad (3.4.6)$$

and 
$$Z_t(y, +0) = Z_t(y, -0) = Z_t(y, 0) \quad (3.4.7)$$

where the continuity of  $Z_t(y, z)$  follows from equations (3.4.3) and (3.4.5).

The boundary conditions for the total fields at  $y = \pm\infty$  and  $z = \pm 0$  are also required. Far from the region of varying integrated conductivity in the negative

and positive  $y$  directions, we assume that the fields behave like the normal fields discussed earlier. Furthermore, we know, from Jones and Price (1970), that the total horizontal magnetic field at the surface due to a uniform source field is the same at the extreme values of  $y$ , even if the conductivity structures in  $z > 0$  at  $y = -\infty$  and  $y = +\infty$  are different. Thus we have that

$$Y_t(-\infty, -0) = Y_t(+\infty, -0) = Y_0 \quad (3.4.8)$$

The boundary values for the total electric field at the surface and the total horizontal magnetic field just below the surface are then obtained by simply replacing  $\tau_n$  in equations (3.3.21) and (3.3.22) by  $\tau^-$  and  $\tau^+$  respectively. The resulting boundary values are denoted by

$$E_t(-\infty, 0) = E_n^-, \quad E_t(+\infty, 0) = E_n^+, \quad (3.4.9)$$

and

$$Y_t(-\infty, +0) = Y_n^-(+0), \quad Y_t(+\infty, +0) = Y_n^+(+0). \quad (3.4.10)$$

In addition, we have that

$$Z_t(\pm\infty, 0) = 0 \quad (3.4.11)$$

since  $Z_t(u, 0) = \frac{\partial}{\partial y} E_t(u, 0)$  and  $E_t(u, 0)$  is assumed constant, far from the region of varying integrated conductivity.

The fields, obtained by subtracting the normal fields at  $y = -\infty$  from the total fields, are defined as the anomalous fields and are given by

$$E(y, z) = E_t(y, z) - E_n^-(z) \quad , \quad (3.4.12)$$

$$Y(y, z) = Y_t(y, z) - Y_n^-(z) = \frac{i}{\omega} E_2(y, z) \quad , \quad (3.4.13)$$

and  $Z(y, z) = Z_t(y, z) = \frac{-i}{\omega} E_1(y, z) \quad (3.4.14)$

where  $E(y, z)$  must satisfy

$$E_{11}(y, z) + E_{22}(y, z) = i\alpha^2 E(y, z) \quad (3.4.15)$$

in  $z > 0$  ,

and  $E_{11}(y, z) + E_{22}(y, z) = 0$  in  $z < 0$  .  $(3.4.16)$

From the surface boundary conditions for the total and normal fields and the definition of the anomalous fields, it follows that

$$E(y, -0) = E(y, +0) = E(y, 0) \quad , \quad (3.4.17)$$

$$Z(y, -0) = Z(y, +0) = Z(y, 0) \quad , \quad (3.4.18)$$

and

$$Y(y, -0) - Y(y, +0) = \mu_0 \tau(y) E(y, 0) + \mu_0 (\tau(y) - \tau^-) E_n^- . \quad (3.4.19)$$

In particular, equation (3.4.19) is found by subtracting equation (3.3.15) from (3.4.6) and then using equation (3.4.13). The boundary values at  $y = \pm\infty$  are found to be

$$E(-\infty, 0) = 0 \quad , \quad E(+\infty, 0) = E_n^+ - E_n^- \quad , \quad (3.4.20)$$

$$Y(-\infty, +0) = 0 \quad , \quad Y(+\infty, +0) = Y_n^+(+0) - Y_n^-(+0) \quad , \quad (3.4.21)$$

$$\text{and } Y(\pm\infty, -0) = 0 \quad , \quad Z(\pm\infty, 0) = 0 \quad . \quad (3.4.22)$$

Clearly these anomalous fields are caused by currents induced in the region of varying integrated conductivity and thus are entirely of internal origin. This property

of the anomalous fields is significant and is used in determining an expression for  $Y(y,-0)$  .

Equation (3.4.19), which links the anomalous horizontal magnetic field just below and just above the surface, is of importance here, as it is this equation which is used to determine the anomalous fields along the surface. We are about to show that  $Y(y,-0)$  and  $Y(y,+0)$  can be expressed as integrals over the surface values of the electric field. By substituting these integral equations back into equation (3.4.19), we then have an equation written only in terms of the surface electric field. This equation may be solved numerically using just a one-dimensional grid in the  $y$ -direction, rather than a two-dimensional grid in the  $y$ - $z$  plane which is normally required to solve two-dimensional induction problems numerically. This is an important feature of the work presented in this thesis since it means that both the computer time and the storage space required for the numerical solution of geomagnetic induction problems with surface anomalies are considerably reduced. Once the anomalous electric field is determined, the horizontal and vertical magnetic fields just above and below the surface can easily be obtained by using the forthcoming integral equations for  $Y(y,-0)$  and  $Y(y,+0)$  , and equation (3.4.14) for  $Z(y,0)$  .

The integral equations for  $Y(y,-0)$  and  $Y(y,+0)$  just mentioned, can be obtained by using a Fourier transform in the  $y$  variable, which is defined, as in Sneddon (1951), to be

$$\hat{f}(\eta) = \frac{1}{\sqrt{2\pi}} \int_{-\infty}^{\infty} f(y) e^{i\eta y} dy, \quad (3.4.23)$$

with the inverse transform being

$$f(y) = \frac{1}{\sqrt{2\pi}} \int_{-\infty}^{\infty} \hat{f}(\eta) e^{-i\eta y} d\eta. \quad (3.4.24)$$

An important relationship between Fourier transformed functions is provided by the Faltung theorem which states that

$$\int_{-\infty}^{\infty} \hat{f}(\eta) \hat{g}(\eta) e^{-i\eta y} d\eta = \int_{-\infty}^{\infty} f(u) g(y-u) du. \quad (3.4.25)$$

In order to determine  $Y(y, -0)$  in integral form, we consider the non-conducting region ( $z < 0$ ) in which the anomalous magnetic field components can be expressed in terms of an anomalous magnetic scalar potential  $\Omega(y, z)$ , by the equations

$$Y(y, z) = -\Omega_1(y, z) \quad (3.4.26)$$

and  $Z(y, z) = -\Omega_2(y, z) \quad (3.4.27)$

where  $\Omega(y, z)$  satisfies

$$\Omega_{11}(y, z) + \Omega_{22}(y, z) = 0 \quad (3.4.28)$$

Following the work of Weaver (1964), we take the Fourier transform of equation (3.4.28) to obtain

$$\hat{\Omega}_{22}(\eta, z) = \eta^2 \hat{\Omega}(\eta, z) \quad (3.4.29)$$

We require the solution to this equation which vanishes as  $z \rightarrow -\infty$ , since the anomalous potential must be of internal origin. It is

$$\hat{\Omega}(\eta, z) = \hat{\Omega}(\eta, 0) e^{|\eta|z} \quad (3.4.30)$$

with the inverse Fourier transform giving,

$$\Omega(y, z) = \frac{1}{\sqrt{2\pi}} \int_{-\infty}^{\infty} \hat{\Omega}(\eta, 0) e^{|\eta|z} e^{-i\eta y} d\eta . \quad (3.4.31)$$

If we differentiate this equation with respect to  $z$  and let  $z \rightarrow 0$ , it follows from equation (3.4.27) that

$$Z(y, 0) = -\Omega_2(y, -0) = \frac{-1}{\sqrt{2\pi}} \int_{-\infty}^{\infty} |\eta| \hat{\Omega}(\eta, -0) e^{-i\eta y} d\eta \quad (3.4.32)$$

which from equation (3.4.24) implies

$$\hat{\Omega}(\eta, -0) = \frac{\hat{Z}(\eta, 0)}{|\eta|} . \quad (3.4.33)$$

Substituting this into equation (3.4.31) and differentiating with respect to  $y$ , we have

$$Y(y, -0) = -\Omega_1(y, -0) = \frac{-i}{\sqrt{2\pi}} \int_{-\infty}^{\infty} \hat{Z}(\eta, 0) \operatorname{sgn}(\eta) e^{-i\eta y} d\eta . \quad (3.4.34)$$

After applying the Faltung theorem, this becomes

$$Y(y, -0) = \frac{-1}{\pi} \int_{-\infty}^{\infty} \frac{Z(u, 0)}{y-u} du \quad (3.4.35)$$

since the inverse Fourier transform of  $\operatorname{sgn}(\eta) = \frac{\eta}{|\eta|}$  is known to be  $\frac{-i}{y} \sqrt{\frac{2}{\pi}}$  (Lighthill, 1958). Here, the

bar across the integral sign signifies that the Cauchy principal value (C.P.V.) of the integral must be taken at  $u = y$  for the improper integral to exist. From equation (3.4.14) we know that

$$Z(y, 0) = \frac{-i}{\omega} E_1(y, 0) \quad (3.4.36)$$

so that the desired integral expression for the anomalous horizontal magnetic field at the surface is

$$Y(y, -0) = \frac{i}{\omega\pi} \int_{-\infty}^{\infty} \frac{E_1(u, 0)}{y-u} du \quad (3.4.37)$$

Following the general procedure used to determine equation (3.4.37), an integral expression for  $Y(y, +0)$  can be found. We begin by determining an expression for the anomalous electric field in the conducting region by taking a Fourier transform of equation (3.4.15) to give

$$\hat{E}_{22}(\eta, z) = (\eta^2 + i\alpha^2) \hat{E}(\eta, z) \quad (3.4.38)$$

with the solution, which vanishes as  $z \rightarrow \infty$ , being

$$\hat{E}(\eta, z) = \hat{E}(\eta, 0) e^{-\gamma z} \quad (3.4.39)$$

where  $\gamma = \eta^2 + i\alpha^2$  . (3.4.40)

The exponential term in equation (3.4.39) can be considered as a Fourier transform  $\hat{g}(\eta)$  , of some function  $g(y)$  which is

$$\begin{aligned} g(y) &= \frac{1}{\sqrt{2\pi}} \int_{-\infty}^{\infty} e^{-\gamma z} e^{-i\eta y} d\eta \\ &= \sqrt{\frac{2}{\pi}} \int_0^{\infty} e^{-\gamma z} \cos \eta y d\eta \\ &= \sqrt{\frac{2}{\pi}} \frac{z\sqrt{i}\alpha K_1(\sqrt{i}\alpha\sqrt{y^2+z^2})}{\sqrt{y^2+z^2}} \end{aligned} \tag{3.4.41}$$

where  $K_1$  is a modified Bessel function of the second kind of order 1. The last step in equation (3.4.41) is a tabulated result (Erdélyi et al., 1954, eq. 1.4.26). In order to simplify the notation, we define a function

$$P(y, z) = \frac{K_1(\sqrt{i}\alpha\sqrt{y^2+z^2})}{\sqrt{y^2+z^2}} . \tag{3.4.42}$$

Now by taking the inverse Fourier transform of equation (3.4.39) and using the Faltung theorem, an expression for the anomalous electric field in the conducting region is obtained, giving

$$E(y, z) = \frac{z\sqrt{i}\alpha}{\pi} \int_{-\infty}^{\infty} E(u, 0) P(y-u, z) du \quad . \quad (3.4.43)$$

In arriving at equation (3.4.43), we have tacitly assumed that  $E(y, 0) = 0$  at  $y = \pm\infty$  (i.e.  $E_n^+ = E_n^-$ ) as this is a requirement of taking the Fourier transform of the second derivative with respect to  $y$  in equation (3.4.15). Now from a tabulated result (Gradshteyn and Ryzhik, 1965, eq. 6.596#3), we know that

$$\int_0^{\infty} P(y, z) dy = \sqrt{\frac{\pi}{2\sqrt{i}\alpha z}} K_{1/2}(\sqrt{i}\alpha z) \quad (\alpha > 0) \quad (3.4.44)$$

which, together with the tabulated result (Abramowitz and Stegun, 1964, eq. 10.2.17)

$$\sqrt{\frac{\pi}{2w}} K_{1/2}(w) = \left(\frac{\pi}{2w}\right) e^{-w}, \quad (w, \text{ a complex number})$$

yields

$$\frac{z\sqrt{i}\alpha}{\pi} \int_{-\infty}^{\infty} P(y, z) dy = e^{-\sqrt{i}\alpha z} \quad . \quad (3.4.45)$$

Using this last equation, equation (3.4.42) may be re-written as

$$E(y, z) = z\sqrt{i\alpha} J(y, z) + E(y, 0) e^{-\sqrt{i\alpha}z} \quad (3.4.46)$$

where

$$\begin{aligned} J(y, z) &= \frac{1}{\pi} \int_{-\infty}^{\infty} [E(u, 0) - E(y, 0)] P(y-u, z) du \\ &= \frac{1}{\pi} \int_{-\infty}^{\infty} [E(y+s, 0) - E(y, 0)] P(s, z) ds \quad . \quad (3.4.47) \end{aligned}$$

In this latter form, we see that  $J(y, z) \rightarrow 0$  as  $y \rightarrow \pm\infty$ . Thus the solution for  $E(y, z)$  is actually valid for more general boundary conditions since  $E(y, z)$  approaches the expected one-dimensional solution at  $y = +\infty$ , being

$$E(+\infty, z) = E_t(+\infty, z) - E_n^-(z) = (E_n^+ - E_n^-) e^{-\sqrt{i\alpha}z}$$

$$(z \geq 0)$$

even when  $E_n^+ \neq E_n^-$ . By the Uniqueness theorem, then,

equation (3.4.46) is the one and only solution to equation (3.4.15) which satisfies the required boundary conditions.

We now differentiate equation (3.4.46) with respect to  $z$  to obtain

$$E_2(y, z) = \sqrt{i\alpha} [J(y, z) + zJ_2(y, z) - e^{-\sqrt{i\alpha}z} E(y, 0)] \quad (3.4.48)$$

The second term on the right above vanishes at  $z = +0$ , since it can be shown (see appendix B) that  $J_2(y, z)$  exists at  $z = +0$ . Hence, the desired integral expression for the anomalous horizontal magnetic field just below the surface follows from equation (3.4.13), being

$$Y(y, +0) = \frac{i}{\omega} E_2(y, +0) = \frac{i\sqrt{i\alpha}}{\omega} [J(y, +0) - E(y, 0)] \quad (3.4.49)$$

$$\text{where } J(y, +0) = \frac{1}{\pi} \int_{-\infty}^{\infty} [E(u, 0) - E(y, 0)] P(y-u, +0) du \quad (3.4.50)$$

$$\text{and } P(y-u, +0) = \frac{K_1(\sqrt{i\alpha}|y-u|)}{|y-u|} \quad (3.4.51)$$

Here, the C.P.V. of the integral is taken at  $u = y$  for the improper integral to exist.

By substituting equation (3.3.21) into (3.4.19) and rearranging, we finally obtain the desired expression for the anomalous electric field at the surface

$$E(y, 0) = \frac{\omega\sigma}{\alpha^2\tau(y)} [Y(y, -0) - Y(y, +0)]$$

$$- \frac{i\omega}{\sqrt{i}\alpha} \left( \frac{Y_0}{1 + \frac{\sqrt{i}\alpha\tau^-}{\sigma}} \right) \left( \frac{\tau(y) - \tau^-}{\tau(y)} \right) \quad (3.4.52)$$

where  $Y(y, -0)$  and  $Y(y, +0)$  are now known in terms of  $E(u, 0)$  by equations (3.4.37) and (3.4.49), respectively. (In the above equation, we have also used  $\alpha^2 = \omega\mu_0\sigma$  as defined in equation (2.1.25).)

In the next chapter we will determine the anomalous electric field numerically using this equation. After  $E(u, 0)$  is determined,  $Y(y, -0)$ ,  $Y(y, +0)$  and  $Z(y, 0)$  may easily be calculated. The total fields can then be found by simply adding the normal field values (at  $y = -\infty$ ) to the anomalous field results.

### 3.5 Anomalous fields in B-polarization

The anomalous B-polarization equations can be determined by following the same procedure used to find the anomalous E-polarization equations. Again the anomalous field components are found by subtracting the normal field components (at  $y = -\infty$ ) from the corresponding total field components. The whole procedure is considerably simplified, though, since from section 2.2, we already know that the total horizontal magnetic field above the surface must be constant. As this must agree with the normal field at  $y = -\infty$ , it follows that in  $z < 0$

$$X_t(y, z) = X_o \quad (3.5.1)$$

which implies that

$$X(y, -0) = X_t(y, -0) - X_o = 0 \quad (3.5.2)$$

The anomalous horizontal magnetic field in the conducting region may be found by solving the differential equation

$$X_{11}(y, z) + X_{22}(y, z) = i\alpha^2 X(y, z) \quad (3.5.3)$$

The solution to this equation has already been determined in section 3.4, as

$$X(y, z) = \frac{\sqrt{i}\alpha z}{\pi} \int_{-\infty}^{\infty} [X(u, +0) - X(y, +0)] P(y-u, z) du$$
$$+ X(y, +0) e^{-\sqrt{i}\alpha z} \quad (3.5.4)$$

with the derivative with respect to  $z$ , at  $z = +0$ ,  
being

$$X_2(y, +0) = \frac{\sqrt{i}\alpha}{\pi} \int_{-\infty}^{\infty} [X(u, +0) - X(y, +0)] P(y-u, +0) du$$
$$- \sqrt{i}\alpha X(y, +0) \quad (3.5.5)$$

From equations (2.2.16), (2.2.17), (3.3.25) and (3.3.23)  
and the definition of the anomalous fields, the anomalous  
electric fields, in  $z > 0$ , are given by

$$F(y, z) = \frac{1}{\mu_0 \sigma} X_2(y, z) \quad (3.5.6)$$

and

$$G(y, z) = \frac{-1}{\mu_0 \sigma} X_1(y, z) \quad (3.5.7)$$

The boundary conditions for the anomalous fields (i) across the surface, and (ii) at  $y = \pm\infty$  ( $z = \pm 0$ ), easily follow from the argument used to determine equations (3.4.17) through (3.4.22) and are

$$(i) \quad F(y, +0) = F(y, -0) = F(y, 0) \quad (3.5.8)$$

$$\begin{aligned} X(y, +0) - X(y, -0) &= X(y, +0) \\ &= \mu_0 \tau(y) F(y, 0) + \mu_0 (\tau(y) - \tau^-) F_n^- \quad , \quad (3.5.9) \end{aligned}$$

and

$$(ii) \quad F(-\infty, 0) = 0 \quad , \quad F(+\infty, 0) = F_n^+ - F_n^- \quad , \quad (3.5.10)$$

$$X(-\infty, +0) = 0 \quad , \quad X(+\infty, +0) = X_n^+(+0) - X_n^-(+0) \quad , \quad (3.5.11)$$

$$X(\pm\infty, -0) = 0 \quad , \quad G(\pm\infty, +0) = 0 \quad (3.5.12)$$

where  $F_n^-$  and  $F_n^+$  , and  $X_n^-(+0)$  and  $X_n^+(+0)$  are obtained by replacing  $\tau_n$  in equations (3.3.32) and (3.3.31) by  $\tau^-$  and  $\tau^+$  , respectively.

As in E-polarization, the equation describing the surface boundary condition for the anomalous horizontal magnetic field is important, since it is this equation

which can be used to determine  $X(y,+0)$  which, in turn, is used to determine  $F(y,0)$  and  $G(y,+0)$ . By substituting equation (3.3.32) into (3.5.9) and remembering that  $\alpha^2 = \omega\mu_0\sigma$  and  $X(y,-0) = 0$ , we obtain

$$X(y,+0) = \frac{\alpha^2 \tau(y)}{\omega\sigma} F(y,0) - \frac{\sqrt{i}\alpha(\tau(y) - \tau^-)X_0}{\sigma(1 + \frac{\sqrt{i}\alpha\tau^-}{\sigma})} \quad (3.5.13)$$

where from equations (3.5.5) and (3.5.6),  $F(y,0)$  is known in terms of  $X(u,+0)$  as

$$F(y,0) = \frac{\omega\sqrt{i}}{\alpha} \left\{ \frac{1}{\pi} \int_{-\infty}^{\infty} [X(u,+0) - X(y,+0)] P(y-u,+0) du - X(y,+0) \right\} \quad (3.5.14)$$

From equation (3.5.7), the vertical electric field just below the surface layer is given by

$$G(y,+0) = \frac{-\omega}{\alpha^2} X_1(y,+0) \quad (3.5.15)$$

These equations could be evaluated numerically in a similar way to the corresponding E-polarization equations.

In this thesis, we prefer to determine the horizontal electric field directly since it is more convenient to have  $E(y,0)$  and  $F(y,0)$ , rather than  $E(y,0)$  and  $X(y,+0)$ , immediately available for boundary values in three-dimensional problems. We will now show that an expression entirely in terms of the surface values of the horizontal electric field may be found. From equations (2.2.19), (2.2.20) and (2.2.1) and the definition of anomalous fields, it follows, in  $z > 0$ , that

$$F_{11}(y,z) + F_{22}(y,z) = i\alpha^2 F(y,z) \quad , \quad (3.5.16)$$

$$G_{11}(y,z) + G_{22}(y,z) = i\alpha^2 G(y,z) \quad , \quad (3.5.17)$$

$$\text{and } F_2(y,z) - G_1(y,z) = i\omega X(y,z) \quad . \quad (3.5.18)$$

From equation (3.4.49) in the previous section, we know that solving equation (3.5.16) leads to the expression

$$F_2(y,+0) = \sqrt{i}\alpha \left\{ \frac{1}{\pi} \int_{-\infty}^{\infty} [F(u,0) - F(y,0)] P(y-u,+0) du \right. \\ \left. - F(y,0) \right\} \quad (3.5.19)$$

An expression for  $G_1(y, +0)$  can be obtained by applying a Fourier transform in the  $y$ -variable to equation (3.5.17). The solution, which vanishes as  $z \rightarrow \infty$ , is

$$\hat{G}(\eta, z) = \hat{G}(\eta, +0) e^{-\gamma z} \quad (3.5.20)$$

where  $\gamma^2 = \eta^2 + i\alpha^2$ .

By differentiating with respect to  $z$  at  $z = +0$ , and rearranging, we find that

$$\hat{G}(\eta, z) = \frac{-\hat{G}_2(\eta, +0) e^{-\gamma z}}{\gamma} \quad (3.5.21)$$

Now, by taking the inverse Fourier transform of the above equation, we obtain

$$G(y, z) = \frac{-1}{\sqrt{2\pi}} \int_{-\infty}^{\infty} \frac{e^{-\gamma z}}{\gamma} \hat{G}_2(\eta, +0) e^{-i\eta y} d\eta \quad (3.5.22)$$

which, after differentiating with respect to  $y$ , becomes

$$G_1(y, z) = \frac{i}{\sqrt{2\pi}} \int_{-\infty}^{\infty} \left( \frac{\eta e^{-\gamma z}}{\gamma} \right) \hat{G}_2(\eta, +0) e^{-i\eta y} d\eta \quad (3.5.23)$$

From tabulated results (Erdélyi et al., 1954, eq. 1.4.27 and eq. 2.4.36), we know that

$$\begin{aligned} \frac{-1}{\sqrt{2\pi}} \int_{-\infty}^{\infty} \frac{e^{-\gamma z}}{\gamma} e^{-i\eta y} d\eta &= -\sqrt{\frac{2}{\pi}} \int_0^{\infty} \frac{e^{-\gamma z}}{\gamma} \cos \eta y d\eta \\ &= -\sqrt{\frac{2}{\pi}} K_0(\alpha\sqrt{i}\sqrt{y^2+z^2}) \end{aligned} \quad (3.5.24)$$

and

$$\begin{aligned} \frac{-1}{\sqrt{2\pi}} \int_{-\infty}^{\infty} \frac{\eta e^{-\gamma z}}{\gamma} e^{-i\eta y} d\eta &= -\sqrt{\frac{2}{\pi}} \int_0^{\infty} \frac{\eta e^{-\gamma z}}{\gamma} \sin \eta y d\eta \\ &= -\sqrt{i}\alpha y P(y, z) \end{aligned} \quad (3.5.25)$$

and since the divergence of the electric field is zero, we also know that, in  $z > 0$

$$G_2(y, z) = -F_1(y, z) \quad (3.5.26)$$

Thus, by applying the Faltung theorem to equations (3.5.22) and (3.5.23) and using the above information, we finally obtain expressions for the vertical electric field and its

derivative with respect to  $y$ , just below the surface,

$$\begin{aligned}
 G(y, +0) &= \frac{1}{\pi} \int_{-\infty}^{\infty} F_1(u, 0) K_0(\sqrt{i}\alpha|y-u|) du \\
 &= \frac{-\sqrt{i}\alpha}{\pi} \int_{-\infty}^{\infty} F(u, 0) (y-u) P(y-u, +0) du \quad (3.5.27)
 \end{aligned}$$

and

$$G_1(y, +0) = \frac{-\sqrt{i}\alpha}{\pi} \int_{-\infty}^{\infty} F_1(u, 0) (y-u) P(y-u, +0) du \quad (3.5.28)$$

The second step in equation (3.5.27) is obtained by integration by parts. The desired expression for the horizontal electric field at the surface is found by substituting equation (3.5.9) into (3.5.18), giving

$$\frac{i\alpha^2 \tau(y)}{\sigma} F(y, 0) = F_2(y, +0) - G_1(y, +0) - i\alpha^2 \left( \frac{\tau(y) - \tau^-}{\sigma} \right) F_n^- \quad (3.5.29)$$

where  $F_2(y, +0)$  and  $G_1(y, +0)$  are known in terms of  $F(y, 0)$  by equations (3.5.19) and (3.5.28), respectively.

In the next chapter, we will determine the horizontal electric field at the surface numerically using the above equation. The horizontal magnetic field and the vertical electric field just below the surface can then be calculated using equations (3.5.13) and (3.5.15), respectively.

CHAPTER 4

NUMERICAL METHOD

4.1 Introduction

We begin this chapter by expressing the field equations of chapter 3 in dimensionless form so that the results will be as general as possible. We do this by scaling the length terms,  $u$  and  $y$ , with respect to the skin depth,  $\delta = \frac{\sqrt{2}}{\alpha}$ , of the lower half-space, i.e.

$$u' = \frac{u}{\delta} = \frac{\alpha u}{\sqrt{2}} \quad \text{and} \quad y' = \frac{y}{\delta} = \frac{\alpha y}{\sqrt{2}} \quad (4.1.1)$$

and by defining new dimensionless fields to be

$$\bar{E}' = \frac{\bar{E}}{\omega \delta B_0} \quad (4.1.2)$$

and  $\bar{B}' = \frac{\bar{B}}{B_0} \quad (4.1.3)$

where  $B_0 = Y_0$  in E-polarization and  $B_0 = X_0$  in B-polarization. Furthermore, we denote the dimensionless form of the integrated conductivity and of the function  $P(y-u, +0)$  by

$$\tau'(y') = \frac{\tau(y)}{\sigma \delta} \quad (4.1.4)$$

and  $P'(y'-u', +0) = \delta P(y-u, +0) \quad (4.1.5)$

Here all dimensionless terms are denoted by primes ('). We may now write the E-polarization equations ((3.4.52), (3.4.37), (3.4.49) and (3.4.36)) in dimensionless form as

$$E'(y', 0) = \left( \frac{Y'(y', -0) - Y'(y', +0)}{2\tau'(y')} \right) + \left( \frac{\sqrt{2i}}{1 + \sqrt{2i}\tau'^-} \right) \left( \frac{\tau'^- - \tau'(y')}{2\tau'(y')} \right), \quad (4.1.6)$$

$$Y'(y', -0) = \frac{i}{\pi} \int_{-\infty}^{\infty} \frac{E_1'(u', 0)}{y' - u'} du' , \quad (4.1.7)$$

$$Y'(y', +0) = i\sqrt{2i} \left\{ \frac{1}{\pi} \int_{-\infty}^{\infty} [E'(u', 0) - E'(y', 0)] P'(y' - u', +0) du' - E'(y', 0) \right\} , \quad (4.1.8)$$

and  $Z'(y', 0) = -iE_1'(y', 0)$  (4.1.9)

and the B-polarization equations ((3.5.26), (3.5.13), (3.5.15), (3.5.19) and (3.5.25)) as

$$F'(Y', 0) = -i \left( \frac{F_2'(Y', +0) - G_1'(Y', +0)}{2\tau'(Y')} \right) + \left( \frac{\sqrt{2i}}{1 + \sqrt{2i}\tau'^{-}} \right) \left( \frac{\tau'^{-} - \tau'(Y')}{2\tau'(Y')} \right), \quad (4.1.10)$$

$$X'(Y', +0) = 2\tau'(Y')F'(Y', 0) + \left( \frac{\sqrt{2i}}{1 + \sqrt{2i}\tau'^{-}} \right) (\tau'^{-} - \tau'(Y')), \quad (4.1.11)$$

$$\text{and } G'(Y', +0) = \frac{-1}{2} X_1'(Y', +0) \quad (4.1.12)$$

where

$$F_2'(Y', +0) = \sqrt{2i} \left\{ \frac{1}{\pi} \int_{-\infty}^{\infty} [F'(u', 0) - F'(Y', 0)] P'(Y'-u', +0) du' - F'(Y', 0) \right\} \quad (4.1.13)$$

and

$$G_1'(Y', +0) = \frac{-\sqrt{2i}}{\pi} \int_{-\infty}^{\infty} (Y'-u') F_1'(u', 0) P'(Y'-u', +0) du'. \quad (4.1.14)$$

To simplify the notation, we will drop the primes from the above equations, in this chapter, since we will only be concerned with dimensionless terms.

The above equations can not be solved analytically so we must use numerical techniques. In order to express these equations in a form suitable for numerical evaluation, we first assume that the fields reach their boundary values at some finite points,  $y_1$ , and  $y_M$  (see figure 4.1) and remain at these values out to  $y = \pm\infty$ . (Note that, as an alternative in the E-polarization case, we can use the improved end condition described in section 4.4.) Within these finite boundaries, we choose a set of grid points  $y_j$  of variable step-size (see figure 4.1) at which we will determine the unknown field values. As a general rule, we choose the grid points in such a way that there are more points per given distance in the region of varying integrated conductivity. The accuracy of the resulting field values in a given region is generally increased by increasing the number of grid points and/or by extending the boundary points. One further point to mention is that the integrated conductivity is initially defined in the region between consecutive grid points. As shown by Brewitt-Taylor and Weaver (1976), the value at the grid point is found by taking a weighted average, given by

$$\tau(y_j) = \frac{k_{j-1}\tau(y_{j-\frac{1}{2}}) + k_j\tau(y_{j+\frac{1}{2}})}{k_{j-1} + k_j}$$

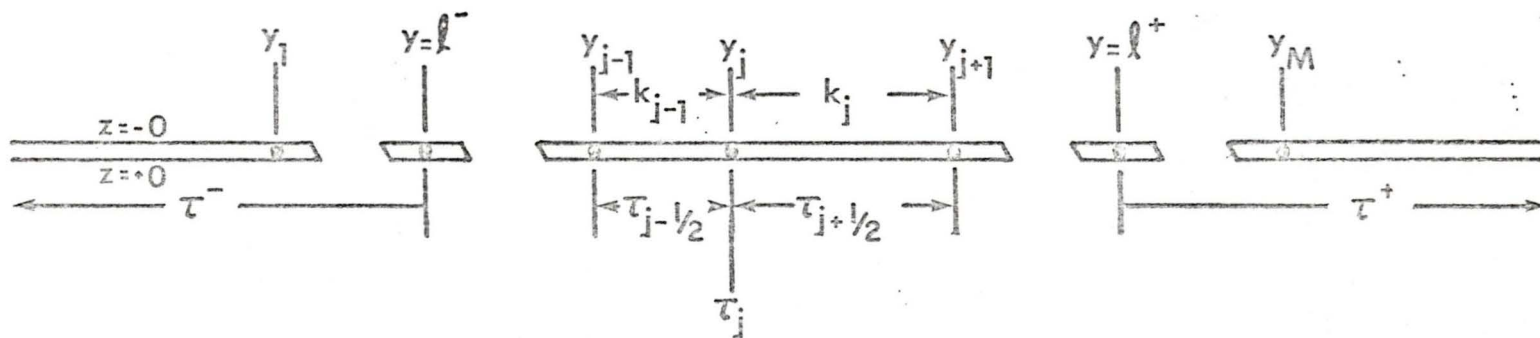


Figure 4.1 The set of grid points and the limited region of varying integrated conductivity ( $l^- < y < l^+$ ).

where  $\tau(y_{j-\frac{1}{2}})$  denotes the constant value of the integrated conductivity in the interval between  $y_{j-1}$  and  $y_j$ , and  $k_j$  denotes the distance between any consecutive grid points,  $y_j$  and  $y_{j+1}$  (i.e.  $k_j = y_{j+1} - y_j$ ).

In the next section, we will see that at each of the  $M-2$  grid points,  $y_j$  ( $j = 2, 3, \dots, M-1$ ), equations (4.1.6) and (4.1.10) can be written in terms of  $M-2$  unknowns. We thus have a system of equations which may easily be expressed in matrix form. The unknown fields,  $E(y_j, 0)$  and  $F(y_j, 0)$ , at each grid point can then be determined by using Gaussian elimination. Once  $E(y_j, 0)$  and  $F(y_j, 0)$  are determined, the other field components may easily be found.

#### 4.2 Numerical form of E-polarization equations

It is convenient to show first the method used to evaluate numerically the integral expression for  $Y(u, -0)$ , assuming  $E(u, 0)$  is known. The same method also applies to the integral expression for  $Y(u, +0)$ . The required discrete form of equation (4.1.6) is then easily found.

We begin by writing the integral in equation (4.1.7) as a sum of integrals

$$\begin{aligned}
 -i\pi Y(y_m, -0) &= \int_{-\infty}^{\infty} \frac{E_1(u, 0)}{y_m^{-u}} du \\
 &= \int_{-\infty}^{y_1} \frac{E_1(u, 0)}{y_m^{-u}} du + \int_{y_{m-1}}^{y_{m+1}} \frac{E_1(u, 0)}{y_m^{-u}} du \\
 &\quad + \int_{y_M}^{\infty} \frac{E_1(u, 0)}{y_m^{-u}} du \\
 &\quad + \sum_{\substack{j=2 \\ (j \neq m, m+1)}}^{M-1} \int_{y_{j-1}}^{y_j} \frac{E_1(u, 0)}{y_m^{-u}} du \quad (4.2.1)
 \end{aligned}$$

Here the first and third terms on the right vanish, since over these intervals,  $E(u, 0)$  is assumed constant (see section 4.1), and thus the derivative is zero.

Hartmann (1963) has pointed out that the effect of putting  $E_1(u,0) = 0$  for  $-\infty < u < y_1$  and  $y_M < u < \infty$  causes results which are inaccurate, because the influence of  $\frac{1}{y_m - u}$  in the infinite integral is cut off at  $y_1$  and  $y_M$ . For a given region, though, this effect can be decreased to a desired accuracy by extending the boundary points. (A much better method of overcoming this effect is described in section 4.4.) Each of the remaining terms in equation (4.2.1) are evaluated by a variation of a method suggested by Hartmann (1963).

We now analyse the term involving the singularity. We begin by expanding  $E(u,0)$  about  $y_m$  in a Taylor's series to second order, to give

$$E(u,0) = E(y_m,0) + (u-y_m)E_1(y_m,0) + \frac{(u-y_m)^2}{2} E_{11}(y_m,0) \quad (4.2.2)$$

which, on differentiation, becomes

$$E_1(u,0) = E_1(y_m,0) + (u-y_m)E_{11}(y_m,0) \quad (4.2.3)$$

$$(y_{m-1} \leq u \leq y_{m+1}) .$$

Three point finite-difference (F.D.) forms are used to evaluate  $E_1(y_m,0)$  and  $E_{11}(y_m,0)$ . These forms can be determined, for variable step-size grids, by again using

equation (4.2.2). In this case, we write

$$E(Y_{m+1}, 0) = E(Y_m, 0) + k_m E_1(Y_m, 0) + \frac{k_m^2}{2} E_{11}(Y_m, 0) \quad (4.2.4)$$

and

$$E(Y_{m-1}, 0) = E(Y_m, 0) - k_{m-1} E_1(Y_m, 0) + \frac{k_{m-1}^2}{2} E_{11}(Y_m, 0) \quad (4.2.5)$$

where  $k_j = Y_{j+1} - Y_j$  . (4.2.6)

The required finite difference expression for  $E_1(u, 0)$  is found by multiplying equation (4.2.4) by  $k_{m-1}^2$  and equation (4.2.5) by  $k_m^2$  and subtracting. The resulting equation can then be rearranged to give

$$E_1(Y_m, 0) = a_m E(Y_{m-1}, 0) + b_m E(Y_m, 0) + c_m E(Y_{m+1}, 0) \quad (4.2.7)$$

where

$$a_m = \frac{-k_m}{k_{m-1} k_m^+} , \quad b_m = \frac{k_m^-}{k_m k_{m-1}} , \quad c_m = \frac{k_{m-1}}{k_m k_m^+} \quad (4.2.8)$$

with  $k_m^+ = k_m + k_{m-1}$  ,  $k_m^- = k_m - k_{m-1}$  . (4.2.9)

Similarly, by multiplying equation (4.2.4) by  $k_{m-1}$  and equation (4.2.5) by  $k_m$  and adding, we obtain

$$E_{11}(y_m, 0) = p_m E(y_{m-1}, 0) + q_m E(y_m, 0) + r_m E(y_{m+1}, 0) \quad (4.1.10)$$

where

$$p_m = \frac{2}{k_{m-1} k_m^+}, \quad q_m = \frac{-2}{k_m k_{m-1}}, \quad r_m = \frac{2}{k_m k_m^+} \quad (4.1.11)$$

To simplify notation, we will denote the fields at the general grid point  $y_j$ , by the grid subscript alone (i.e.  $E_j = E(y_j, 0)$ ). Using equation (4.2.3) and the F.D. forms for  $E_1(y_m, 0)$  and  $E_{11}(y_m, 0)$ , we may now write

$$\begin{aligned} \int_{y_{m-1}}^{y_{m+1}} \frac{E_1(u, 0)}{y_m - u} du &= E_1(y_m, 0) \int_{y_{m-1}}^{y_{m+1}} \frac{du}{y_m - u} + E_{11}(y_m, 0) \int_{y_{m-1}}^{y_{m+1}} \frac{u - y_m}{y_m - u} du \\ &= -(a_m E_{m-1} + b_m E_m + c_m E_{m+1}) \ln \left( \frac{k_m}{k_{m-1}} \right) \\ &\quad - (p_m E_{m-1} + q_m E_m + r_m E_{m+1}) k_m^+ \end{aligned} \quad (4.1.12)$$

where the first integral on the right-hand side has been evaluated by taking the C.P.V. of the integral as follows,

$$\begin{aligned}
 - \int_{y_{m-1}}^{y_{m+1}} \frac{du}{y_m - u} &= \int_{-k_{m-1}}^{k_m} \frac{dv}{v} = \lim_{\epsilon \rightarrow 0} \left\{ \int_{-k_{m-1}}^{-\epsilon} + \int_{\epsilon}^{k_m} \right\} \frac{dv}{v} \\
 &= \lim_{\epsilon \rightarrow 0} \left\{ \int_{\epsilon}^{k_m} - \int_{\epsilon}^{k_{m-1}} \right\} \frac{dv}{v} \\
 &= \lim_{\epsilon \rightarrow 0} \left\{ \ln k_m - \ln \epsilon - \ln k_{m-1} + \ln \epsilon \right\} \\
 &= \ln \left( \frac{k_m}{k_{m-1}} \right) \quad . \quad (4.2.13)
 \end{aligned}$$

Clearly the representation of  $E_1(u, 0)$  by equation (4.2.3) is equivalent to fitting a quadratic through the values of  $E(u, 0)$  at  $y_{m-1}$ ,  $y_m$  and  $y_{m+1}$  and then differentiating with respect to  $u$ .

Away from the singularity, it is assumed that  $E(u, 0)$  varies approximately linearly between consecutive grid points so that  $E_1(u, 0)$  may be expressed by a simple two point F.D. form, given by

$$E_1(u, 0) = \frac{E_j - E_{j-1}}{y_j - y_{j-1}} \left( \begin{array}{l} y_1 \leq y_{j-1} \leq u \leq y_j \leq y_{m-1} \\ y_{m+1} \leq y_{j-1} \leq u \leq y_j \leq y_M \end{array} \right) \quad (4.2.14)$$

so that

$$\begin{aligned}
 \sum_{\substack{j=2 \\ (j \neq m, m+1)}}^M \int_{Y_{j-1}}^{Y_j} \frac{E_1(u, 0)}{Y_m - u} du &= \sum_{\substack{j=2 \\ (j \neq m, m+1)}}^M \left( \frac{E_j - E_{j-1}}{Y_j - Y_{j-1}} \right) \int_{Y_{j-1}}^{Y_j} \frac{du}{Y_m - u} \\
 &= - \sum_{\substack{j=2 \\ (j \neq m, m+1)}}^M \left\{ \left( \frac{E_j}{Y_j - Y_{j-1}} \right) \ell n \left( \frac{Y_j - Y_m}{Y_{j-1} - Y_m} \right) - \left( \frac{E_{j-1}}{Y_j - Y_{j-1}} \right) \ell n \left( \frac{Y_j - Y_m}{Y_{j-1} - Y_m} \right) \right\} \\
 &= - \sum_{\substack{j=2 \\ (j \neq m-1, m, m+1)}}^{M-1} E_j \left\{ \frac{1}{k_{j-1}} \ell n \left( \frac{Y_j - Y_m}{Y_{j-1} - Y_m} \right) - \frac{1}{k_j} \ell n \left( \frac{Y_{j+1} - Y_m}{Y_j - Y_m} \right) \right\} \\
 &\quad + \frac{E_1}{k_1} \ell n \left( \frac{Y_2 - Y_m}{Y_1 - Y_m} \right) - \frac{E_{m-1}}{k_{m-2}} \ell n \left( \frac{k_{m-1}}{k_{m-1}^+} \right) + \frac{E_{m+1}}{k_{m+1}} \ell n \left( \frac{k_{m+1}^+}{k_m} \right) \\
 &\quad - \frac{E_M}{k_{M-1}} \ell n \left( \frac{Y_M - Y_m}{Y_{M-1} - Y_m} \right) \tag{4.2.15}
 \end{aligned}$$

where  $E_1$  stands for  $E(Y_1, 0)$  and is not to be confused with the partial derivative  $E_1(u, 0)$ . We may now write equation (4.2.1) in a form suitable for programming on a computer, as

$$-i\pi Y(Y_m, -0) \cong \sum_{j=1}^M Q_{mj} E_j \tag{4.2.16}$$

where

$$Q_{mj} = \left\{ \begin{array}{l} \frac{1}{k_j} \ell n \left( \frac{y_m - y_{j+1}}{y_m - y_j} \right) - \frac{1}{k_{j-1}} \ell n \left( \frac{y_m - y_j}{y_m - y_{j-1}} \right) \quad \left( \begin{array}{l} 2 \leq j \leq m-2 \\ m+2 \leq j \leq M-1 \end{array} \right) \\ \\ \frac{1}{k_1} \ell n \left( \frac{y_m - y_2}{y_m - y_1} \right) \quad (j = 1) \\ \\ a_m \ell n \left( \frac{k_{m-1}}{k_m} \right) - p_m k_m^+ - \frac{1}{k_{m-2}} \ell n \left( \frac{k_{m-1}}{k_{m-1}^+} \right) \quad (j = m-1) \\ \\ b_m \ell n \left( \frac{k_{m-1}}{k_m} \right) - q_m k_m^+ \quad (j = m) \\ \\ c_m \ell n \left( \frac{k_{m-1}}{k_m} \right) - r_m k_m^+ - \frac{1}{k_{m+1}} \ell n \left( \frac{k_m}{k_{m-1}^+} \right) \quad (j = m+1) \\ \\ \frac{1}{k_{M-1}} \ell n \left( \frac{y_m - y_{M-1}}{y_m - y_M} \right) \quad (j = M) \end{array} \right. \quad (4.2.17)$$

with special cases when  $m = 2$  and  $m = M-1$ , being

$$Q_{21} = a_2 \ln \left( \frac{k_1}{k_2} \right) - p_2 k_2^+ \quad (4.2.18)$$

and

$$Q_{M-1,M} = c_{M-1} \ln \left( \frac{k_{M-1}}{k_m} \right) - r_{M-1} k_{M-1}^+$$

Here,  $m$  varies from 2 to  $M-1$ . (Unless the improved boundary condition of section 4.4 is used, the term  $Q_{m1}$  is not required since  $E_1$  is zero by the boundary conditions. Here and later, terms associated with  $E_1$  will be included for the sake of completeness.)

Following the procedure used to evaluate  $Y(y_m, -0)$  the integral expression for the horizontal magnetic field just below the surface, given by equation (4.1.8), may be written as

$$\begin{aligned} -\sqrt{\frac{1}{2}} \pi Y(y_m, +0) &= \int_{-\infty}^{\infty} [E(u, 0) - E(y_m, 0)] P(y_m - u, +0) du - \pi E(y_m, 0) \\ &= \left\{ \int_{-\infty}^{Y_1} + \int_{Y_M}^{\infty} \right\} E(u, 0) P(y_m - u, +0) du + \sum_{\substack{j=2 \\ j \neq m, m+1}}^M \left\{ \int_{Y_{j-1}}^{Y_j} E(u, 0) P(y_m - u, +0) du \right\} \end{aligned}$$

$$\begin{aligned}
 & - \left[ \pi + \left\{ \int_{-\infty}^{Y_{m-1}} + \int_{Y_{m+1}}^{\infty} \right\} P(Y_m^{-u}, +0) du \right] E_m \\
 & + \int_{Y_{m-1}}^{Y_{m+1}} [E(u, 0) - E(Y_m, 0)] P(Y_m^{-u}, +0) du \\
 = & E_1 \int_{-\infty}^{Y_1} P(Y_m^{-u}, +0) du + E_M \int_{Y_M}^{\infty} P(Y_m^{-u}, +0) du \\
 & + \sum_{j=2}^{m-1} \left\{ E_j \int_{Y_{j-1}}^{Y_j} P(Y_m^{-u}, +0) du + \left( \frac{E_j - E_{j-1}}{Y_j - Y_{j-1}} \right) \int_{Y_{j-1}}^{Y_j} (u - Y_j) P(Y_m^{-u}, +0) du \right\} \\
 & + \sum_{j=m+1}^{M-1} \left\{ E_j \int_{Y_j}^{Y_{j+1}} P(Y_m^{-u}, +0) du + \left( \frac{E_{j+1} - E_j}{Y_{j+1} - Y_j} \right) \int_{Y_j}^{Y_{j+1}} (u - Y_j) P(Y_m^{-u}, +0) du \right\} \\
 & - E_m \left[ \pi + \left\{ \int_{-\infty}^{Y_{m-1}} + \int_{Y_{m+1}}^{\infty} \right\} P(Y_m^{-u}, +0) du \right] \\
 & + E_1(Y_m, 0) \int_{Y_{m-1}}^{Y_{m+1}} (u - Y_m) P(Y_m^{-u}, +0) du \\
 & + \frac{E_{11}(Y_m, 0)}{2} \int_{Y_{m-1}}^{Y_{m+1}} (u - Y_m)^2 P(Y_m^{-u}, +0) du
 \end{aligned} \tag{4.2.19}$$

Here we have represented  $E(u,0)$  near the singularity  $(y_{m-1} < u < y_{m+1})$  by equation (4.2.2) and between consecutive grid points away from the singularity by

$$E(u,0) = E_j + (u-y_j) \left( \frac{E_j - E_{j-1}}{y_j - y_{j-1}} \right) \quad (4.2.20)$$

$$\left( \begin{array}{l} y_1 \leq y_{j-1} \leq u \leq y_j \leq y_{m-1} \\ y_{m+1} \leq y_{j-1} \leq u \leq y_j \leq y_M \end{array} \right)$$

We now denote the integral coefficients in equation (4.2.19) by the symbols  $U_{mj}$ ,  $V_{mj}$  and  $W_m$  as follows:

$$U_{mj} = \begin{cases} -\sqrt{2i} \int_{-\infty}^{Y_1} P(Y_m - u, +0) du & (j = 1) \\ -\sqrt{2i} \int_{Y_{j-1}}^{Y_j} P(Y_m - u, +0) du & (2 \leq j \leq m-1) \\ \sqrt{2i} \pi + \sqrt{2i} \left\{ \int_{-\infty}^{Y_{m-1}} + \int_{Y_{m+1}}^{\infty} \right\} P(Y_m - u, +0) du & (j = m) \\ -\sqrt{2i} \int_{Y_j}^{Y_{j+1}} P(Y_m - u, +0) du & (m+1 \leq j \leq M-1) \\ -\sqrt{2i} \int_{Y_M}^{Y_j} P(Y_m - u, +0) du & (j = M) \end{cases} \quad (4.2.21)$$

$$V_{mj} = \begin{cases} \sqrt{2i} \int_{Y_{j-1}}^{Y_j} (u - Y_j) P(Y_m - u, +0) du & (2 \leq j \leq m-1) \\ -\sqrt{2i} \int_{Y_{m-1}}^{Y_{m+1}} (u - Y_m) P(Y_m - u, +0) du & (j = m) \\ -\sqrt{2i} \int_{Y_j}^{Y_{j+1}} (u - Y_j) P(Y_m - u, +0) du & (m+1 \leq j \leq M-1) \end{cases} \quad (4.2.22)$$

$$W_m = \frac{-\sqrt{2i}}{2} \int_{Y_{m-1}}^{Y_{m+1}} (u - Y_m)^2 P(Y_m - u, +0) du \quad (4.2.23)$$

Each of these terms is written in a form suitable for programming in appendix A. In doing this, the handbook by Abramowitz and Stegun (1964) has been used extensively.

Using the above defined coefficients we may write equation (4.2.19) as

$$i\pi Y(y_m, +0) = \sum_{j=1}^M R_{mj} E_j \quad (4.2.25)$$

where

$$R_{mj} = \left\{ \begin{array}{ll} U_{m1} - \frac{V_{m2}}{k_1} & (j = 1) \\ U_{mj} + \frac{V_{mj}}{k_{j-1}} - \frac{V_{mj+1}}{k_j} & (2 \leq j \leq m-2) \\ U_{mm-1} + \frac{V_{mm-1}}{k_{m-2}} + a_m V_{mm} + p_m W_m & (j = m-1) \\ U_{mm} + b_m V_{mm} + q_m W_m & (j = m) \quad (4.2.26) \\ U_{m+1} - \frac{V_{m+1}}{k_{m+1}} + c_m V_{mm} + r_m W_m & (j = m+1) \\ U_{mj} - \frac{V_{mj}}{k_j} + \frac{V_{mj-1}}{k_{j-1}} & (m+2 \leq j \leq M-1) \\ U_{mM} + \frac{V_{mM-1}}{k_{M-1}} & (j = M) \end{array} \right.$$

with special cases when  $m = 2$  and  $m = M-1$ , being

$$R_{21} = U_{m1} + a_2 V_{22} + p_2 W_2$$

and 
$$R_{M-1M} = U_{M-1M} + c_{M-1} V_{M-1M-1} + r_{M-1} W_{M-1}$$

Again,  $m$  varies from 2 to  $M-1$ .

Finally, equation (4.1.6) can be written as

$$E_m = \frac{i}{2\pi\tau_m} \left\{ \sum_{j=1}^M (Q_{mj} + R_{mj}) E_j + i\sqrt{2i}\pi \frac{(\tau_m - \tau^-)}{(1 + \sqrt{2i}\tau^-)} \right\} \quad (4.2.27)$$

As mentioned in section 4.1, there are  $M-2$  equations of this form in the  $M-2$  unknowns,  $E_j$  ( $j = 2, \dots, M-1$ ).

( $E_1$  and  $E_M$  are the known boundary values.) The  $E_j$ 's may be determined by expressing the system of equations in matrix form as

$$[A][E] = [B] \quad (4.2.28)$$

where

$$A_{mj} = Q_{mj} + R_{mj} + 2\pi i \delta_{mj} \tau_m$$

and

$$B_m = \frac{(1-i)\pi(\tau_m - \tau^-)}{(1 + \sqrt{2i}\tau^-)} - (R_{m1} + Q_{m1})E_1 - (R_{mM} + Q_{mM})E_M, \quad (4.2.29)$$

and then using Gaussian elimination. Here,  $\delta_{mj}$  is the Kronecker delta.

With the horizontal electric field known at the grid points, the horizontal magnetic field just above the surface can easily be determined from equation (4.2.16). The horizontal magnetic field just below the surface could be determined from equation (4.2.25) but, with  $Y(y_m, -0)$  known, we can find  $Y(y_m, +0)$  by simply rearranging equation (4.1.6). The vertical magnetic field  $Z(u, 0)$  can be determined at the midpoint between consecutive grid points by

$$Z(y_{m-\frac{1}{2}}, 0) = -i \left( \frac{E_m - E_{m-1}}{Y_m - Y_{m-1}} \right) \quad (4.2.30)$$

where  $Y_{m-\frac{1}{2}} = \frac{Y_m + Y_{m-1}}{2}$  . (4.2.31)

The total fields can then be obtained by adding the normal fields at  $y = -\infty$  to the corresponding anomalous fields.

In dimensionless form, the normal fields are

$$E_n^-(0) = \sqrt{\frac{i}{2}} \left( \frac{1}{1 + \sqrt{2i}\tau^-} \right) , \quad (4.2.32)$$

$$y_n^-(+0) = \left( \frac{1}{1 + \sqrt{2i}\tau^-} \right) , \quad (4.2.33)$$

$$y_n^-(-0) = 1 , \quad (4.2.34)$$

and  $z_n^-(0) = 0$  . (4.2.35)

Here the subscript  $n$  follows the notation used in section 3.3 for normal fields and the postscripted  $-$  sign indicates that these are the fields determined at  $y = -\infty$  .

#### 4.3 Numerical form of B-polarization equations

Having described the procedure required to express the E-polarization equations in numerical form, we can now easily express the B-polarization equations in the appropriate form. By comparing equation (4.1.13) with (4.1.8), the integral expression for  $F_2(y_m, +0)$  may be written immediately as

$$F_2(y_m, +0) = \frac{-i}{\pi} \sum_{j=1}^M R_{mj} F_j \quad (4.3.1)$$

where the  $R_{mj}$ 's are the same coefficients as given by equation (4.2.26). Furthermore, following the method of presentation used in the previous section and remembering that we have assumed  $F(u, 0)$  is constant (i.e.  $F_1(u, 0) = 0$ ) in the regions  $-\infty < u < y_1$  and  $y_M < u < \infty$ , we write

$$G_1(y_m, +0) = -\frac{\sqrt{2i}}{\pi} \int_{-\infty}^{\infty} (y_m - u) F_1(u, 0) P(y_m - u, +0) du$$

$$\begin{aligned}
 &= \frac{-\sqrt{2i}}{\pi} \left[ \left\{ \int_{-\infty}^{Y_1} + \int_{Y_M}^{\infty} \right\} (y_m - u) F_1(u, 0) P(y_m - u, +0) du \right. \\
 &\quad + \sum_{\substack{j=2 \\ (j \neq m, m+1)}}^M \left\{ \int_{Y_{j-1}}^{Y_j} (y_m - u) F_1(y, 0) P(y_m - u, +0) du \right\} \\
 &\quad \left. + \int_{Y_{m-1}}^{Y_{m+1}} (y_m - u) F_1(u, 0) P(y_m - u, +0) du \right] \\
 &= \frac{1}{\pi} \left[ \sum_{j=2}^{m-1} \left( \frac{F_j - F_{j-1}}{Y_j - Y_{j-1}} \right) \tilde{V}_{mj} + F_1(y_m, 0) \tilde{V}_{mm} + F_{11}(y_m, 0) \tilde{W}_m \right. \\
 &\quad \left. + \sum_{j=m+1}^{M-1} \left( \frac{F_{j+1} - F_j}{Y_{j+1} - Y_j} \right) \tilde{V}_{mj} \right] \\
 &= \frac{1}{\pi} \sum_{j=1}^M S_{mj} F_j \tag{4.3.2}
 \end{aligned}$$

where

$$\tilde{V}_{mj} = \begin{cases} \sqrt{2i} \int_{Y_{j-1}}^{Y_j} (u - y_m) P(y_m - u, +0) du & (2 \leq j \leq m-1) \\ \sqrt{2i} \int_{Y_{m-1}}^{Y_{m+1}} (u - y_m) P(y_m - u, +0) du & (j=m) \\ \sqrt{2i} \int_{Y_j}^{Y_{j+1}} (u - y_m) P(y_m - u, +0) du & (m+1 \leq j \leq M-1) \end{cases} \tag{4.3.3}$$

$$\tilde{W}_m = \sqrt{2i} \int_{y_{m-1}}^{y_{m+1}} (y_m - u)^2 P(y_m - u, +0) du \quad (4.3.4)$$

and

$$S_{mj} = \begin{cases} \frac{-\tilde{V}_{m2}}{k_1} & (j=1) \\ \frac{\tilde{V}_{mj}}{k_{j-1}} - \frac{\tilde{V}_{mj+1}}{k_j} & (2 \leq j \leq m-2) \\ a_m \tilde{V}_{mm} + p_m \tilde{W}_m + \frac{\tilde{V}_{mm-1}}{k_{m-2}} & (j=m-1) \\ b_m \tilde{V}_{mm} + q_m \tilde{W}_m & (j=m) \\ c_m \tilde{V}_{mm} + r_m \tilde{W}_m - \frac{\tilde{V}_{mm+1}}{k_{m+1}} & (j=m+1) \\ \frac{\tilde{V}_{mj-1}}{k_{j-1}} - \frac{\tilde{V}_{mj}}{k_j} & (m+2 \leq j \leq M-1) \\ \frac{\tilde{V}_{mM-1}}{k_{M-1}} & (j=M) \end{cases} \quad (4.3.5)$$

with special cases when  $m = 2$  and  $m = M-1$ , being

$$S_{21} = a_2 \tilde{V}_{22} + p_2 \tilde{W}_2 \quad (4.3.6)$$

and  $S_{M-1 M} = c_{M-1} \tilde{V}_{M-1 M-1} + r_{M-1} \tilde{W}_{M-1}$ .

Both  $\tilde{V}_{mj}$  and  $\tilde{W}_m$  are written in a form suitable for programming in appendix A. Now, by substituting equations (4.3.1) and (4.3.2) into (4.1.10), we finally obtain  $M-2$  equations of the form

$$F_m = \frac{-1}{2\pi i \tau_m} \left[ \sum_{j=1}^M (R_{mj} + S_{mj}) F_j + i\sqrt{2i}\pi \frac{\tau^- - \tau_m}{1 + \sqrt{2i}\tau^-} \right] \quad (4.3.7)$$

which can be written in matrix form as

$$[A][F] = [B] \quad (4.3.8)$$

where

$$A_{mj} = R_{mj} + S_{mj} + 2\pi i \delta_{mj} \tau_m \quad (4.3.9)$$

and  $B_m = (1-i)\pi \left( \frac{\tau^- - \tau_m}{1 + \sqrt{2i}\tau^-} \right) - (R_{m1} + S_{m1})F_1 - (R_{mM} + S_{mM})F_M$ .

The  $F_j$ 's can then be determined using Gaussian elimination. With the  $F_j$ 's known, it is a simple matter to calculate  $X_m$  using equation (4.1.11). The vertical electric field just below the surface can be calculated at the mid-point between consecutive grid points by writing equation (4.1.12) as

$$G(Y_{m-\frac{1}{2}}, +0) = -\frac{1}{2} \left( \frac{X_m - X_{m-1}}{Y_m - Y_{m-1}} \right) \quad (4.3.10)$$

The total fields are again determined by adding the normal fields at  $y = -\infty$  to the corresponding anomalous fields. Here, the normal fields, in dimensionless units, are given by

$$F_n^-(0) = -\sqrt{\frac{i}{2}} \left( \frac{1}{1 + \sqrt{2i}\tau^-} \right) \quad (4.3.11)$$

$$X_n^-(+0) = \frac{1}{1 + \sqrt{2i}\tau^-} \quad (4.3.12)$$

and  $G_n^-(+0) = 0 \quad (4.3.13)$

It is interesting to note that if we had evaluated the horizontal magnetic field directly by substituting equation (3.5.14) into (3.5.13), the resulting expression would lead to an ill-conditioned matrix when high conductivity contrasts are studied.

#### 4.4 Improved boundary conditions for E-polarization

It has been shown (Weaver and Brewitt-Taylor, 1978) that

$$E_1(u, 0) \rightarrow \frac{D^\pm}{u^2} \quad (4.4.1)$$

$$\text{and } E(u, 0) \rightarrow E_n^\pm - \frac{D^\pm}{u} \quad (4.4.2)$$

as  $u \rightarrow \pm\infty$  ( $D^-, D^+$ , constants). In section 4.2, it was assumed that  $E(u, 0)$  is constant (and, thus,  $E_1(u, 0) = 0$ ) in the regions  $-\infty < u < y_1$  and  $y_M < u < \infty$ . This assumption can be greatly improved (in the above intervals) by including the information given in relations (4.4.1) and (4.4.2). In the next chapter, it will be shown that the inclusion of these modifications in our numerical technique gives much better results than our earlier assumption and considerably reduces the computer time and storage space required to determine the values of the field components in the region of interest (i.e. varying conductivity).

We begin by assuming that

$$E_1(u, 0) = \begin{cases} \frac{D^-}{u^2} & (-\infty < u \leq y_1) \\ \frac{D^+}{u^2} & (y_M \leq u < \infty) \end{cases} \quad (4.4.3)$$

and

$$E(u, 0) = \begin{cases} E_n^- - \frac{D^-}{u} & (-\infty < u \leq Y_1) \\ E_n^+ - \frac{D^+}{u} & (Y_M \leq u < \infty) \end{cases} \quad (4.4.4)$$

for  $Y_1$  and  $Y_M$  sufficiently far from the region of interest. By evaluating equation (4.4.4) at  $u = Y_1$  and  $u = Y_M$ , we immediately see that

$$D^- = Y_1 (E_n^- - E_1) \quad (4.4.5)$$

$$\text{and } D^+ = Y_M (E_n^+ - E_M) \quad (4.4.6)$$

(Note that  $E_1$  and  $E_M$  are no longer the values at  $u = \pm\infty$ .) Furthermore, we can use two-point F.D. forms to represent numerically the derivatives in equation (4.4.3) at the end grid points, giving

$$D^- = Y_1^2 \left( \frac{E_2 - E_1}{Y_2 - Y_1} \right) \quad (4.4.7)$$

$$\text{and } D^+ = Y_M^2 \left( \frac{E_M - E_{M-1}}{Y_M - Y_{M-1}} \right) \quad (4.4.8)$$

Now by substituting  $D^-$  and  $D^+$  back into equations (4.4.5) and (4.4.6) and solving for  $E_1$  and  $E_M$ , we obtain

$$E_1 = s^- E_n^- + t^- E_2 \quad (4.4.9)$$

and 
$$E_M = s^+ E_n^+ + t^+ E_{M-1} \quad (4.4.10)$$

where 
$$s^- = \frac{Y_2 - Y_1}{Y_2 - 2Y_1}, \quad t^- = \frac{Y_1}{2Y_1 - Y_2},$$

$$s^+ = \frac{Y_M - Y_{M-1}}{2Y_M - Y_{M-1}}, \quad t^+ = \frac{Y_M}{2Y_M - Y_{M-1}}.$$

Finally we can eliminate  $E_1$  and  $E_M$  from equations (4.4.5) and (4.4.6), to give

$$D^- = \left( \frac{Y_1^2}{2Y_1 - Y_2} \right) (E_n^- - E_2) \quad (4.4.11)$$

and 
$$D^+ = \left( \frac{Y_M^2}{2Y_M - Y_{M-1}} \right) (E_n^+ - E_{M-1}) \quad (4.4.12)$$

Modifications can now be made to the expressions for the horizontal magnetic field just above and below the

surface (given by equations (4.2.16) and (4.2.25)) to include the new boundary conditions. Clearly, we can write

$$\begin{aligned}
 -i\pi Y(y_m, -0) = & \sum_{j=2}^{M-1} Q_{mj} E_j + Q_{m1} E_1 + Q_{mM} E_M \\
 & + D_m^- H_m^- + D_m^+ H_m^+ \qquad (4.4.13)
 \end{aligned}$$

and

$$\begin{aligned}
 -i\pi Y(y_m, +0) = & \sum_{j=2}^{M-1} R_{mj} E_j + (R_{m1} - U_{m1}) E_1 + U_{m1} E_n^- \\
 & - D_m^- I_m^- + (R_{mM} - U_{mM}) E_M \\
 & + U_{mM} E_n^+ - D_m^+ I_m^+ \qquad (4.4.14)
 \end{aligned}$$

where  $H_m^- = \int_{-\infty}^{y_1} \frac{du}{u^2 (y_m - u)}$  ,  $H_m^+ = \int_{y_M}^{\infty} \frac{du}{u^2 (y_m - u)}$

and  $I_m^- = -\sqrt{2i} \int_{-\infty}^{y_1} \frac{P(y_m - u, +0)}{u} du$  ,

$I_m^+ = -\sqrt{2i} \int_{y_M}^{\infty} \frac{P(y_m - u, +0)}{u} du$  .

Both  $H_m^-$  and  $H_m^+$  are easily found to be

$$H_m^- = \begin{cases} -\frac{1}{Y_m} \left[ \frac{1}{Y_1} + \frac{1}{Y_m} \ln \left( 1 - \frac{Y_m}{Y_1} \right) \right] & (y_m \neq 0) \\ \frac{1}{2Y_1^2} & (y_m = 0) \end{cases} \quad (4.4.15)$$

and

$$H_m^+ = \begin{cases} \frac{1}{Y_m} \left[ \frac{1}{Y_M} + \frac{1}{Y_m} \ln \left( 1 - \frac{Y_m}{Y_M} \right) \right] & (y_m \neq 0) \\ -\frac{1}{2Y_M^2} & (y_m = 0) \end{cases} \quad (4.4.16)$$

whereas  $I_m^-$  and  $I_m^+$  are evaluated numerically and the procedure is described in detail at the end of appendix A. Now by substituting the expressions for  $D^-$ ,  $D^+$ ,  $E_1$  and  $E_M$  in equations (4.4.9) through (4.4.12) into equations (4.4.13) and (4.4.14), we can define new coefficients  $\tilde{Q}_{mj}$  and  $\tilde{R}_{mj}$  such that

$$-i\pi Y(y_m, -0) = \sum_{j=2}^{M-1} \tilde{Q}_{mj} E_j + \tilde{Q}_{m1} E_n^- + Q_{mM} E_n^+ \quad (4.4.17)$$

where

$$\tilde{Q}_{mj} = \begin{cases} s^- Q_{m1} + y_1 t^- H_m^- & (j=1) \\ Q_{m2} + t^- (Q_{m1} - y_1 H_m^-) & (j=2) \\ Q_{mj} & (3 \leq j \leq M-2) \\ Q_{mM-1} + t^+ (Q_{mM} - y_M H_m^+) & (j=M-1) \\ s^+ Q_{mM} + y_M t^+ H_m^+ & (j=M) \end{cases}$$

and

$$i\pi Y(y_m, +0) = \sum_{j=2}^{M-1} \tilde{R}_{mj} E_j + \tilde{R}_{m1} E_n^- + \tilde{R}_{mM} E_n^+ \quad (4.4.18)$$

where

$$\tilde{R}_{mj} = \begin{cases} U_{m1} + s^- (R_{m1} - U_{m1}) - y_1 t^- I_m^- & (j=1) \\ R_{m2} + t^- (R_{m1} - U_{m1} + y_1 I_m^-) & (j=2) \\ R_{mj} & (3 \leq j \leq M-2) \\ R_{mM} + t^+ (R_{mM} - U_{mM} + y_M I_m^+) & (j=M-1) \\ U_{mM} + s^+ (R_{mM} - U_{mM}) - y_M t^+ I_m^+ & (j=M) \end{cases}$$

(Note that we still have  $M-2$  equations in  $M-2$  unknowns as in section 4.2.)

CHAPTER 5

RESULTS AND DISCUSSION

5.1 Introductory remarks

Following the notation of the previous chapter, we define the dimensionless form of the total fields (indicated by primes) as

$$\bar{E}'_t = \frac{\bar{E}_t}{\omega \delta B_0}$$

and 
$$\bar{B}'_t = \frac{\bar{B}_t}{B_0}$$

where  $B_0 = Y_0$  in E-polarization and  $B_0 = X_0$  in B-polarization. Furthermore, in this chapter, we denote the total fields just below and above the surface by superscripts as

$$A_t^{\pm} \equiv A(y, \pm 0)$$

where  $A_t$  represents  $X_t$ ,  $Y_t$ , or  $G_t$ . We also recall, from section 4.1, that the dimensionless grid points and integrated conductivity are given by

$$y' = \frac{y}{\delta}$$

and 
$$\tau' = \frac{\tau}{\sigma \delta} = \sqrt{\frac{\pi \mu_0 f}{\sigma}} \tau \quad (5.1.1)$$

By taking a quick glance at equation (4.2.17), (4.2.26), (4.3.5) and the appropriate terms in appendix A, we find that the integral coefficients  $Q_{mj}$ ,  $R_{mj}$  and  $S_{mj}$  are dependent only on the set of dimensionless grid points. Hence, these coefficients need be calculated only once for each grid and stored for future use. From equations (4.2.29) and (4.3.9), we also know that the matrix of coefficients  $A_{mj}$  and  $B_m$ , and consequently, the resulting field values, are known entirely in terms of the above integral coefficients, the dimensionless values of the integrated conductivity and the given boundary values. Thus we immediately see that a given set of dimensionless field results may be scaled to represent the field values for various conductivity structures and source frequencies since, for a given  $\tau'$ , the model parameters  $f$ ,  $\sigma$ , and  $\tau$  may be varied in accordance with equation (5.1.1). We must remember, though, that the limitations imposed by the thin sheet approximation somewhat restrict the choice of values for the model parameters.

5.2 Demonstration of the effectiveness of the improved boundary condition for E-polarization problems

The effect of the improved E-polarization boundary condition, discussed in section 4.4, can be seen by setting up a 75 point grid (-8.5 + 8.5) and then comparing results obtained from the full grid with results obtained from a 45 point subset of this grid (-2.5 to 2.5). To illustrate this effect, a model is chosen in which the integrated conductivity is

$$\tau' = \tau/\sigma\delta = \begin{cases} 10^4 & (y' < 0) \\ 0 & (y' > 0) \end{cases}$$

and the grid (symmetrical about  $y' = 0$ ) is

$$y' = y/\delta = \begin{cases} 0, .05, .1, .15, .2, .25, .3, .35, .4, .45, .5, .6, .7, \\ .8, .9, 1, 1.2, 1.4, 1.6, 1.8, 2, 2.25, 2.5, 2.75, 3, \\ 3.25, 3.5, 3.75, 4, 4.5, 5, 5.5, 6, 6.5, 7, 7.5, 8, 8.5 \end{cases} .$$

The values for the field components at some discrete points are given in Table 5.1. As expected, the field values, determined with or without the correction, are almost identical when the full grid is used. With the correction term applied to the partial grid, the agreement is still very good whereas, without the correction, the values are considerably different. The largest relative differences

TABLE 5.1

A comparison of field values, showing the effect of the improved boundary conditions for E-polarization problems.

\* × 10<sup>-4</sup>

	y/δ	FULL GRID WITH CORRECTION		FULL GRID WITHOUT CORRECTION		PARTIAL GRID WITH CORRECTION		PARTIAL GRID WITHOUT CORRECTION	
		Real	Imag	Real	Imag	Real	Imag	Real	Imag
$\frac{E}{E_0}$	-2.0	.533 *	-.028 *	.533 *	-.028 *	.533 *	-.027 *	.532 *	-.029 *
	-1.0	.559 *	-.058 *	.559 *	-.058 *	.559 *	-.058 *	.553 *	-.061 *
	-0.5	.622 *	-.116 *	.622 *	-.116 *	.622 *	-.115 *	.619 *	-.119 *
	-0.1	1.017 *	-.347 *	1.016 *	-.347 *	1.018 *	-.345 *	1.008 *	-.355 *
	-0.05	1.316 *	-.491 *	1.316 *	-.492 *	1.317 *	-.489 *	1.303 *	-.502 *
	0.0	4.995 *	-1.996 *	4.983 *	-1.998 *	4.990 *	-1.986 *	4.931 *	-2.044 *
	0.05	.0515	.1210	.0516	.1210	.0513	.1212	.0527	.1197
	0.1	.0777	.1781	.0778	.1780	.0774	.1783	.0796	.1760
	0.5	.1962	.3728	.1963	.3726	.1953	.3734	.2010	.3672
	1.0	.2867	.4595	.2869	.4592	.2852	.4604	.2960	.4502
	2.0	.3880	.5054	.3883	.5050	.3837	.5063	.4204	.4502
$\frac{I}{I_0}$	-2.0	1.070	-.0546	1.070	-.0550	1.070	-.0539	1.069	-.0579
	-1.0	1.126	-.0909	1.126	-.0914	1.127	-.0899	1.125	-.0964
	-0.5	1.219	-.1443	1.219	-.1449	1.219	-.1429	1.216	-.1521
	-0.1	1.651	-.3583	1.651	-.3591	1.652	-.3557	1.642	-.3726
	-0.05	1.957	-.4988	1.957	-.4997	1.958	-.4955	1.944	-.5166
	0.0	3.140	1.000	3.139	-1.002	3.142	-.9946	3.113	-1.031
	0.05	.656	.0061	.656	.0057	.656	.0072	.656	-.0008
	0.1	.664	.0133	.664	.0130	.664	.0144	.664	.0064
	0.5	.726	.0578	.726	.0574	.726	.0592	.728	.0481
	1.0	.794	.0841	.794	.0836	.793	.0860	.798	.0767
	2.0	.887	.0859	.887	.0853	.884	.0886	.902	.0651
$\frac{E}{E_0}$	-1.9	-.015 *	-.014 *	-.015 *	-.014 *	-.015 *	-.014 *	-.016 *	-.013 *
	-1.1	-.053 *	-.047 *	-.053 *	-.047 *	-.053 *	-.047 *	-.054 *	-.046 *
	-0.55	-.177 *	-.215 *	-.177 *	-.215 *	-.176 *	-.216 *	-.180 *	-.211 *
	-0.025	-.003	-.007	-.003	-.007	-.003	-.007	-.003	-.007
	0.025	2.425	-1.021	2.424	-1.022	2.428	-1.016	2.399	-1.045
	0.55	.247	-.213	.246	-.213	.247	-.212	.239	-.220
	1.1	.087	-.136	.087	-.136	.088	-.134	.080	-.148
	1.9	.017	-.072	.016	-.072	.016	-.068	.014	-.110

are noted in the imaginary components.

In order not to waste computer time and storage space, the improved boundary condition is used in all of the following E-polarization calculations.

### 5.3 Comparison with other work

In this section, results obtained by the method described in this thesis are compared with those calculated by other authors for the particular model of an infinitely conducting half-sheet, i.e.

$$\tau' = \begin{cases} \infty & (y' < 0) \\ 0 & (y' > 0) \end{cases}$$

covering a conducting half-space. In determining our results for both polarizations, we have approximated  $\tau' = \infty$  by  $\tau' = 10^{12}$  and used the following 75 point grid (symmetrical about  $y' = 0$ )

$$y' = \begin{cases} .0, .01, .02, .04, .06, .08, .1, .125, .15, .175, .2, .25, .3, \\ .35, .4, .45, .5, .6, .7, .8, .9, 1, 1.2, 1.4, 1.6, 1.8, 2.0, \\ 2.2, 2.4, 2.6, 2.8, 3.0, 3.2, 3.4, 3.6, 3.8, 4, 4.2 \end{cases}$$

Fischer et al. (1978a,1978b) have obtained the solution for this particular model in the E-polarization case, by incorporating directly into the theory the fact that the horizontal electric field must be zero at the surface of the infinitely conducting half-sheet. They solved their integral equation (which can be shown to be a special case of our equation (3.4.52)) numerically by assuming the electric field is constant between each grid point and by using an evenly-spaced grid. Initially, they used

90 grid points between 0 and 9. Then, to improve the resolution in the vicinity of the origin, the field values were recalculated using 80 grid points between 0 and 2. (The advantages of incorporating uneven grid spacing and the improved boundary conditions into the theory as we have done can be seen immediately.) On comparing our results with those of Fischer et al., we see from figures 5.1 and 5.3 that the real and imaginary parts of the horizontal electric field and the vertical magnetic field agree well. The real and imaginary parts of the horizontal magnetic field also agree well for  $y' < 0$  but quite different results are obtained for  $y' > 0$  (see figure 5.2). At the interface ( $y' = 0$ ), we find that the real and imaginary parts of the horizontal magnetic field are discontinuous, diverging as  $y' \rightarrow 0$  and smoothly approaching the finite values, .65 and 0, as  $y' \rightarrow +0$ . Fischer et al. suggest a different value of -1.14 for the real part of the magnetic field at  $y' = +0$ . To help resolve this discrepancy, we note that Weidelt (1971) obtained an analytical solution to a similar problem by using the Weiner-Hopf technique. (He considered a model having an infinitely conducting half-sheet separated from an infinitely conducting sheet by a non-conducting region.) In his paper (Weidelt, 1971, fig. 6),

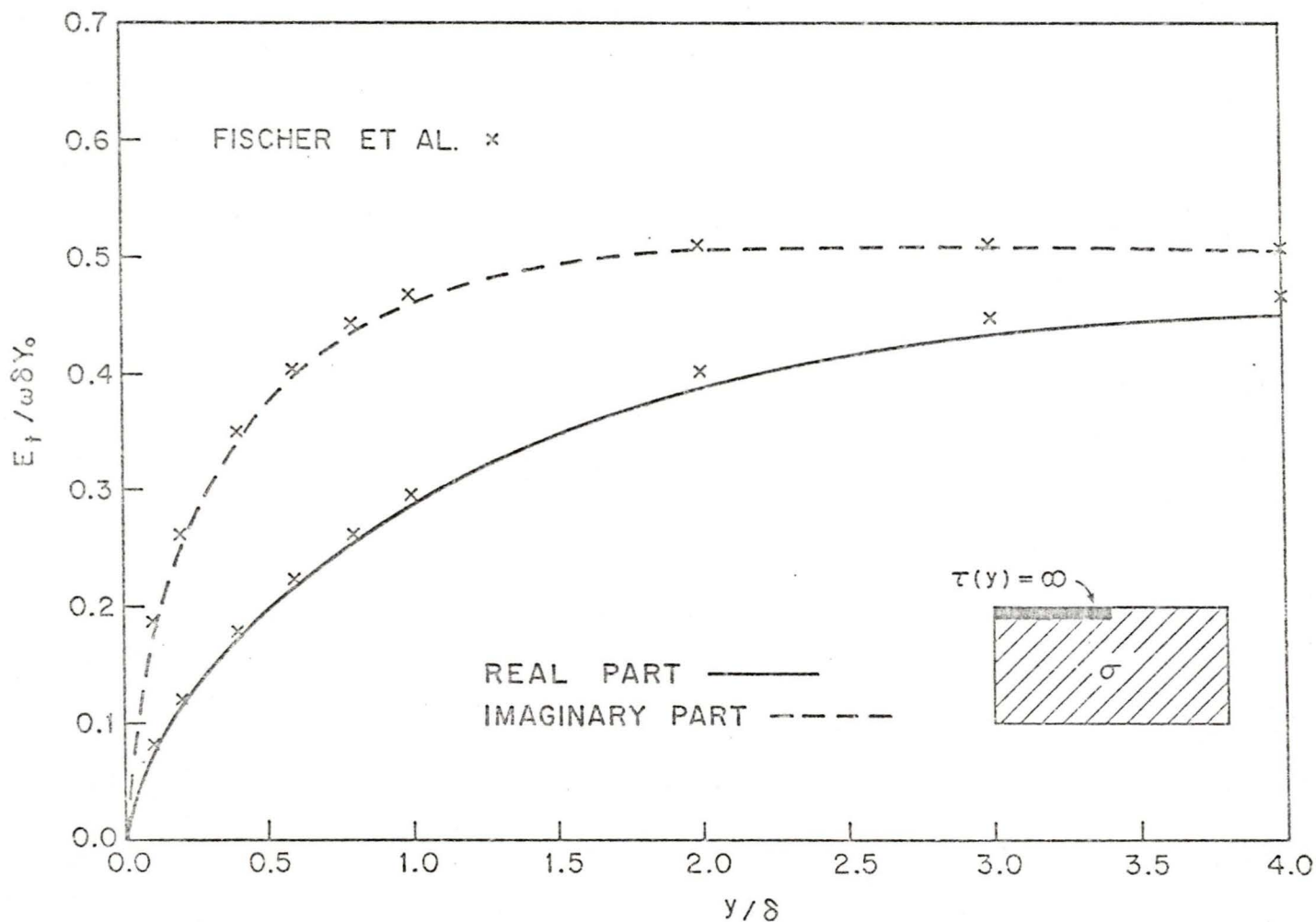


Figure 5.1 The real and imaginary parts of the horizontal electric field ( $z=0$ ) for a perfectly conducting thin sheet ( $z=0, y < 0$ ) covering a conducting half-space shown in the diagram (E-polarization). (Results are compared with those of Fischer et al. (1978b).)

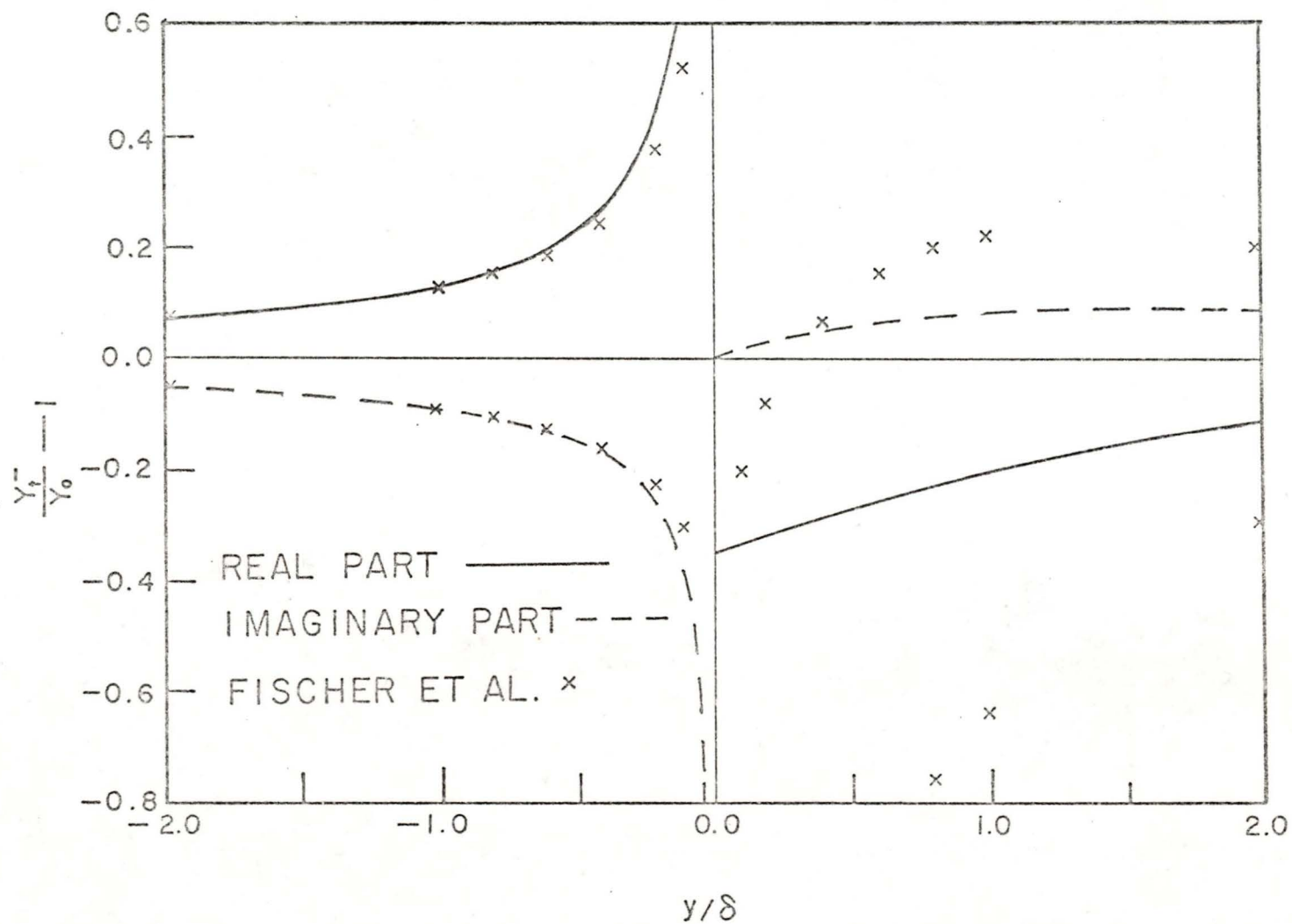


Figure 5.2 The real and imaginary parts of the horizontal magnetic field ( $z = -0$ ) for the model shown in Figure 5.1 (E-polarization). (Results are compared with those of Fischer et al. (1978b).)

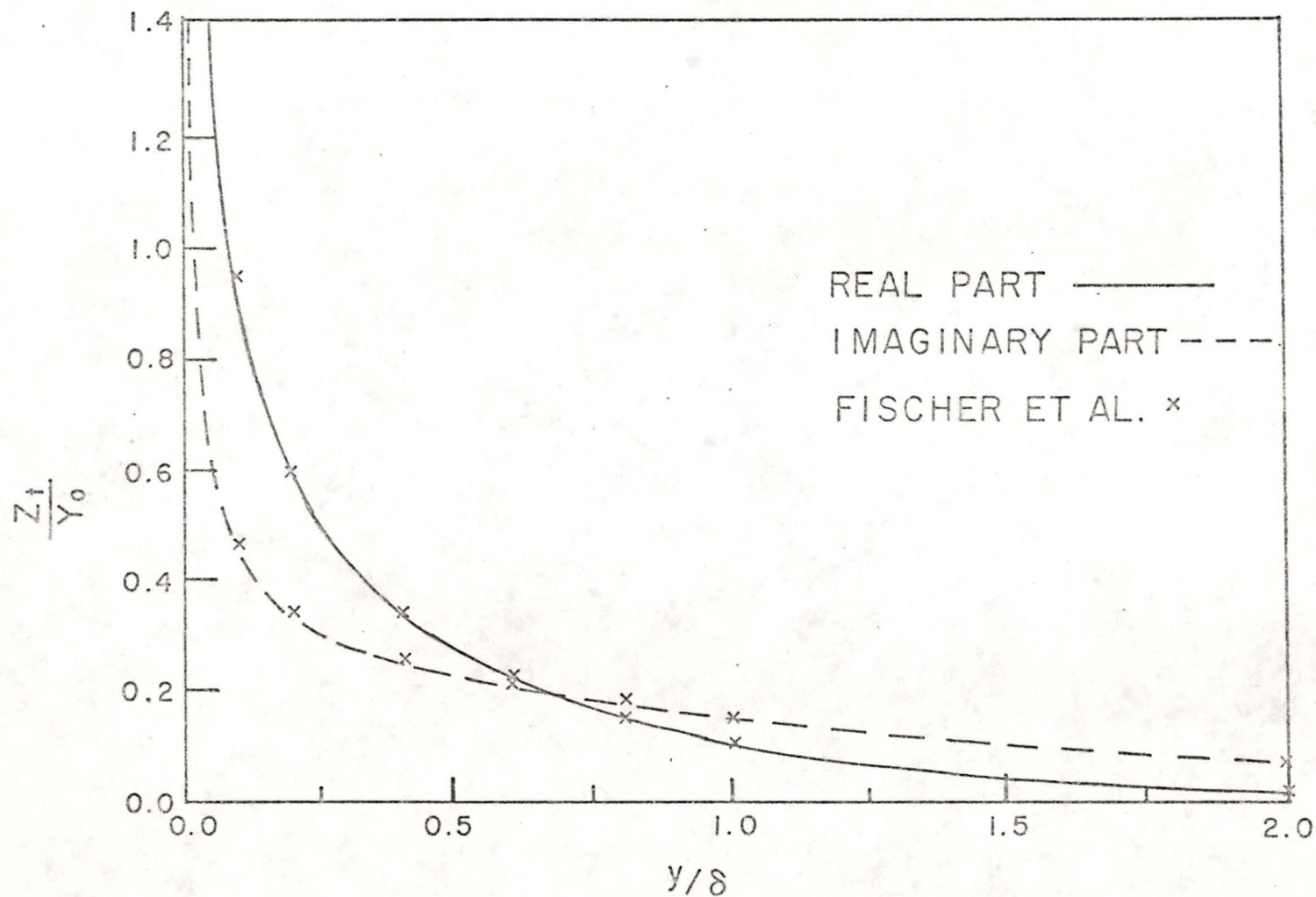


Figure 5.3 The real and imaginary parts of the vertical magnetic field ( $z = 0$ ) for the model shown in Figure 5.1 (E-polarization). (Results are compared with those of Fischer et al. (1978b).)

we find, at  $y' = +0$ , that

$$\frac{H_{xi} - H_o}{H_o} \approx -.67 \quad (5.3.1)$$

where  $H_o$  denotes the uniform external magnetic field and  $H_{xi}$  denotes the internal horizontal magnetic field and also that total horizontal field  $H_x$ , is given by

$$H_x = H_{xi} + H_o .$$

Hence, we obtain  $H_x(\pm\infty, 0) = 2H_o$  since  $H_{xi}(\pm\infty, 0) = H_o$ .

Clearly, equation (5.3.1) becomes

$$\frac{H_x(+0, 0)}{2H_o} \approx .67$$

which compares directly with our result of

$$\frac{Y_t(+0, -0)}{Y_o} \approx .65 .$$

This leads us to believe that our results for the horizontal magnetic field for  $y' > 0$  are indeed reasonable. As a further check on our numerical procedure, work is continuing at the University of Victoria to solve the problem of E-polarization and B-polarization induction in two half-sheets of finite

integrated conductivity covering a conducting half-space.

From figures 5.4, 5.5, and 5.6, all field component values, in the B-polarization case, agree well with field values obtained by Nicoll and Weaver (1977) whose analytical solution was determined by applying the Weiner-Hopf technique to the problem.

Later, in section 5.5, we also compare our results with those determined by a finite difference method and obtain excellent agreement. This gives additional verification of the validity of our numerical scheme.

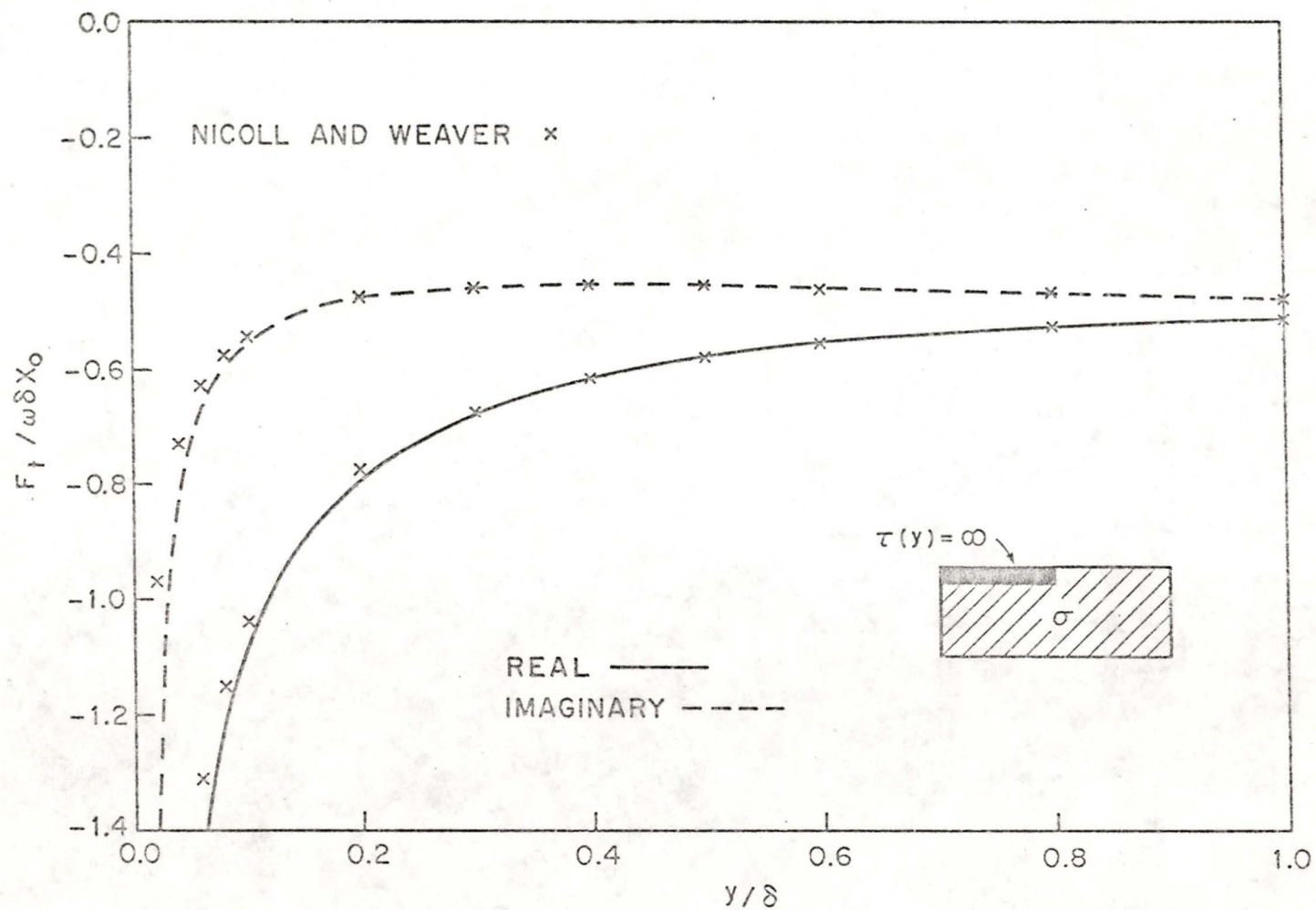


Figure 5.4 The real and imaginary parts of the horizontal electric field ( $z = 0$ ) for a perfectly conducting thin sheet ( $z = 0, y < 0$ ) covering a conducting half-space shown in the diagram (B-polarization). (Results are compared with those of Nicoll and Weaver (1977).)

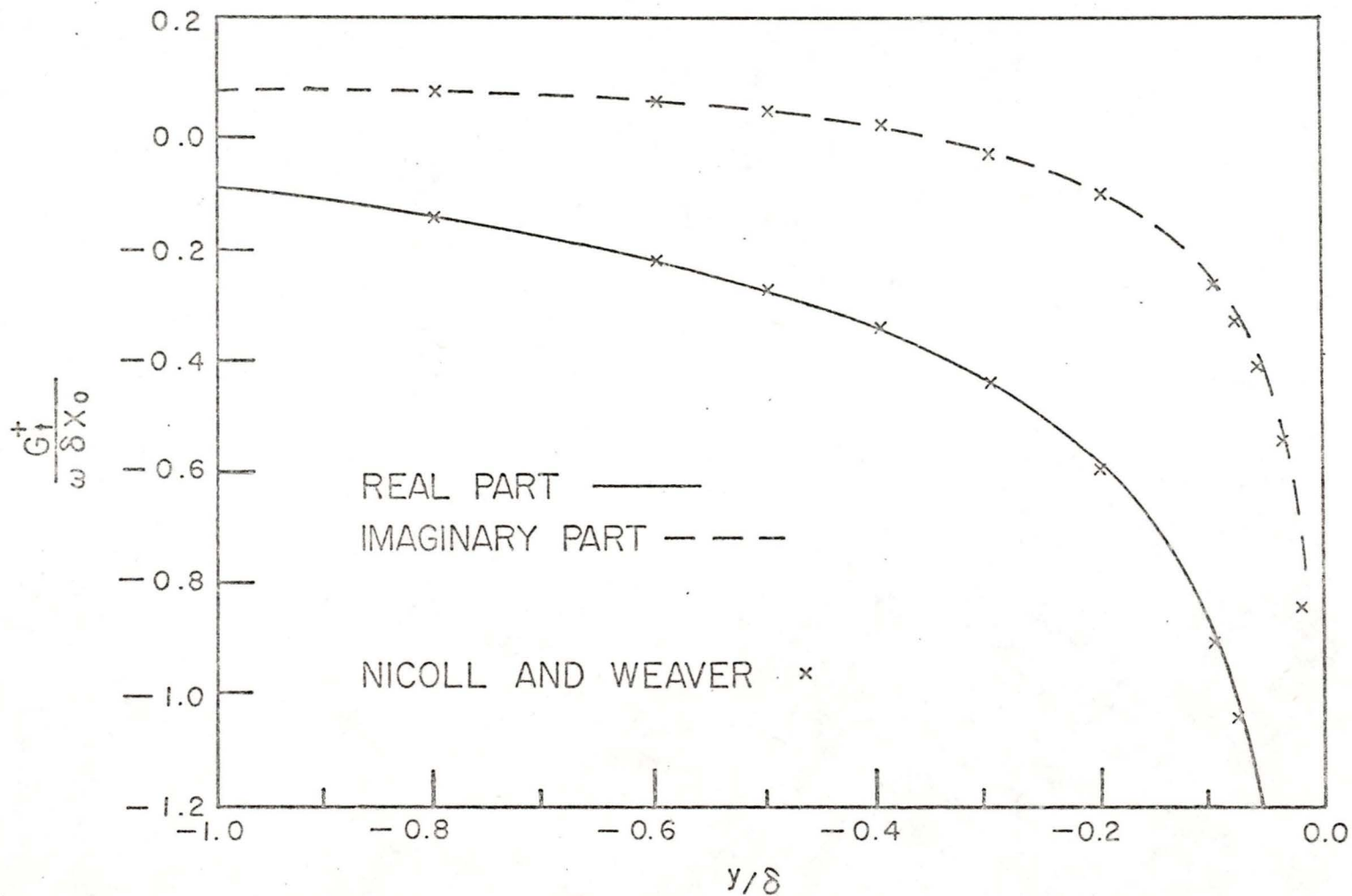


Figure 5.5 The real and imaginary parts of the vertical electric field ( $z=+0$ ) for the model shown in Figure 5.4 (B-polarization). (Results are compared with those of Nicoll and Weaver (1977).)

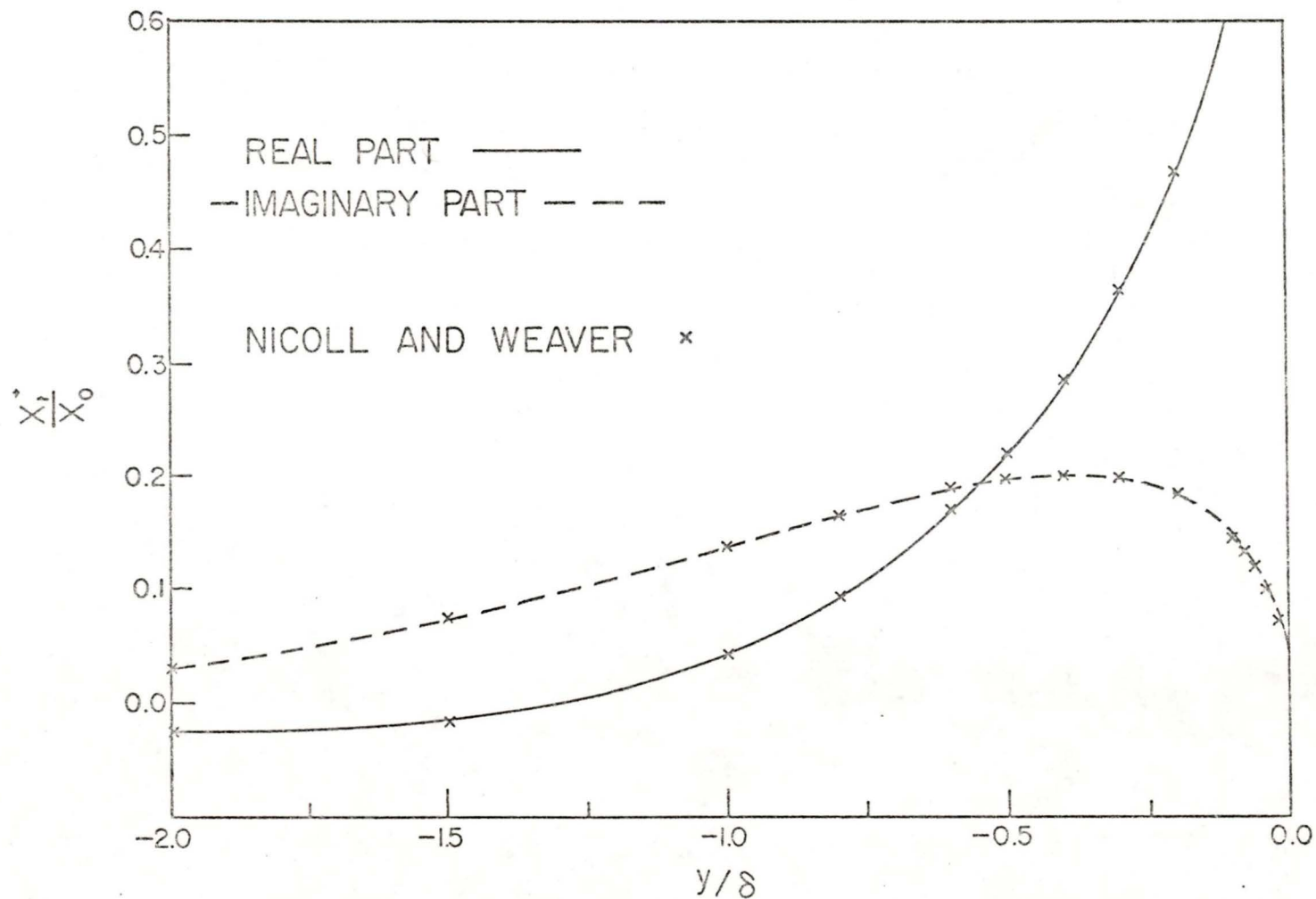


Figure 5.6 The real and imaginary parts of the horizontal magnetic field ( $z=+0$ ) for the model shown in Figure 5.4 (B-polarization). (Results are compared with those of Nicoll and Weaver (1977).)

#### 5.4 Comparison of abrupt and gradual changes in integrated conductivity

In this section, two similar models are considered in which  $\tau'$  changes from  $2\pi$  to  $\pi$ . In the first model,  $\tau'$  changes abruptly at  $y' = 0$  while, in the second model,  $\tau'$  changes smoothly over one-half skin-depth (see figures 5.7 through 5.13).

For the E-polarization case, with an abrupt change in  $\tau'$ , the real component of the vertical magnetic field diverges as the interface is approached while the real part of the horizontal magnetic field jumps discontinuously at the interface. The remaining E-polarization components are continuous in this region. As in section 5.3, this is consistent with results obtained by Weidelt (1971, figure 2) for a similar model of two half-sheets having integrated conductivities  $\tau_1 = 1$  and  $\tau_2 = 4$ , respectively, overlying a non-conducting region.

Similarly in B-polarization, for an abrupt change in  $\tau'$ , the real part of the vertical electric field diverges as  $y' \rightarrow 0$  and the real part of the horizontal electric field jumps discontinuously at  $y' = 0$ , while the remaining field components are continuous in the region.

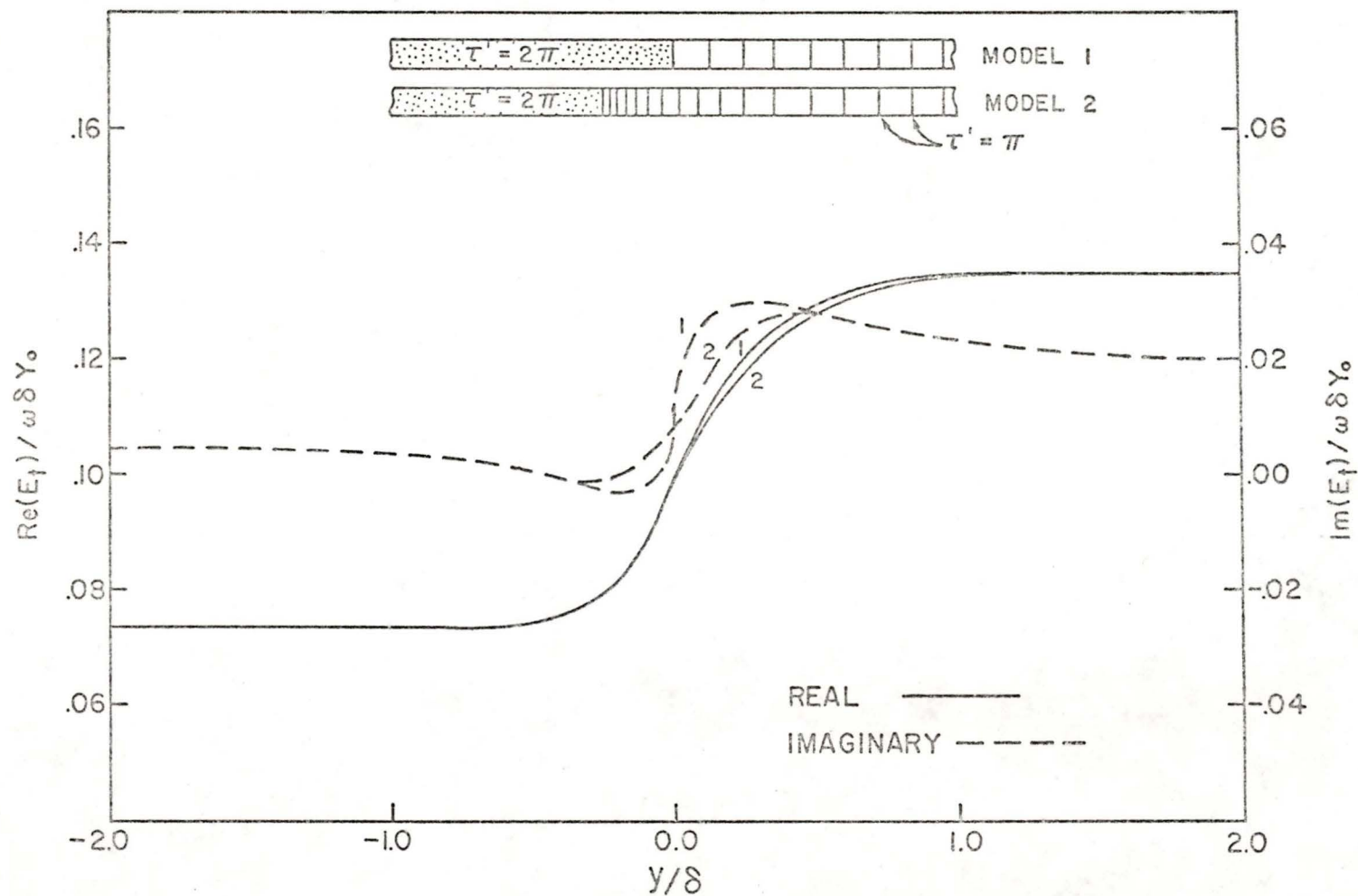


Figure 5.7 The effect of abrupt and gradual changes in integrated conductivity on the horizontal electric field at the surface (E-polarization).

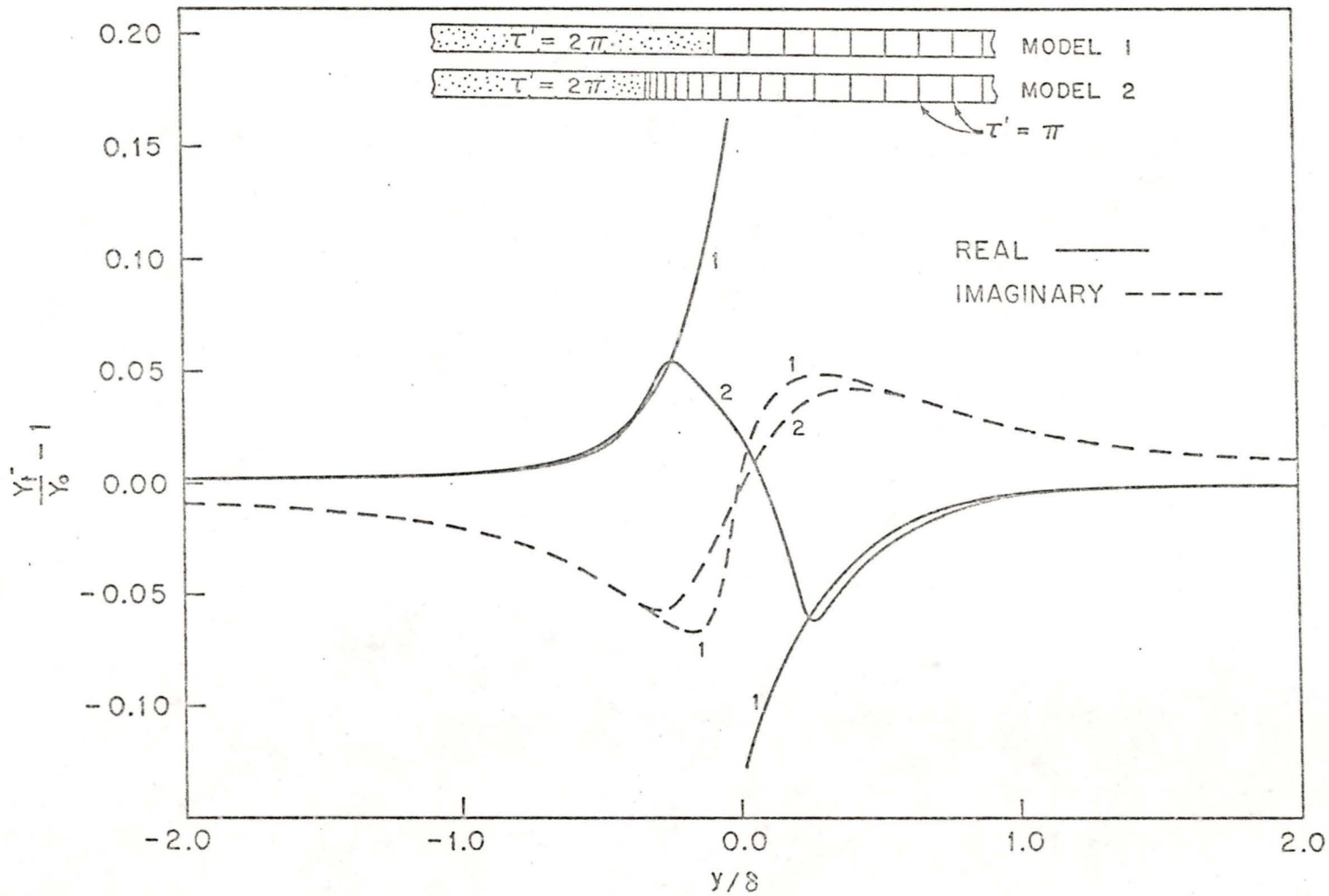


Figure 5.8 The effect of abrupt and gradual changes in integrated conductivity on the horizontal magnetic field at the surface (E-polarization).

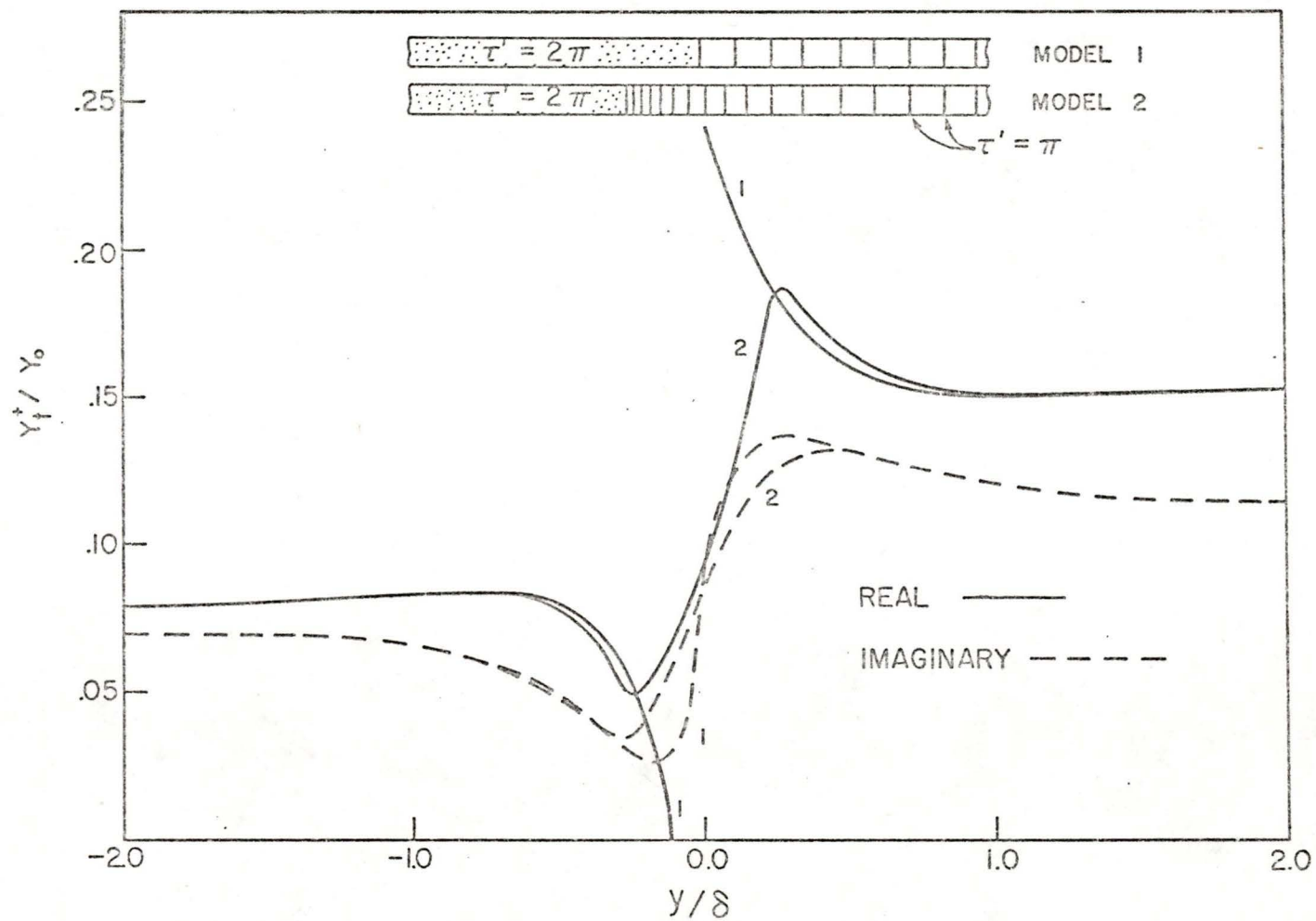


Figure 5.9 The effect of abrupt and gradual changes in integrated conductivity on the horizontal magnetic field just below the infinitely thin sheet (E-polarization).

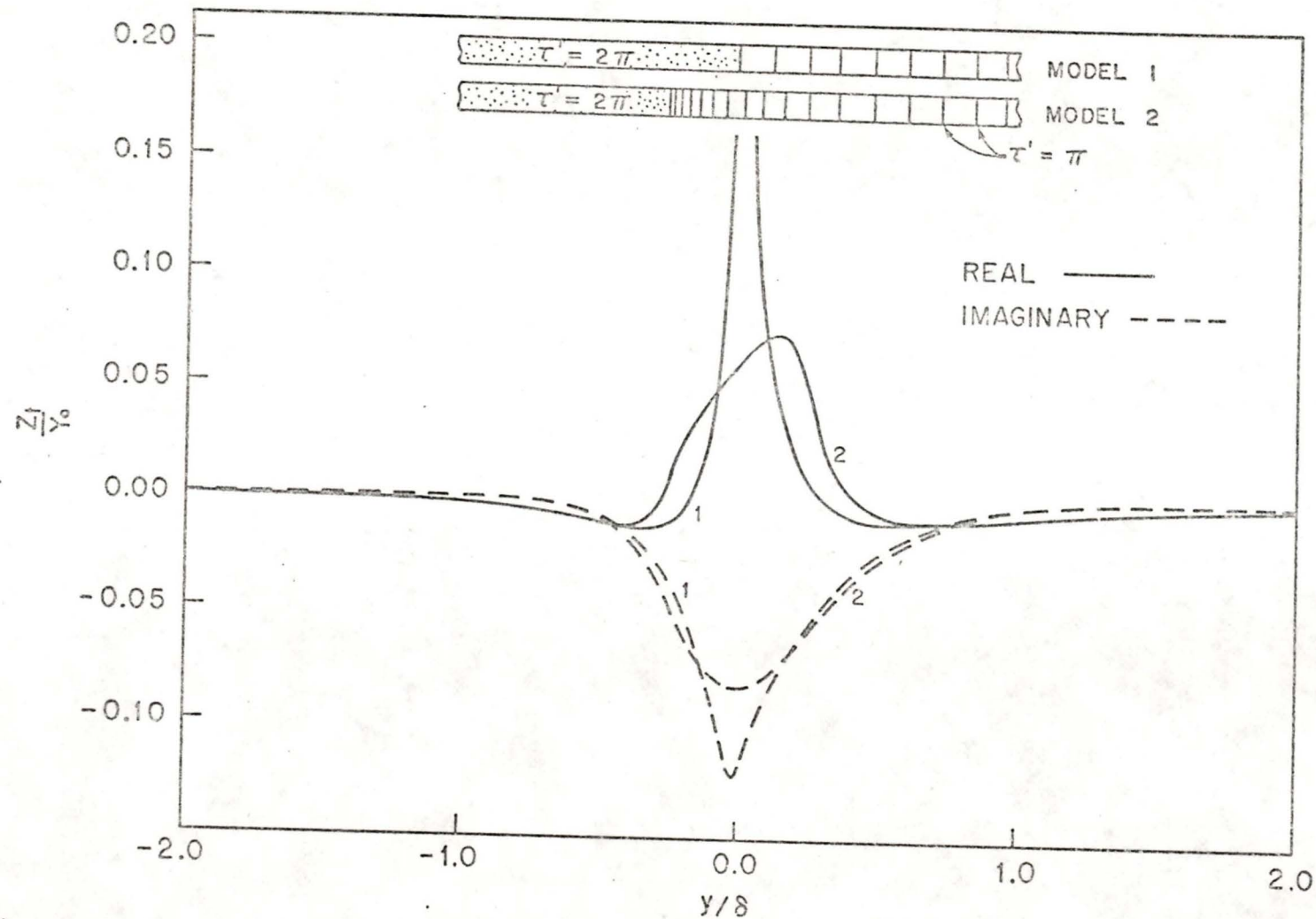


Figure 5.10 The effect of abrupt and gradual changes in integrated conductivity on the vertical magnetic field at the surface (E-polarization).

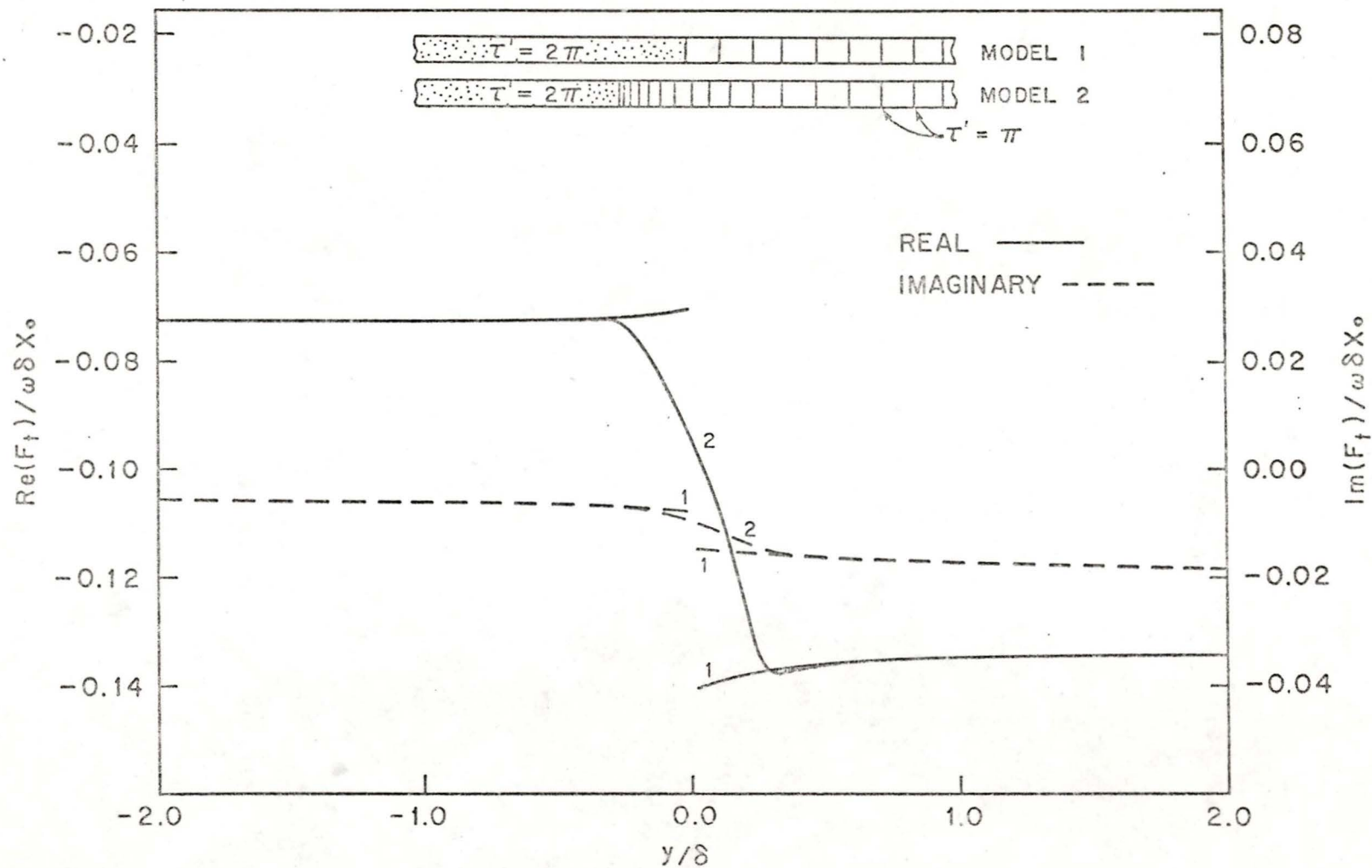


Figure 5.11 The effect of abrupt and gradual changes in integrated conductivity on the horizontal electric field at the surface (B-polarization).

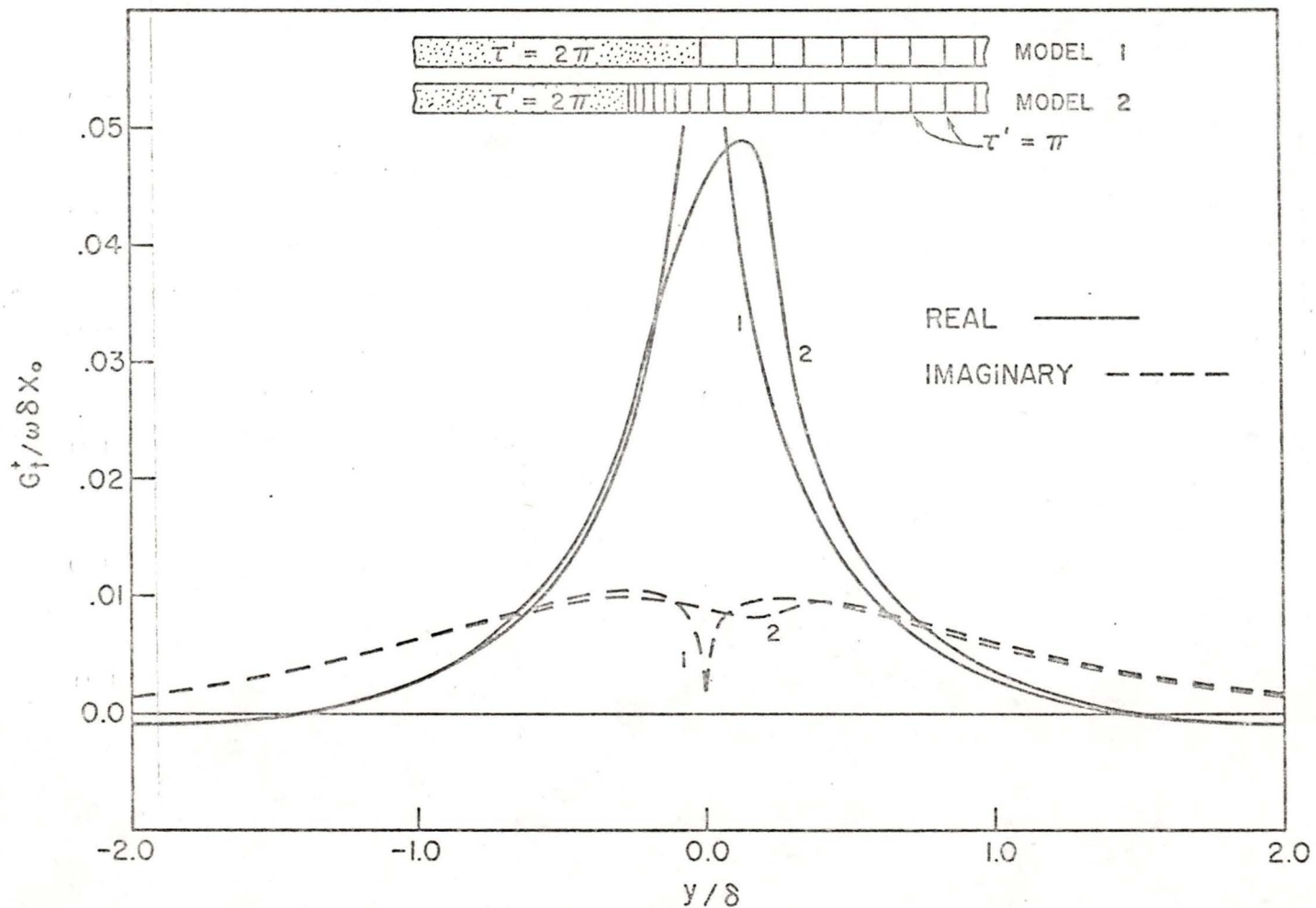


Figure 5.12 The effect of abrupt and gradual changes in integrated conductivity on the vertical electric field just below the infinitely thin sheet (B-polarization).

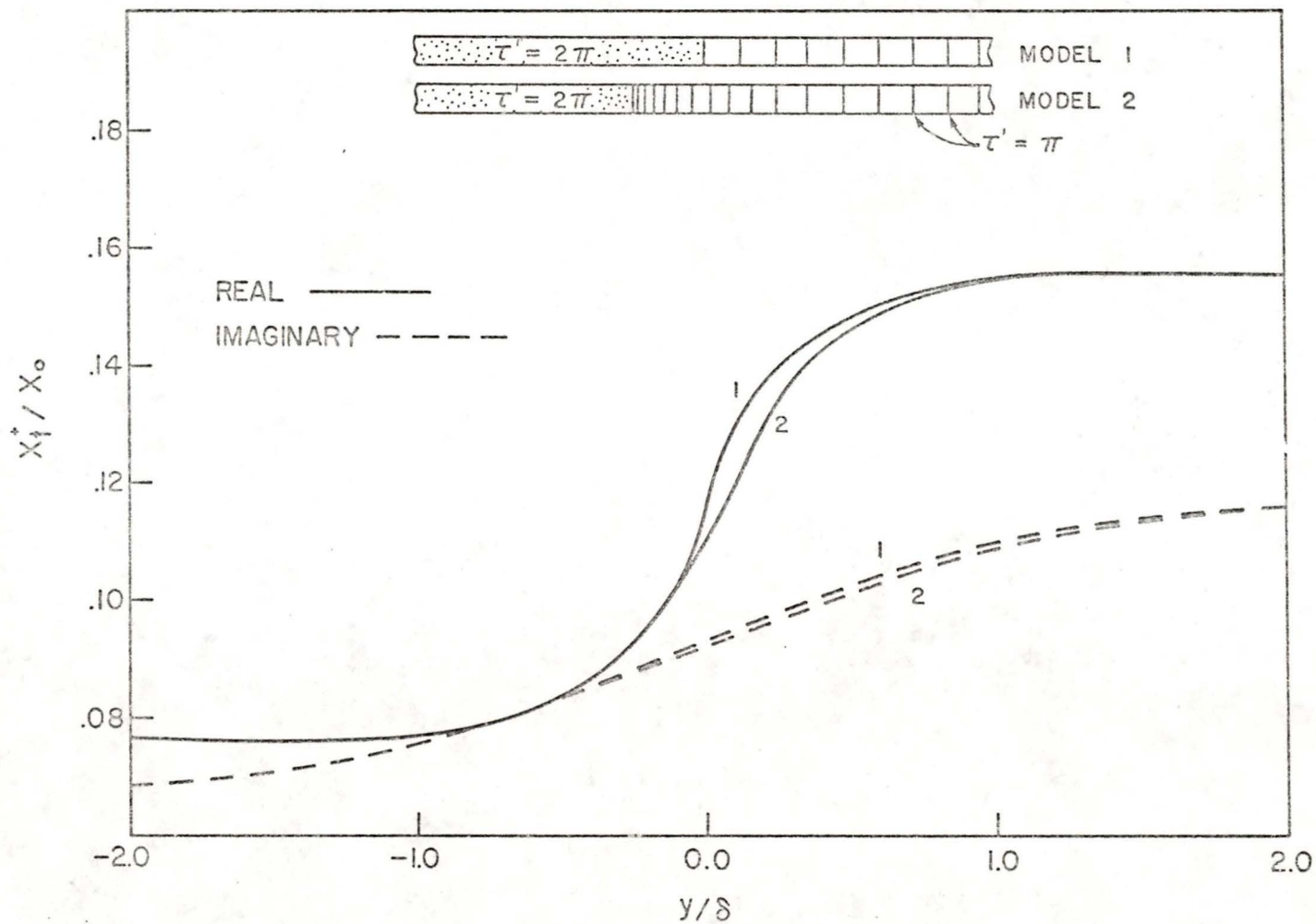


Figure 5.13 The effect of abrupt and gradual changes in integrated conductivity on the horizontal magnetic field just below the infinitely thin sheet (B-polarization).

When  $\tau'$  changes smoothly from one value to the other, all field components remain continuous, in both polarizations, while crossing the zone of varying integrated conductivity (see Ashour, 1971). It is important to notice, with this model, that the peaks in the field components have shifted away from  $y' = 0$ . This indicates that for realistic results the sloping continental shelf should be modelled more closely than by an abrupt change in conductivity. In the next section, a coast model, which includes a continental slope, is considered.

### 5.5 Vancouver Island Model

As a final illustration of the method developed in this thesis, we consider a two-dimensional E-polarization model roughly representing a cross-section through Vancouver Island which includes the continental slope, the continental shelf and the inner strait between the island and the mainland.

We have compared our results for the amplitude of the horizontal and vertical magnetic fields at the surface with results obtained using the finite-difference formulation of Brewitt-Taylor and Weaver (1976). As seen in figure 5.14, the agreement is excellent. It is interesting to note that the computer time required to determine the fields at the surface using their numerical procedure (with a 59 point surface grid by 40 point vertical grid) is approximately 15 minutes compared to about 1 minute using our method for the same 59 point surface grid. Also, extra disk space must be used in their method.

From our results, for the frequency of 1 cph ( $\sim .3$  mHz), there are minima in the vertical field at the island coastline facing the continent and just off the island coastline facing the ocean. There are maxima at the continental coastline and the island coastline facing the deep ocean with the main maximum occurring well out over the continental slope. Slight

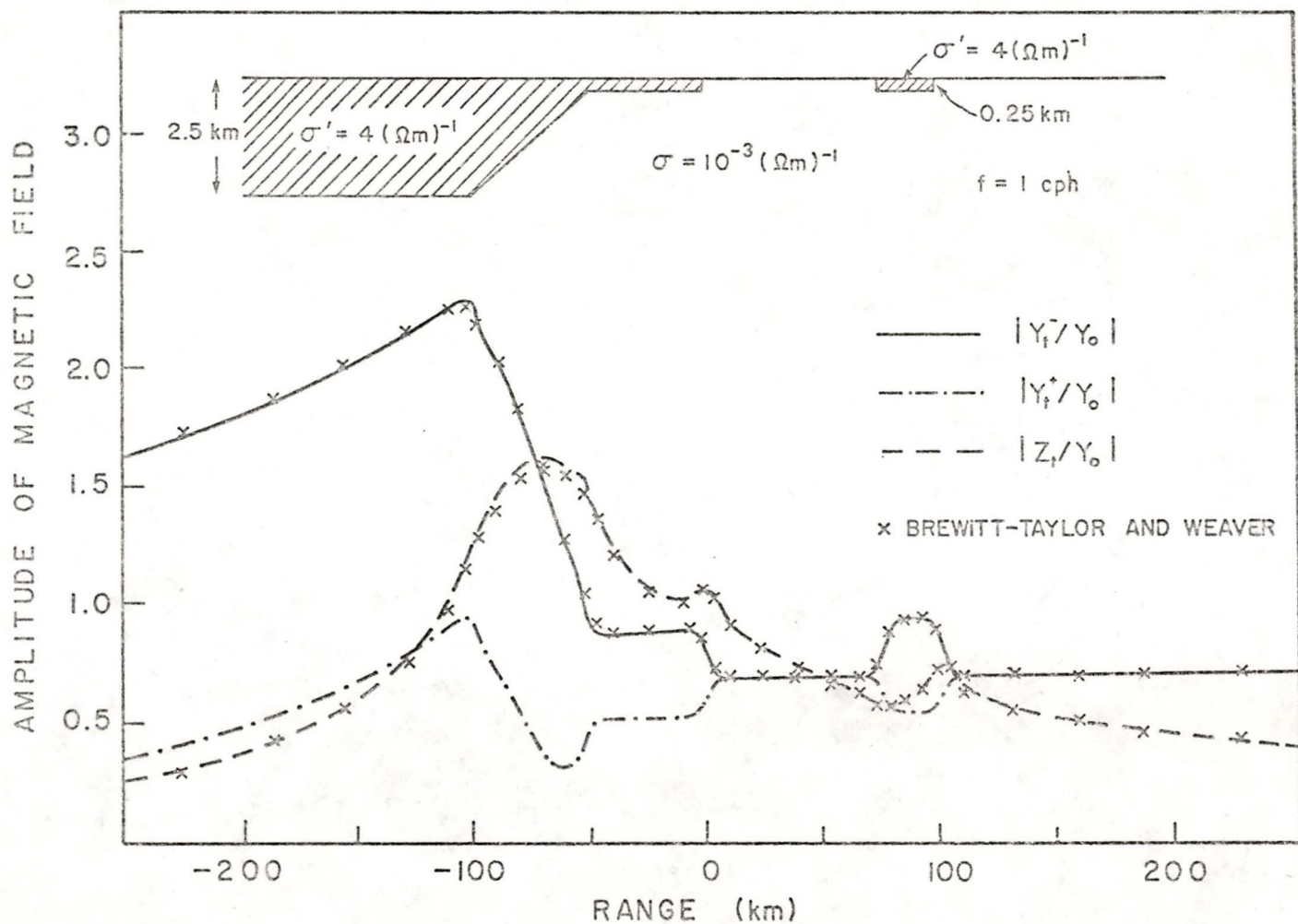


Figure 5.14 Amplitudes of the horizontal magnetic field at the surface and below the ocean and the vertical magnetic field at the surface for the model of Vancouver Island (E-polarization).

enhancements of the field also occur at the beginning and end of the continental slope. The amplitude of the surface horizontal field decreases considerably from a maximum obtained where the deep ocean first meets the continental slope and then clearly distinguishes the continental shelf by a levelling off of the field followed by an abrupt change at the coastline. The island and strait are similarly distinguished by a levelling off of the field and abrupt changes at the edges. The horizontal magnetic field at the ocean bottom has a maximum at the point where the deep ocean meets the continental slope and has a minimum just before reaching the continental shelf. Along the continental shelf and at the bottom of the strait, the field roughly behaves like a mirror image of the surface field.

In the region of the continental slope and shelf, we see that the fields are quite perturbed at this frequency. Thus, when trying to infer information about the conductivity structure of the Earth in this region, we conclude that field measurements should be taken either at the surface or bottom of the ocean as well as over the land.

## 5.6 Summary and future work

In this thesis, a method for studying problems of electromagnetic induction in two-dimensional conductivity anomalies confined to near the Earth's surface has been developed using the thin sheet approximation. Both E-polarization and B-polarization cases have been considered.

A number of important features have been included in the numerical evaluation of the integral equations used to determine the field values. In particular, the electric field is approximated by a quadratic function near the singularity and by a linear function between consecutive grid points elsewhere. Also, even or uneven grid-spacing may be used. Furthermore, the integrated conductivity may vary over a limited range along the y-axis and may have different values at the extreme ends of the model. Its value at a grid point is determined by a weighted average of the conductivity in the two adjoining regions. Additionally, the fact that the horizontal electric field along the surface,  $E(u,0)$ , far from the region of varying conductivity, dies off as  $1/u$  has been incorporated into the procedure.

In section 5.3, it has been shown that the accuracy of our results is excellent when compared to the analytical solution of Nicoll and Weaver (1977) (B-polarization

case) but that some differences do occur when comparing our results with those of Fischer et al. (1978a,1978b) (E-polarization case). However, the similarity between our results and those obtained by Weidelt (1971) analytically leads us to conclude that our calculations are indeed accurate. For the complex model of Vancouver Island (E-polarization case), our results have also been compared with those obtained by the finite-difference formulation of Brewitt-Taylor and Weaver (1976) which requires much more computer time and storage space than our method. The excellent agreement between the results obtained by these two different approaches is further verification of the validity of our procedure. Moreover, the considerable saving in computer time and storage space provides one of the main reasons for developing the theory using the thin sheet approximation.

It has been mentioned previously that work is in progress to determine analytical solutions to some geometrically simple thin sheet models (using the Weiner-Hopf technique) in order to provide further checks on our numerical procedure. Work is also being done to extend the two-dimensional theory to include a layered half-space in the present model. As a final comment, it should be pointed out that a two-dimensional model

can not be used to study the additional effect of channelling of electric currents around an island. The extension of this theory to analyse problems in three-dimensions would give a mathematical technique for studying this 'channelling effect' which would be more practical, in terms of computer time and storage space, than a finite-difference formulation. The extension to three-dimensions is presently being developed.

REFERENCES

- Abramowitz, M., and Stegun, I.A., 1964. Handbook of Mathematical Functions. U.S. Government Printing Office, Washington.
- Ashour, A.A., 1971. Electromagnetic induction in thin finite sheets having conductivity decreasing to zero at the edge, with geomagnetic applications - I. *Geophys. J. R. astr. Soc.*, 22, 417-443.
- Ashour, A.A., 1973. Theoretical models for electromagnetic induction in the oceans. *Phys. Earth Planet. Inter.*, 7, 303-312.
- Ashour, A.A., and Chapman, S., 1965. The magnetic field of electric currents in an unbounded plane sheet, uniform except for a circular area of different uniform conductivity. *Geophys. J.*, 10, 31-44.
- Bailey, R.C., 1977. Electromagnetic induction over the edge of a perfectly conducting ocean: the H-polarization case. *Geophys. J. R. astr. Soc.*, 48, 385-392.
- Brewitt-Taylor, C.R., 1975. A model for the coast-effect. *Phys. Earth Planet. Inter.*, 10, 151-158.
- Brewitt-Taylor, C.R., 1976. A model for the coast-effect - further results. *Phys. Earth Planet. Inter.*, 13, 9-14.
- Brewitt-Taylor, C.R., and Weaver, J.T., 1976. On the finite difference solution of two-dimensional induction problems. *Geophys. J. R. astr. Soc.*, 47, 375-396.
- D'Erceville, I., and Kunetz, G., 1962. The effect of a fault on the earth's natural electromagnetic field. *Geophysics*, 27, 651-665.
- Dosso, H.W., 1973. A review of analogue model studies of the coast effect. *Phys. Earth Planet. Inter.*, 7, 294-302.
- Erdelyi, A., Magnus, W., Oberhettinger, F., and Tricomi, F., 1954. Tables of Integral Transforms, 1. McGraw-Hill Book Co. Inc., New York.
- Fischer, G., Schnegg, P.-A., and Usadel, K.D., 1978a. Electromagnetic response of an ocean coast model to E-polarization induction. *Geophys. J. R. astr. Soc.*, 52, in press.

- Fischer, G., Schnegg, P.-A., and Usadel, K.D., 1978b. Electromagnetic induction at a model ocean coast. *J. Geomag. Geoelectr.*, in press.
- Gradshteyn, I.S., and Ryzhik, I.M., 1965. Table of Integrals, Series, and Products. Academic Press, New York.
- Hartmann, O., 1963. Behandlung lokaler erdmagnetischer Felder als Randwertaufgabe der Potentialtheorie. *Abhandl. Akad. Wiss Gottingen, Math.-Phys. Kl., Beitr. Internat. Geophys. Jahr.*, 9, 1-50.
- Jones, D.S., 1964. The Theory of Electromagnetism. Pergamon Press, Oxford.
- Jones, F.W., and Price, A.T., 1970. The perturbations of alternating geomagnetic fields by conductivity anomalies. *Geophys. J. R. astr. Soc.*, 20, 317-334.
- Kaplan, W., 1973. Advanced Calculus, second edition. Addison-Wesley Publishing Company, Don Mills.
- Lighthill, M.J., 1958. An Introduction to Fourier Analysis and Generalised Functions. Cambridge University Press, Cambridge.
- Nicoll, M.A., and Weaver, J.T., 1977. H-polarization induction over an ocean edge coupled to the mantle by a conducting crust. *Geophys. J. R. astr. Soc.*, 49, 427-442.
- Nienaber, W., Dosso, H.W., Law, L.K., Ramaswamy, V., and Jones, F.W., 1978. An analogue study of electromagnetic induction in the Vancouver Island region. *J. Geomag. Geoelectr.*, in press.
- Parker, R.L., 1968. Electromagnetic induction in a thin strip. *Geophys. J. R. astr. Soc.*, 14, 487-495.
- Price, A.T., 1949. The induction of electric currents in non-uniform thin sheets and shells. *Quart. J. Mech. Appl. Math.*, 2, 283-310.
- Price, A.T., 1950. Electromagnetic induction in a semi-infinite conductor with a plane boundary. *Quart. J. Mech. Appl. Math.*, 3, 385-410.
- Rikitake, T., 1966. Electromagnetism and the Earth's Interior. Elsevier Publishing Company, Amsterdam.

- Rikitake, T., 1968. Electromagnetic induction in uniform and non-uniform sheets underlain by an undulating perfect conductor. *Bull. Earthquake Res. Inst., Tokyo Univ.*, 46, 361-384.
- Rikitake, T., 1973. Global electrical conductivity of the earth. *Phys. Earth Planet. Inter.*, 7, 245-250.
- Roden, R.B., 1964. The effect of an ocean on magnetic diurnal variations. *Geophys. J. R. astr. Soc.*, 8, 375-388.
- Schmucker, U., 1970. Anomalies of geomagnetic variations in the Southwestern United States. *Bull. Scripps Inst. Oceanogr. Univ. Calif.*, 13.
- Schmucker, U., 1971. Interpretations of induction anomalies above nonuniform surface layers. *Geophysics*, 36, 156-165.
- Sneddon, I.N., 1951. Fourier Transforms. McGraw-Hill Book Co. Inc., New York.
- Summers, D.M., and Weaver, J.T., 1973. Electromagnetic induction in a stratified conducting half-space by an arbitrary periodic source. *Can. J. Phys.*, 51, 1064-1074.
- Weaver, J.T., 1963. The electromagnetic field within a discontinuous conductor with reference to geomagnetic micropulsations near a coastline. *Can. J. Phys.*, 41, 484-495.
- Weaver, J.T., 1964. On the separation of local geomagnetic fields into external and internal parts. *Z. Geophys.*, 30, 29-36.
- Weaver, J.T., 1971. The general theory of electromagnetic induction in a conducting half-space. *Geophys. J. R. astr. Soc.*, 22, 83-100.
- Weaver, J.T., 1973. Induction in a layered plane-Earth by uniform and non-uniform source fields. *Phys. Earth Planet. Inter.*, 7, 266-281.
- Weaver, J.T., and Brewitt-Taylor, C.R., 1978. Improved boundary conditions for the numerical solution of E-polarization problems in geomagnetic induction. *Geophys. J. R. astr. Soc.*, in press.

Weaver, J.T., and Thomson, D.J., 1972. Induction in a non-uniform conducting half-space by an external line current. *Geophys. J. R. astr. Soc.*, 28, 163-185.

Weidelt, P., 1971. The electromagnetic induction in two thin half-sheets. *Z. Geophys.*, 37, 649-665.

APPENDIX A

EVALUATION OF INTEGRAL COEFFICIENTS  
CONTAINING BESSEL FUNCTIONS

In order to determine the coefficients  $U_{mj}$ ,  $V_{mj}$ , and  $W_m$  (defined in section 4.2),  $\tilde{V}_{mj}$  and  $\tilde{W}_m$  (defined in section 4.3) and  $I_m^-$  and  $I_m^+$  (defined in section 4.4) in a form suitable for programming on a computer, some expressions for the integrals of Modified Bessel functions of the second kind are required. From the handbook by Abramowitz and Stegun (1964), appropriate series representations of  $K_0(w)$  and  $K_1(w)$  are available almost directly. Also, from tabulated results (Abramowitz and Stegun, 1964, eq. 11.4.23 and eq. 11.1.9), we know that

$$\int_0^{\infty} K_0(w) dw = \frac{\pi}{2} \quad (A.1)$$

and 
$$\int_0^z K_0(w) dw = z \sum_{k=0}^{\infty} a_k \left(\frac{z}{2}\right)^{2k} \quad (A.2)$$

where  $z = \sqrt{2i} x$ , ( $x$ , real and positive)

$$z = \sqrt{2} x$$

$$a_k = p_k + iq_k$$

$$p_0 = 1 - \gamma + \frac{\ln 2}{2} - \ln x$$

$$q_0 = \frac{-\pi}{4} ,$$

$$p_k = \frac{p_0 + r_k + 1/(2k+1)}{(k!)^2 (2k+1)} ,$$

$$q_k = \frac{q_0}{(k!)^2 (2k+1)} ,$$

$$r_k = \sum_{j=2}^k \frac{1}{j} ,$$

$\gamma = .57721566490153$  , Euler's constant.

After some rearrangements, equation (A.2) may be written as

$$A(z) = \int_0^z K_0(w) dw = x \left[ (R(x) - S(x)) + i(R(x) + S(x)) \right] \quad (A.3)$$

where

$$R(x) = \sum_{k=0}^{\infty} (-1)^k b_k u^{2k} , \quad S(x) = \sum_{k=0}^{\infty} (-1)^k c_k u^{2k} ,$$

$$b_k = 32^k (p_{2k} - 32 \cdot u \cdot q_{2k+1}) , \quad c_k = 32^k (q_{2k} + 32 \cdot u \cdot p_{2k+1}) ,$$

$$u = \left( \frac{x}{8} \right)^2 .$$

Both  $R(x)$  and  $S(x)$  are convergent alternating series of real terms. If these series are terminated when  $k = n$ , it is well known that the remainder is less than the first term neglected for  $n > N$ , provided that the terms of the remainder are monotonically decreasing. For instance, for  $x \leq 8$ ,  $N = 2$  (see Table A.1). For convenience in programming, the above series representation is used for  $x < 8$  with  $n = 10$ . In this case, the maximum remainder for  $R(x)$  is then  $|b_{11}| = .33 \times 10^{-10}$  and, for  $S(x)$ , is  $|c_{11}| = .16 \times 10^{-10}$ . Note that the coefficients  $b_k$  and  $c_k$  are multiplied by  $\left(\frac{x}{8}\right)^{4k}$  so that for  $x < 8$ , the terms in  $R(x)$  and  $S(x)$  die off extremely quickly.

Now by using equation (A.1), we can define the following two functions:

$$\tilde{H}(z) = \int_0^z K_0(w) dw = \begin{cases} A(z) & (x < 8) \\ \frac{\pi}{2} - B(z) & (x \geq 8) \end{cases} \quad (\text{A.4})$$

and

$$\tilde{I}(z) = \int_z^\infty K_0(w) dw = \begin{cases} \frac{\pi}{2} - A(z) & (x < 8) \\ B(z) & (x \geq 8) \end{cases} \quad (\text{A.5})$$

A series representation of  $B(z) = \int_z^\infty K_0(w) dw$ , for  $x \geq 8$ , is given in the handbook by Abramowitz and Stegun

TABLE A.1

Coefficients used to determine A(z) to the desired accuracy

k	b <sub>k</sub>			c <sub>k</sub>		
	x = .001	x = 1.0	x = 8.0	x = .001	x = 1.0	x = 8.0
1	.43 × 10 <sup>3</sup>	.77 × 10 <sup>2</sup>	.71 × 10 <sup>2</sup>	.40 × 10 <sup>2</sup>	.37 × 10 <sup>2</sup>	.84 × 10 <sup>2</sup>
2	.18 × 10 <sup>4</sup>	.40 × 10 <sup>3</sup>	.14 × 10 <sup>3</sup>	.15 × 10 <sup>3</sup>	.15 × 10 <sup>3</sup>	.15 × 10 <sup>3</sup>
3	.15 × 10 <sup>4</sup>	.37 × 10 <sup>3</sup>	.11 × 10 <sup>3</sup>	.13 × 10 <sup>3</sup>	.12 × 10 <sup>3</sup>	.94 × 10 <sup>2</sup>
4	.38 × 10 <sup>3</sup>	.10 × 10 <sup>3</sup>	.30 × 10 <sup>2</sup>	.32 × 10 <sup>2</sup>	.31 × 10 <sup>2</sup>	.23 × 10 <sup>2</sup>
5	.39 × 10 <sup>2</sup>	.11 × 10 <sup>2</sup>	.35 × 10 <sup>1</sup>	.32 × 10 <sup>1</sup>	.32 × 10 <sup>1</sup>	.25 × 10 <sup>1</sup>
6	.20 × 10 <sup>1</sup>	.58 × 10 <sup>0</sup>	.20 × 10 <sup>0</sup>	.16 × 10 <sup>0</sup>	.16 × 10 <sup>0</sup>	.13 × 10 <sup>0</sup>
7	.53 × 10 <sup>-1</sup>	.16 × 10 <sup>-1</sup>	.58 × 10 <sup>-2</sup>	.42 × 10 <sup>-2</sup>	.42 × 10 <sup>-2</sup>	.35 × 10 <sup>-2</sup>
8	.84 × 10 <sup>-3</sup>	.27 × 10 <sup>-3</sup>	.99 × 10 <sup>-4</sup>	.66 × 10 <sup>-4</sup>	.65 × 10 <sup>-4</sup>	.56 × 10 <sup>-4</sup>
9	.83 × 10 <sup>-5</sup>	.27 × 10 <sup>-5</sup>	.10 × 10 <sup>-5</sup>	.64 × 10 <sup>-6</sup>	.64 × 10 <sup>-6</sup>	.55 × 10 <sup>-6</sup>
10	.54 × 10 <sup>-7</sup>	.18 × 10 <sup>-7</sup>	.71 × 10 <sup>-8</sup>	.41 × 10 <sup>-8</sup>	.41 × 10 <sup>-8</sup>	.36 × 10 <sup>-8</sup>
11	.23 × 10 <sup>-9</sup>	.80 × 10 <sup>-10</sup>	.33 × 10 <sup>-10</sup>	.18 × 10 <sup>-10</sup>	.18 × 10 <sup>-10</sup>	.16 × 10 <sup>-10</sup>
12	.74 × 10 <sup>-12</sup>	.25 × 10 <sup>-12</sup>	.11 × 10 <sup>-12</sup>	.55 × 10 <sup>-13</sup>	.55 × 10 <sup>-13</sup>	.50 × 10 <sup>-13</sup>

(1964, eq. 11.1.18) (see computer listing - subroutine BESSEL - for further details).

From the well-known recurrence relations for modified Bessel functions of the second kind (Abramowitz and Stegun, 1964, eq. 9.6.26 and eq. 9.6.27), we know that

$$K_1(w) = -K_0'(w)$$

and 
$$\frac{K_1(w)}{w} = -K_0(w) - K_1'(w)$$

Furthermore, both  $K_0(w)$  and  $K_1(w)$  vanish at infinity.

With these relations, we find that

$$\int_{z_1}^{z_2} \frac{K_1(w)}{w} dw = - \int_{z_1}^{z_2} [K_0(w) + K_1'(w)] dw = M(z_2) - M(z_1) , \quad (\text{A.6})$$

$$\int_{z_1}^{\infty} \frac{K_1(w)}{w} dw = - \int_{z_1}^{\infty} [K_0(w) + K_1'(w)] dw = L(z_1) , \quad (\text{A.7})$$

$$\int_{z_1}^{z_2} K_1(w) dw = - \int_{z_1}^{z_2} K_0'(w) dw = K_0(z_1) - K_0(z_2) , \quad (\text{A.8})$$

$$\int_0^{z_1} wK_1(w) dw = -wK_0(w) \Big|_0^{z_1} + \int_0^{z_1} K_0(w) dw = N(z_1) , \quad (\text{A.9})$$

where  $L(z) = -\tilde{I}(z) + K_1(z)$  ,

$$M(z) = -\tilde{H}(z) - K_1(z) ,$$

and  $N(z) = -zK_0(z) + \tilde{H}(z)$  .

Here,  $z_1 = \sqrt{2i} x_1$  and  $z_2 = \sqrt{2i} x_2$  with  $0 < x_1 < x_2$  .

Now, by using the above results, we can express the coefficients

$U_{mj}$  ,  $V_{mj}$  ,  $W_m$  ,  $\tilde{V}_{mj}$  and  $\tilde{W}_m$  , given by equations

(4.2.21), (4.2.22), (4.2.23), (4.3.3) and (4.3.4) respectively,

as

$$U_{mj} = \begin{cases} -\sqrt{2i} L(g_{m1}) & (j = 1) \\ \sqrt{2i} [M(g_{mj}) - M(g_{mj-1})] & (2 \leq j \leq m-1) \\ -\sqrt{2i} [M(g_{mm-1}) + M(g_{mm+1})] & (j = m) \\ \sqrt{2i} [M(g_{mj}) - M(g_{mj+1})] & (m+1 \leq j \leq M-1) \\ -\sqrt{2i} L(g_{mM}) & (j = M) \end{cases} \quad (A.10)$$

$$V_{mj} = \begin{cases} K_0(g_{mj}) - K_0(g_{mj-1}) + (y_m - y_j)U_{mj} & (2 \leq j \leq m-1) \\ K_0(g_{mm+1}) - K_0(g_{mm-1}) & (j = m) \\ K_0(g_{mj+1}) - K_0(g_{mj}) + (y_m - y_j)U_{mj} & (m+1 \leq j \leq M-1) \end{cases} \quad (\text{A.11})$$

$$W_m = \frac{-1}{2} [N(g_{mm+1}) + N(g_{mm-1})] \quad (\text{A.12})$$

$$\tilde{V}_{mj} = \begin{cases} K_0(g_{mj-1}) - K_0(g_{mj}) & (2 \leq j \leq m-1) \\ K_0(g_{mm-1}) - K_0(g_{mm+1}) & (j = m) \\ K_0(g_{mj}) - K_0(g_{mj+1}) & (m+1 \leq j \leq M-1) \end{cases} \quad (\text{A.13})$$

and  $\tilde{W}_m = N(g_{mm+1}) + N(g_{mm-1}) \quad (\text{A.14})$

where  $g_{mj} = \sqrt{2i} |y_m - y_j|$ . In the above, we have taken the Cauchy Principal Value of the integral denoted by

$V_{mm}$  and noted that  $\int_{\infty} (u - y_j) = (u - y_m) + (y_m - y_j)$  in  $V_{mj}$  ( $m \neq j$ ).

Finally, consider the integrals  $I_m^-$  and  $I_m^+$ , defined as

$$I_m^- = -\sqrt{2i} \int_{-\infty}^{y_1} \frac{P(y_m - u, +0)}{u} du$$

and

$$I_m^+ = -\sqrt{2i} \int_{y_M}^{\infty} \frac{P(y_m - u, +0)}{u} du ,$$

and recall that  $P(y_m - u, +0) = \frac{K_1(\sqrt{2i}|y_m - u|)}{|y_m - u|}$ . For

$y_m \neq 0$ , we make a change of variable ( $w = \sqrt{2i}|y_m - u|$ )

and note that

$$\frac{1}{(w \pm \sqrt{2i} y_m)} = \pm \frac{1}{\sqrt{2i} y_m} \left( \frac{1}{w} - \frac{1}{w \pm \sqrt{2i} y_m} \right).$$

Next, we integrate the term involving  $\left( \frac{1}{w \pm \sqrt{2i} y_m} \right)$

by parts. For  $y_m = 0$ , we make the same change in variable and integrate by parts directly. The result is

$$I_m^\pm = \begin{cases} \frac{1}{y_m} \left( -\sqrt{2i} L(\sqrt{2i} h_m^\pm) + \frac{K_0(\sqrt{2i} h_m^\pm)}{h_0^\pm} + \tilde{M}^\pm(\sqrt{2i} h_m^\pm) \right) & (y_m \neq 0) \\ \pm \left( \frac{K_0(\sqrt{2i} h_0^\pm)}{h_0^\pm} + \tilde{N}(\sqrt{2i} h_0^\pm) \right) & (y_m = 0) \end{cases} \quad (\text{A.15})$$

where

$$\tilde{M}^{\pm}(z) = -\sqrt{2i} \int_z^{\infty} \frac{K_0(w) dw}{(w \pm \sqrt{2i} y_m)^2} \quad (\text{A.16})$$

and

$$\tilde{N}(z) = -2i \int_z^{\infty} \frac{K_0(w) dw}{w^3} \quad (\text{A.17})$$

with  $h_m^- = y_m - y_1$  ,  $h_m^+ = y_M - y_m$  ,

$h_0^- = -y_1$  ,  $h_0^+ = y_M$  .

To evaluate  $\tilde{M}^{\pm}(\sqrt{2i} h_m^{\pm})$  , we discretize the integral

as

$$-\sqrt{2i} \int_{\sqrt{2i} h_m^{\pm}}^{\infty} \frac{K_0(w) dw}{(w \pm \sqrt{2i} y_m)^2} = -2i \left\{ \int_{\sqrt{2i} h_m^{\pm}}^{\sqrt{2i} s_n} + \sum_{j=n}^{159} \int_{\sqrt{2i} s_j}^{\sqrt{2i} s_{j+1}} \right. \\ \left. + \int_{\sqrt{2i} s_N}^{\infty} \right\} \frac{K_0(w) dw}{(w \pm \sqrt{2i} y_m)^2}$$

where  $s_N = 8$  ,  $s_j = .02 j$  ( $1 \leq j \leq 400$ ) , and

$s_{n-1} < h_m^{\pm} \leq s_n$  , and then replace  $1/(w \pm \sqrt{2i} y_m)^2$  by

the constant value

$$\frac{1}{4i} \left[ \frac{1}{(h_m^\pm \pm y_m)^2} + \frac{1}{(s_n \pm y_m)^2} \right]$$

in the interval  $h_m^\pm < \frac{w}{\sqrt{2i}} < s_n$ , and similarly, by

$$\frac{1}{4i} \left[ \frac{1}{(s_j \pm y_m)^2} + \frac{1}{(s_{j+1} \pm y_m)^2} \right]$$

in each of the remaining intervals,  $\sqrt{2i} s_j < w \leq \sqrt{2i} s_{j+1}$ .

The resulting expression is then

$$\begin{aligned} \tilde{M}^\pm(\sqrt{2i} h_m^\pm) &\approx \left(\frac{i-1}{4}\right) \left\{ \left[ \frac{1}{(h_m^\pm \pm y_m)^2} + \frac{1}{(s_n \pm y_m)^2} \right] [\tilde{H}(\sqrt{2i} s_n) - \tilde{H}(\sqrt{2i} h_m^\pm)] \right. \\ &\quad \left. + \sum_{j=n}^{399} \left[ \frac{1}{(s_j \pm y_m)^2} + \frac{1}{(s_{j+1} \pm y_m)^2} \right] [\tilde{H}(\sqrt{2i} s_{j+1}) - \tilde{H}(\sqrt{2i} s_j)] \right\} \end{aligned}$$

(A.18)

Similarly, we find that

$$\begin{aligned} \tilde{N}(\sqrt{2i} h_0^\pm) &\approx \frac{(i-1)}{2} \left\{ \left[ \frac{1}{h_0^{\pm 3}} + \frac{1}{s_n^3} \right] [\tilde{H}(\sqrt{2i} s_n) - \tilde{H}(\sqrt{2i} h_0^\pm)] \right. \\ &\quad \left. + \sum_{j=n}^{399} \left[ \frac{1}{s_j^3} + \frac{1}{s_{j+1}^3} \right] [\tilde{H}(\sqrt{2i} s_{j+1}) - \tilde{H}(\sqrt{2i} s_j)] \right\} \quad (\text{A.19}) \end{aligned}$$

In the above, we have assumed that

$$\int_{\sqrt{2i} s_N}^{\infty} \frac{K_0(w) dw}{(w \pm \sqrt{2i} y_m)^2} \quad \text{and} \quad \int_{\sqrt{2i} s_N}^{\infty} \frac{K_0(w) dw}{w^3}$$

are negligible.

APPENDIX B

VERIFICATION THAT  $J_2(+0)$  EXISTS

To show that  $J_2(z)$  exists at  $z = +0$ , we need to be familiar with two theorems concerning uniform convergence (u.c.) and differentiation of certain integrals (Kaplan, 1973, pp. 447-449). The first theorem may be stated as follows:

If  $|g(s,z)| < h(s)$  on  $0 \leq z \leq 1$  and  
if  $\int_1^\infty h(s) ds$  exists, then  $\int_1^\infty g(s,z) ds$  is  
u.c. on  $0 \leq z \leq 1$ .

The second theorem may be stated as:

Given  $\int_1^\infty g(s,z) ds$  where  $g_2(s,z)$  exists and  
 $\int_1^\infty g_2(s,z) ds$  is u.c. on  $0 \leq z \leq 1$ , then  
 $\frac{\partial}{\partial z} \left\{ \int_1^\infty g(s,z) ds \right\} = \int_1^\infty g_2(s,z) ds$  on  $0 \leq z \leq 1$ .

After scaling all lengths in equation (3.4.47) by  $1/\alpha$  and rearranging, we have that

$$J(z) = \frac{1}{\pi} \int_0^\infty f(y,s) P(s,z) ds \quad (B.1)$$

$$\text{where } f(y, s) = E(y+s, 0) + E(y-s, 0) - 2E(y, 0) \quad (\text{B.2})$$

$$\text{and } P(s, z) = \frac{K_1(\sqrt{i} \sqrt{s^2 + z^2})}{\sqrt{s^2 + z^2}} \quad (\text{B.3})$$

For convenience in this verification, we further subdivide  $J(z)$  as

$$J(z) = I(z) + H(z) \quad (\text{B.4})$$

$$\text{where } I(z) = \int_0^1 f(y, s) P(s, z) ds \quad (\text{B.5})$$

$$\text{and } H(z) = \int_1^\infty f(y, s) P(s, z) ds \quad (\text{B.6})$$

We now wish to show that  $H'(+0)$  exists. We first use the Mean Value Theorem (M.V.T.) to immediately state that

$$|f(y, s)| < M s^2 \quad (\text{B.7})$$

where  $|E_{1,1}(\bar{s}, 0)| < M$  for some  $\bar{s}$ ,  $0 < \bar{s} < 1$ .

Then, from a tabulated result (Abramowitz and Stegun, 1964, eq. 9.6.28)

$$P_2(s, z) = \frac{-\sqrt{i} z K_2(\sqrt{i} \sqrt{s^2 + z^2})}{(s^2 + z^2)}$$

we obtain

$$|P_2(s, z)| \leq \frac{z}{s^2+z^2} |K_2(\sqrt{i}\sqrt{s^2+z^2})| \leq \frac{1}{s^2} |K_2(\sqrt{i}\sqrt{s^2+z^2})| \quad (\text{B.8})$$

on  $0 \leq z \leq 1$ . From another tabulated result (Abramowitz and Stegun, 1964, eq. 9.6.23)

$$K_2(\omega) = \frac{\omega^2}{3} \int_1^\infty e^{-\omega t} (t^2-1)^{3/2} dt \quad ,$$

we find that

$$|K_2(v+iv)| < v^2 \int_1^\infty e^{-vt} t^3 dt = e^{-v} (v + 3 + \frac{6}{v} + \frac{6}{v^2}) \quad (\text{B.9})$$

since

$$|(t^2-1)^{3/2}| < |t^3| \quad ,$$

$$\left| \frac{(1+i)^2}{3} \right| = \frac{2}{3} < 1 \quad ,$$

and  $|e^{-i\omega t}| \leq 1$  .

Now, since  $v = \sqrt{\frac{s^2+z^2}{2}}$  and  $s \geq 1$  on  $0 \leq z \leq 1$  ,

we see that

$$\frac{s}{\sqrt{2}} \leq v \leq \frac{\sqrt{s^2+1}}{\sqrt{2}} \leq s$$

which implies

$$|K_2(\sqrt{i}\sqrt{s^2+z^2})| < e^{-s/\sqrt{2}} \left( s + 3 + \frac{6\sqrt{2}}{s} + \frac{12}{s^2} \right) < Ds e^{-s/\sqrt{2}} \quad (\text{B.10})$$

where  $D = (16 + 6\sqrt{2})$ . After substituting this into (B.8), we obtain

$$|P_2(s, z)| < \frac{De^{-s/\sqrt{2}}}{s} \quad (\text{B.11})$$

Finally, from the inequalities given by (B.7) and (B.11), we can determine that

$$|f(y, s)| |P_2(s, z)| < Ms^2 \frac{De^{-s/\sqrt{2}}}{s} = Nse^{-s/\sqrt{2}} \quad (\text{B.12})$$

on  $0 \leq z \leq 1$ .

and that

$$\int_1^\infty Nse^{-s/\sqrt{2}} ds = (2 + \sqrt{2}) Ne^{-1/\sqrt{2}}, \quad (\text{B.13})$$

a finite value.

By the first theorem,  $\int_1^\infty f(y, s) P_2(s, z) ds$  is u.c. on  $0 \leq z \leq 1$ , and by the second theorem

$$H'(z) = \int_1^\infty f(y, s) P_2(s, z) ds \quad \text{on } 0 \leq z \leq 1.$$

In particular,  $H'(+0)$  exists.

Now consider  $I(z)$ . By the M.V.T., we can write that

$$|P(s, z) - P(s, 0)| = z |P_2(s, c)| = z \left| \frac{cK_2(\sqrt{i}\sqrt{s^2+c^2})}{s^2 + c^2} \right| \quad (\text{B.14})$$

for some  $c$  between 0 and 1. From (B.9), we immediately see that

$$|K_2(v + iv)| \leq e^{-v} \left( v + 3 + \frac{6}{v} + \frac{6}{v^2} \right) < \frac{16}{v^2} \quad (\text{B.15})$$

since, in this case,

$$v = \sqrt{\frac{s^2 + c^2}{2}}$$

and thus  $0 < v < 1$ . After substituting (B.15) into (B.14), we obtain

$$|P(s, z) - P(s, 0)| < \frac{16zc}{s^2 v^2} = \frac{32zc}{s^2 (s^2 + c^2)} \quad (\text{B.16})$$

From (B.5), (B.7) and (B.16), we find that

$$\begin{aligned} \left| \frac{I(z) - I(0)}{z} \right| &\leq \frac{1}{z} \int_0^1 |f(y, s)| |P(s, z) - P(s, 0)| ds \\ &< \frac{1}{z} \int_0^1 \left( Ms^2 \cdot \frac{32cz}{s^2 (s^2 + c^2)} \right) ds \\ &= 32 M \tan^{-1} \frac{1}{c} \quad (\text{B.17}) \end{aligned}$$

Now, as  $z \rightarrow +0$  in the above, we obtain the desired result that  $|I'(+0)| < 16 M \pi$ . Since both  $I'(+0)$  and  $H'(+0)$  exist, we may finally state that

$$\frac{\partial}{\partial z} \left\{ \frac{z\sqrt{i}}{\pi} J(z) \right\}_{z=+0} = \frac{\sqrt{i}}{\pi} J(+0) \quad . \quad (\text{B.18})$$

APPENDIX C

LISTING OF THE FORTRAN PROGRAM

This program calculates the electromagnetic field components in both E- and B-polarization for the model of a thin sheet of variable integrated conductivity covering a conducting half-space. As near as possible, the program follows the notation used in chapter 4.

It should be noted that the listing of the subroutine LINSYS which is used to calculate the horizontal electric fields by Gaussian elimination is not included here. Information on this subroutine is available from the University of Victoria Computer Centre.

```
C --- THIS PROGRAM CALCULATES 2-DIMENSIONAL ELECTROMAGNETIC INDUCTION GRN00100
C          FIELDS FOR THE MODEL OF A THIN SHEET OF VARIABLE GRN00200
C          INTEGRATED CONDUCTIVITY COVERING A CONDUCTING HALF-SPACE. GRN00300
C GRN00400
C----- MAIN -----GRN00500
C --- READS DATA, SETS PROGRAM CONSTANTS AND CALLS REQUIRED ROUTINES. GRN00600
C GRN00700
C          IMPLICIT COMPLEX*16 (E,F,G,I,X,Y,Z), REAL*8 (A-D,K,O-W) GRN00800
C          REAL*8 Y GRN00900
C          COMMON/A0/ IA,IB,IC,ROOT2,PID2,PID4,PID8,D2,D8,SJ,NP,NN,NDIMA,NRHS GRN01000
C          COMMON/A1/ Y(75),DIC(75),KKK(75),XX(75),YY(75),YP(75),ZZ(75) GRN01100
C          COMMON/A2/ DEL,SIG,DREQ,OMEG,I,IPW,O,W,T,PI,M1,MM,M2,ML,M3,MK,JER GRN01200
C          COMMON/A3/ ZH(75,75),ZS(75,75),QQ(75,75) GRN01300
C          COMMON/A5/ A(75),B(75),C(75),P(75),Q(75),R(75),AA(75),KK(75) GRN01400
C          COMMON/A6/ ZUL(75),ZUR(75),ZKOL(75),ZKOR(75) GRN01500
C GRN01600
C          5 FORMAT(10D7.0) GRN01700
C          6 FORMAT(2D15.5,11I2) GRN01800
C GRN01900
C --- PROGRAM CONSTANTS GRN02000
C          O = 0.0D0 GRN02100
C          W = 1.0D0 GRN02200
C          T = 2.0D0 GRN02300
C          I = (0.0D0,1.0D0) GRN02400
C          IPW = (1.0D0,1.0D0) GRN02500
C          PI = DARCOS(-1.0D0) GRN02600
C          PID2 = .5D0*PI GRN02700
C          PID4 = .25D0*PI GRN02800
C          PID8 = .125D0*PI GRN02900
C          ROOT2 = DSQRT(T) GRN03000
C          IA = W/IPW GRN03100
C          IB = IPW/ROOT2 GRN03200
C          IC = (I-W)/ROOT2 GRN03300
C          D2 = W/8.0D0**2 GRN03400
C          D8 = W/8.0D0**8 GRN03500
C          UO = PI*4.0D-7 GRN03600
C          SJ = .02D0 GRN03700
C          NP = 400 GRN03800
C          NDIMA = 73 GRN03900
C          NRHS = 1 GRN04000
C GRN04100
C-----GRN04200
C          PROGRAM OPTIONS GRN04300
C          TO INPUT GRID AND INTEGRATED CONDUCTIVITY IN KILOMETERS AND MHOS, GRN04400
C          SET JDIM = 0. GRN04500
C          TO INPUT GRID AND INTEGRATED CONDUCTIVITY IN DIMENSIONLESS UNITS, GRN04600
C          SET JDIM = 1. GRN04700
C          TO HAVE RESULTS PUNCHED ONTO CARDS, SET JC = 1. JN IS THEN SOME GRN04800
C          NUMBER WHICH IS PUNCHED ONTO THE CARDS TO INDICATE THE GRN04900
C          PARTICULAR SET OF RESULTS. GRN05000
C          TO CALCULATE MATRIX COEFFICIENTS AND FIELDS, SET JCF = 0. GRN05100
C          TO CALCULATE MATRIX COEFFICIENTS AND STORE ON UNIT 11 (DISC), GRN05200
C          SET JCF = 1. (FIELDS ARE ALSO DETERMINED.) GRN05300
C          TO USE COEFFICIENTS STORED ON UNIT 11 (DISC) FROM A PREVIOUS GRN05400
C          RUN, SET JCF = 2. (FIELDS ARE ALSO DETERMINED.) GRN05500
C          TO CALCULATE MATRIX COEFFICIENTS ONLY AND STORE ON UNIT 11 (DISC), GRN05600
C          SET JCF = 3. (FIELDS ARE NOT DETERMINED.) GRN05700
C          TO CALCULATE E-POLARIZATION FIELDS, SET JBP = 1. GRN05800
C          TO CALCULATE H-POLARIZATION FIELDS, SET JEP = 1. GRN05900
C          TO DETERMINE MATRIX COEFFICIENTS FOR IMPROVED BOUNDARY CONDITIONS GRN06000
C          FOR E-POLARIZATION PROBLEMS, SET JCOR = 1. GRN06100
C          TO RESTART PROGRAM, SET JM = 1. GRN06200
```

```
C      IF DIMENSIONLESS GRID POINTS ARE THE SAME FOR THE NEXT RUN, THE      GRN06300
C      MATRIX COEFFICIENTS NEED NOT BE RECALCULATED.  SEE SECTION GRN06400
C      5.1 IN THESIS.  (IE. SET JCF = 1 IN THE FIRST RUN, THEN GRN06500
C      SET JCF = 2 IN FUTURE RUNS.) GRN06600
C      ----- GRN06700
C      GRN06800
C      --- READ INPUT DATA (FREQUENCY, CONDUCTIVITY, END GRID POINTS, OPTIONS) GRN06900
C      11 READ(5,6) DPREQ, SIG, M1, MM, JBP, JEP, JC, JCF, JT, JN, JDIM, JM, JCOR GRN07000
C      GRN07100
C      --- MORE PROGRAM CONSTANTS. GRN07200
C      M2 = M1 + 1 GRN07300
C      M3 = M1 + 2 GRN07400
C      MK = MM - 2 GRN07500
C      ML = MM - 1 GRN07600
C      NN = ML - M1 GRN07700
C      OMEG = T*PI*DFREQ GRN07800
C      DEL = DSQRT(T/(OMEG*UO*SIG)) GRN07900
C      GRN08000
C      --- READ INTEGRATED CONDUCTIVITY GRN08100
C      READ(5,5) (DIC(J), J=M1, ML) GRN08200
C      GRN08300
C      --- READ COEFFICIENTS FROM STORAGE. GRN08400
C      IF(JCF.EQ.2) READ(11) GRN08500
C      1 ((ZR(M,J), J=M1, MM), M=M1, MM), ((ZS(M,J), J=M1, MM), M=M1, MM), (ZKOL(J), GRN08600
C      1 ZKOR(J), ZUL(J), ZUR(J), J=M1, MM), ((QQ(M,J), J=M1, MM), M=M1, MM), GRN08700
C      1 (Y(J), KK(J), AA(J), A(J), B(J), C(J), P(J), Q(J), R(J), J=M1, MM) GRN08800
C      GRN08900
C      IF(JCF.EQ.2) GO TO 10 GRN09000
C      GRN09100
C      --- READ GRID DATA. GRN09200
C      READ(5,5) (Y(J), J=M1, MM) GRN09300
C      GRN09400
C      --- IF JDIM = 0, CONVERT KILOMETERS TO DIMENSIONLESS UNITS. GRN09500
C      IF(JDIM.EQ.1) GOTO 9 GRN09600
C      DSCALE = 1.03/DEL GRN09700
C      DO 1 J = M1, MM GRN09800
C      1 Y(J) = Y(J) * DSCALE GRN09900
C      GRN10000
C      --- CALCULATION OF GRID STEP-SIZES. GRN10100
C      9 DO 2 J = M1, ML GRN10200
C      M = J + 1 GRN10300
C      KK(J) = Y(J+1) - Y(J) GRN10400
C      2 AA(M) = W/KK(J) GRN10500
C      GRN10600
C      --- CALCULATION OF FINITE DIFFERENCE COEFFICIENTS. GRN10700
C      DO 3 J = M2, ML GRN10800
C      K = KK(J) GRN10900
C      K1 = KK(J-1) GRN11000
C      KP = K + K1 GRN11100
C      KM = K - K1 GRN11200
C      A(J) = -K/(KP*K1) GRN11300
C      B(J) = KM/(K*K1) GRN11400
C      C(J) = K1/(KP*K) GRN11500
C      P(J) = T/(KP*K1) GRN11600
C      Q(J) = -T/(K*K1) GRN11700
C      3 R(J) = T/(KP*K) GRN11800
C      GRN11900
C      --- CALCULATION OF DIMENSIONLESS AVERAGED INTEGRATED CONDUCTIVITY. GRN12000
C      --- IF JDIM = 0, CONVERT MHOS TO DIMENSIONLESS UNITS. GRN12100
C      10 SD = W GRN12200
C      IF(JDIM.EQ.0) SD = W/(SIG*DEL) GRN12300
C      DO 4 J = M2, ML GRN12400
```

```
4 KKK(J) = SD*(KK(J)*DIC(J)*KK(J-1)*DIC(J-1))/(KK(J)+KK(J-1)) GRN12500
  KKK(M1) = SD*DIC(M2) GRN12600
  KKK(MM) = SD*DIC(ML) GRN12700
C IF(JCF.NE.2) CALL COEFF GRN12800
C GRN12900
C GRN13000
C --- STORE COEFFICIENTS FOR FUTURE USE. GRN13100
  IF(JCF.EQ.1.OR.JCF.EQ.3) WRITE(11) GRN13200
  1 ((ZR(M,J),J=M1,MM),M=M1,MM),((ZS(M,J),J=M1,MM),M=M1,MM),(ZKOL(J), GRN13300
  1 ZKOR(J),ZUL(J),ZUR(J),J=M1,MM),((QQ(M,J),J=M1,MM),M=M1,MM), GRN13400
  1 (Y(J),KK(J),AA(J),A(J),B(J),C(J),P(J),Q(J),R(J),J=M1,MM) GRN13500
  IF(JCF.EQ.3) STOP GRN13600
C GRN13700
C --- CALCULATION OF B-POLARIZATION FIELDS. GRN13800
  IF(JBP.NE.1) GOTO 7 GRN13900
  CALL BPOL GRN14000
  CALL RESULT(1,JBP,JEP,JC,JCF,JT,JN,JDIM,JM,JCOR) GRN14100
C GRN14200
C --- CALCULATION OF E-POLARIZATION FIELDS. GRN14300
  7 IF(JEP.NE.1) GOTO 8 GRN14400
  IF(JCOR.EQ.1) CALL EPOLC GRN14500
  CALL EPOL(JCOR) GRN14600
  CALL RESULT(2,JBP,JEP,JC,JCF,JT,JN,JDIM,JM,JCOR) GRN14700
  8 CONTINUE GRN14800
C GRN14900
  REWIND 11 GRN15000
  IF(JM.EQ.1) GOTO 11 GRN15100
C GRN15200
  STOP GRN15300
C GRN15400
  END GRN15500
```

```

C----- COEFF -----GRN15600
C --- DETERMINATION OF MATRIX COEFFICIENTS FOR E-POL AND B-POL PROBLEMS GRN15700
C          (SEE CHAPTER 4) GRN15800
C GRN15900
C SUBROUTINE COEFF GRN16000
C IMPLICIT COMPLEX*16 (E,F,G,I,X,Y,Z), REAL*8 (A-D,K,O-W) GRN16100
C REAL*8 Y GRN16200
C COMMON/A1/ Y (75), DIC (75), KKK (75), XX (75), YY (75), YP (75), ZZ (75) GRN16300
C COMMON/A2/ DEL, SIG, DFREQ, OMEG, I, IPW, O, W, T, PI, M1, MM, M2, ML, M3, MK, JEB GRN16400
C COMMON/A3/ ZR (75, 75), ZS (75, 75), QQ (75, 75) GRN16500
C COMMON/A5/ A (75), B (75), C (75), P (75), Q (75), R (75), AA (75), KK (75) GRN16600
C COMMON/A6/ ZUL (75), ZUR (75), ZKOL (75), ZKOR (75) GRN16700
C COMMON/WS/ ZKO (75), ZM (75), ZN (75), ZU (75), ZV (75), ZW (75), GRN16800
C          ZZV (75), ZZW (75), DL (75) GRN16900
C GRN17000
C --- CALCULATION OF COEFFICIENTS ZUL AND ZUR. GRN17100
C CALL BESSEL (M1) GRN17200
C CALL BESSEL (MM) GRN17300
C GRN17400
C DO 10 M = M2, ML GRN17500
C   NN = M - 1 GRN17600
C   MP = M + 1 GRN17700
C   CALL BESSEL (M) GRN17800
C   KP = Y (MP) - Y (MM) GRN17900
C GRN18000
C DL (M) = DLOG ((Y (MP) - Y (M)) / (Y (M) - Y (MM))) GRN18100
C DO 30 J = M2, MM GRN18200
C 30 IF (J.LT.M.OR.J.GT.MP) DL (J) = DLOG ((Y (M) - Y (J)) / (Y (M) - Y (J-1))) GRN18300
C GRN18400
C --- CALCULATION OF U, V, W, V (TILDA) AND W (TILDA). (SEE APPENDIX A) GRN18500
C DO 60 J = M2, ML GRN18600
C DD = Y (M) - Y (J) GRN18700
C IF (J.GE.M) GOTO 61 GRN18800
C ZU (J) = IPW * (ZM (J) - ZN (J-1)) GRN18900
C ZV (J) = ZKO (J) - ZKO (J-1) + DD * ZU (J) GRN19000
C ZZV (J) = ZKO (J-1) - ZKO (J) GRN19100
C ZZW (J) = ZN (J-1) - ZN (J) + DD * ZZV (J) GRN19200
C GOTO 60 GRN19300
C 61 IF (J.LE.M) GOTO 60 GRN19400
C ZU (J) = IPW * (ZM (J) - ZN (J+1)) GRN19500
C ZV (J) = ZKO (J+1) - ZKO (J) + DD * ZU (J) GRN19600
C ZZV (J) = ZKO (J) - ZKO (J+1) GRN19700
C ZZW (J) = ZN (J+1) - ZN (J) + DD * ZZV (J) GRN19800
C 60 CONTINUE GRN19900
C ZU (M) = -IPW * (ZM (MP) + ZM (MM)) GRN20000
C ZV (M) = ZKO (MP) - ZKO (MM) GRN20100
C ZW (M) = -.5D0 * (ZN (MP) + ZN (MM)) GRN20200
C ZZV (M) = ZKO (MM) - ZKO (MP) GRN20300
C ZZW (M) = ZN (MP) + ZN (MM) GRN20400
C GRN20500
C --- CALCULATE COEFFICIENTS FOR Y(U,-0) - SEE EQUATION 4.2.16 - AND GRN20600
C FOR Y(U,+0) AND G1(U,+0) - SEE EQUATIONS 4.2.25 AND 4.3.2. GRN20700
C DO 20 J = M2, ML GRN20800
C IF (J.GE.MM) GOTO 21 GRN20900
C QQ (M, J) = AA (J+1) * DL (J+1) - AA (J) * DL (J) GRN21000
C ZS (M, J) = AA (J) * ZZV (J) - AA (J+1) * ZZV (J+1) GRN21100
C ZR (M, J) = ZU (J) + AA (J) * ZV (J) - AA (J+1) * ZV (J+1) GRN21200
C GOTO 20 GRN21300
C 21 IF (J.LE.MP) GOTO 20 GRN21400
C QQ (M, J) = AA (J+1) * DL (J+1) - AA (J) * DL (J) GRN21500
C ZR (M, J) = ZU (J) + AA (J) * ZV (J-1) - AA (J+1) * ZV (J) GRN21600
C ZS (M, J) = AA (J) * ZZV (J-1) - AA (J+1) * ZZV (J) GRN21700

```

20	CONTINUE		GRN21800
	QQ(M, M) = -B(M)*DL(M) - Q(M)*KP		GRN21900
	ZR(M, M) = ZU(M) + B(M)*ZV(M) + Q(M)*ZW(M)		GRN22000
	ZS(M, M) = B(M)*ZZV(M) + Q(M)*ZZW(M)		GRN22100
	IF(M, EQ, M2) GOTO 1		GRN22200
	QQ(M, MN) = -(AA(MN)*DL(MN) + A(M)*DL(M) + P(M)*KP)		GRN22300
	QQ(M, M1) = AA(M2)*DL(M2)		GRN22400
	ZR(M, MN) = ZU(MN) + AA(MN)*ZV(MN) + A(M)*ZV(M) + P(M)*ZW(M)		GRN22500
	ZR(M, M1) = ZUL(M) - AA(M2)*ZV(M2)		GRN22600
	ZS(M, MN) = A(M)*ZZV(M) + P(M)*ZZW(M) + AA(MN)*ZZV(MN)		GRN22700
	ZS(M, M1) = -AA(M2)*ZZV(M2)		GRN22800
	GOTO 2		GRN22900
1	QQ(M, M1) = -A(M)*DL(M) - P(M)*KP		GRN23000
	ZR(M, M1) = ZUL(M) + A(M)*ZV(M) + P(M)*ZW(M)		GRN23100
	ZS(M, M1) = A(M)*ZZV(M) + P(M)*ZZW(M)		GRN23200
2	IF(M, EQ, M1) GOTO 3		GRN23300
	QQ(M, MP) = AA(M+2)*DL(M+2) - C(M)*DL(M) - R(M)*KP		GRN23400
	QQ(M, MM) = -AA(MM)*DL(MM)		GRN23500
	ZR(M, MP) = ZU(MP) - AA(M+2)*ZV(MP) + C(M)*ZV(M) + R(M)*ZW(M)		GRN23600
	ZR(M, MM) = ZUR(M) + AA(MM)*ZV(ML)		GRN23700
	ZS(M, MP) = C(M)*ZZV(M) + R(M)*ZZW(M) - AA(M+2)*ZZV(MP)		GRN23800
	ZS(M, MM) = AA(MM)*ZZV(ML)		GRN23900
	GOTO 10		GRN24000
3	QQ(M, MM) = -C(M)*DL(M) - R(M)*KP		GRN24100
	ZR(M, MM) = ZUR(M) + C(M)*ZV(M) + R(M)*ZW(M)		GRN24200
	ZS(M, MM) = C(M)*ZZV(M) + R(M)*ZZW(M)		GRN24300
10	CONTINUE		GRN24400
	RETURN		GRN24500
	END		GRN24600
			GRN24700

C

```

----- BESSEL -----GRN24800
C --- CALCULATION OF BESSEL FUNCTIONS. (SEE A+S AND APPENDIX A) GRN24900
C --- A+S - DENOTES REFERENCE TEXT: HANDBOOK OF MATHEMATICAL FUNCTIONS GRN25000
C BY ABRAMOWITZ AND STEGUN, 1964. GRN25100
C GRN25200
SUBROUTINE BESSEL (M) GRN25300
IMPLICIT COMPLEX*16 (F, P, G, L, X, Y, Z), REAL*8 (A-D, K, O-W) GRN25400
REAL*8 Y, X, X8, X8DX GRN25500
COMPLEX*16 CDEXP GRN25600
COMMON/A0/ IA, IB, IC, ROOT2, PID2, PID4, PID8, D2, D8, SJ, NP, NN, NDIMA, NRHS GRN25700
COMMON/A1/ Y (75), DIC (75), KKK (75), XX (75), YY (75), YP (75), ZZ (75) GRN25800
COMMON/A2/ DEL, SIG, DFREQ, OMEG, I, IP#, O, W, F, PI, M1, MM, M2, ML, M3, MK, JER GRN25900
COMMON/A6/ ZUL (75), ZUR (75), ZKOL (75), ZKOR (75) GRN26000
COMMON/WS/ ZKO (75), ZM (75), ZN (75) GRN26100
C GRN26200
C --- A+S - 9.11.11 GRN26300
ZTHETA (U) = -.3926991D0*I+U*(.0110486D0-.0110485D0*I+U*( GRN26400
1-.0009765D0*I+U*(-.0000906D0-.0000901D0*I+U*(-.0000252D0+U*( GRN26500
2-.0000034D0+.0000051D0*I+U*(-.0000006D0+.0000019D0*I)))))) GRN26600
C GRN26700
C --- A+S - 9.11.14 GRN26800
ZPHI (U) = .7071068D0*IPW+U*(-.0625001D0-.0000001D0*I+U*(-.0013813D0 GRN26900
1+.0013811D0*I+U*(-.0000005D0+.0002452D0*I+U*(.0000346D0+.0000338D0 GRN27000
2*I+U*(-.0000117D0-.0000024D0*I+U*(-.0000016D0-.0000032D0*I)))))) GRN27100
C GRN27200
C --- A+S - 9.11.9 GRN27300
FF (U, V) = DSQRT (PID2/U) *CDEXP (-U*IB+ZTHETA (-V)) GRN27400
C GRN27500
C --- A+S - 9.11.1 GRN27600
BER (U, V, SV) = W+V*(113.77777774D0+V*(2.64191397D0+V*(.00122552D0))) GRN27700
1-SV*(64.D0+V*(32.36345652D0+V*(.08349609D0+V*.00000901D0))) GRN27800
C GRN27900
C --- A+S - 9.11.2 GRN28000
BEI (U, V, SV) = (16.D0+V*(72.817777742D0+V*(.52185615D0+V*.00011346D0 GRN28100
1)))-SV*(113.77777774D0+V*(10.56765779D0+V*.01103667D0)))*U*U*D2 GRN28200
C GRN28300
C --- A+S - 9.11.5 GRN28400
BERP (U, V, SV) = (SV*(14.22222222D0+V*(.66047849D0+V*.00045957D0)) GRN28500
1-(4.D0+V*(6.0681481D0+V*(.02609253D0+V*.00000394D0))))*U*U*U*D2 GRN28600
C GRN28700
C --- A+S - 9.11.6 GRN28800
BEIP (U, V, SV) = (.5D0+V*(11.377777772D0+V*(.14677204D0+V*.00004609D0)) GRN28900
1-SV*(10.66666666D0+V*(2.31167514D0+V*.00379386D0)))*U GRN29000
C GRN29100
DO 30 J = M1, MM GRN29200
IF (J.EQ.M) GOTO 30 GRN29300
D = DABS (Y (M)-Y (J)) GRN29400
X = D * ROOT2 GRN29500
X8 = D8*X**8 GRN29600
SQX8 = DSQRT (X8) GRN29700
KFACT = -DLOG (.5D0 * X) GRN29800
Z = D * IPW GRN29900
Z2 = D2*Z**2 GRN30000
IF (X.GT.8.D0) GOTO 40 GRN30100
BERX = BER (X, X8, SQX8) GRN30200
BEIX = BEI (X, X8, SQX8) GRN30300
BERPX = BERP (X, X8, SQX8) GRN30400
BEIPX = BEIP (X, X8, SQX8) GRN30500
C GRN30600
C --- A+S - 9.11.3 GRN30700
KER = KFACT*BERX+PID4*BEIX-.57721566D0-SQX8*(59.05819744D0+X8* GRN30800
1(60.60977451D0+X8*(-.19636347D0+X8*.00002458D0)))*X8* GRN30900

```

```

2(171.36272133D0+X8*(5.65539121D0+X8*.00309699D0))
C
C --- A+S - 9.11.4
KEI = KFACT*BEIX-PID4*BERX+(X*X*D2)*(6.76454936D0+X8*(
1124.2356965D0+X8*(1.17509064D0+X8*.00029532D0)))-(X*X*D2)*
25QX8*(142.91827687D0+X8*(21.30060904D0+X8*.02695875D0))
C
C --- A+S - 9.11.7
KERP = KFACT*BERPX-(BERX/X)+PID4*BEIPX+(X*X*X*D2)*(-3.69113734D0
1-X8*(11.36433272D0+X8*(.06136358D0+X8*.00001075D0)))+(X*X*X*D2)
2*(5QX8*(21.42034017D0+X8*(1.4138478D0+X8*.00116137D0))
C
C --- A+S - 9.11.8
KEIP = KFACT*BEIPX-(BEIX/X)-PID4*BERPX+X*.21139217D0-X*SQX8*(
113.39858846D0+X8*(4.65950823D0+X8*.00926707D0))+X*X8*
2(19.41182758D0+X8*(.33049424D0+X8*.00011997D0))
C
C --- A+S - 9.9.2
ZKO(J) = KER + I*KEI
C
C --- A+S - 9.9.2 , 9.9.17
ZK1 = IC * (KERP + I*KEIP)
GO TO 50
40 X8DX = 8.D0/X
C
C --- A+S - 9.11.9
ZKO(J) = FF(X,X8DX)
C
C --- A+S - 9.9.2, 9.9.17, 9.11.12
ZK1 = (W-I)*ZKO(J)*ZPH1(-X8DX)
C
50 CALL INTRO(D,Z,ZH,ZI)
C
C --- A+S - 11.4.23
IF(M.EQ.M1) ZOL(J) = IPW*(ZI-ZK1)
IF(M.EQ.M2) ZOR(J) = IPW*(ZI-ZK1)
ZH(J) = -ZH-ZK1
ZN(J) = IA*ZH - D*ZKO(J)
30 CONTINUE
ZKOL(M) = ZKO(M1)
ZKOR(M) = ZKO(M2)
C
RETURN
END
C

```

GRN31000  
GRN31100  
GRN31200  
GRN31300  
GRN31400  
GRN31500  
GRN31600  
GRN31700  
GRN31800  
GRN31900  
GRN32000  
GRN32100  
GRN32200  
GRN32300  
GRN32400  
GRN32500  
GRN32600  
GRN32700  
GRN32800  
GRN32900  
GRN33000  
GRN33100  
GRN33200  
GRN33300  
GRN33400  
GRN33500  
GRN33600  
GRN33700  
GRN33800  
GRN33900  
GRN34000  
GRN34100  
GRN34200  
GRN34300  
GRN34400  
GRN34500  
GRN34600  
GRN34700  
GRN34800  
GRN34900  
GRN35000  
GRN35100  
GRN35200  
GRN35300  
GRN35400

```

C----- INTKO -----GRN35500
C --- CALCULATION OF INTEGRAL OVER K0. (SEE APPENDIX A) GRN35600
C GRN35700
SUBROUTINE INTKO(D,Z,ZH,ZI) GRN35800
IMPLICIT COMPLEX*16 (E,F,G,I,X,Y,Z),REAL*8 (A-D,K,O-W) GRN35900
REAL*8 Y,X GRN36000
COMPLEX*16 CDEXP GRN36100
COMMON/A0/ IA,IB,IC,ROOT2,PID2,PID4,PID8,D2,D8,SJ,HP,NN,NDIMA,NRHS GRN36200
COMMON/A2/ DEL,SIG,DPREQ,OMEG,I,IPW,O,W,T,PI,M1,MM,M2,ML,M3,MK,JK,JKR GRN36300
COMMON/SV/ AA(23),PP(23),Q(23),P(23),B(11),C(11),Q0,P00,IR4,NQ GRN36400
C GRN36500
C --- A+S - 11.1.18 GRN36600
ZF(C) = 1.25331014D0+G*(.11190289D0+G*(.02576646D0+G*(.00933994D0+ GRN36700
1 G*(.00417454D0+G*(.00163271D0+G*(.00033934D0)))) GRN36800
C GRN36900
IF(NQ.NE.0) GO TO 1 GRN37000
NQ = 1 GRN37100
IR4 = DCOS(PID8)+I*DSIN(PID8) GRN37200
P00 = W - .57721566490153D0 + .5D0*DLOG(T) GRN37300
R = 0 GRN37400
Q0 = -PID4 GRN37500
AA(1) = 32.D0/3.D0 GRN37600
Q(1) = AA(1)*Q0 GRN37700
PP(1) = AA(1)*(P00+W/3.D0) GRN37800
DO 2 N = 2,23 GRN37900
A = W*N GRN38000
AA(N) = 32.D0*(A+A-W)/((A+A+W)*A*A)*AA(N-1) GRN38100
Q(N) = AA(N)*Q0 GRN38200
R = R + W/A GRN38300
2 PP(N) = AA(N)*(P00+R+W/(W+A+A)) GRN38400
C GRN38500
1 IF(D.GE.8.D0) GOTO 5 GRN38600
C GRN38700
C --- A+S - 11.1.9 (SEE APPENDIX A) GRN38800
DL = DLOG(D) GRN38900
DO 3 N = 1,23 GRN39000
3 P(N) = PP(N) - AA(N)*DL GRN39100
DD = D*D*D2 GRN39200
BU = P00 - DL - DD*Q(1) GRN39300
CO = Q0 + DD*P(1) GRN39400
DO 4 N = 1,11 GRN39500
B(N) = P(N+N) - DD*Q(N+N+1) GRN39600
4 C(N) = Q(N+N) + DD*P(N+N+1) GRN39700
D4 = -DD*DD GRN39800
R = BU+D4*(B(1)+D4*(B(2)+D4*(B(3)+D4*(B(4)+D4*(B(5)+D4*(B(6)+D4* GRN39900
1 (B(7)+D4*(B(8)+D4*(B(9)+D4*(B(10)+D4*B(11))))))))) GRN40000
S = CO+D4*(C(1)+D4*(C(2)+D4*(C(3)+D4*(C(4)+D4*(C(5)+D4*(C(6)+D4* GRN40100
1 (C(7)+D4*(C(8)+D4*(C(9)+D4*(C(10)+D4*(C(11))))))))) GRN40200
ZH = D*((R-S) + I*(R+S)) GRN40300
ZI = PID2 - ZH GRN40400
C GRN40500
GOTO 6 GRN40600
C GRN40700
5 GG = -7.D0/Z GRN40800
X = ROOT2*D GRN40900
ZI = ZF(GG)/(IR4*DSQRT(X)*CDEXP(Z)) GRN41000
ZH = PID2 - ZI GRN41100
6 CONTINUE GRN41200
C GRN41300
RETURN GRN41400
END GRN41500
C GRN41600

```

```

C----- EPOLC -----GRN41700
C --- CALCULATION OF COEFFICIENTS FOR IMPROVED BOUNDARY CONDITION GRN41800
C          FOR E-POLARIZATION PROBLEMS (SEE SECTION 4.4 AND APPENDIX A) GRN41900
C GRN42000
SUBROUTINE EPOLC GRN42100
IMPLICIT COMPLEX*16 (E, F, G, I, X, Y, Z), REAL*8 (A-D, K, O-W) GRN42200
REAL*8 Y, HN, HP GRN42300
COMMON/A0/ IA, IB, IC, ROOT2, PID2, PID4, PID8, D2, D8, SJ, NP, NN, NDIMA, NRHS GRN42400
COMMON/A1/ Y (75), DIC (75), KKK (75), XX (75), YY (75), YP (75), ZZ (75) GRN42500
COMMON/A2/ DEL, SIG, DFREQ, OMEG, L, IPW, O, W, T, PL, M1, MM, M2, ML, M3, MK, JER GRN42600
COMMON/A3/ ZR (75, 75), ZS (75, 75), QQ (75, 75) GRN42700
COMMON/A4/ SN, TN, SP, TP GRN42800
COMMON/A6/ ZUL (75), ZUR (75), ZKOL (75), ZKOR (75) GRN42900
COMMON/WS/ ZHH (400), G (400), S (400), DN (400), DP (400), D3 (400) GRN43000
1          , IN (75), IP (75), HN (75), HP (75) GRN43100
C GRN43200
C --- CALCULATION OF INTEGRALS HN AND HP (N=NEGATIVE, P=POSITIVE). GRN43300
DO 10 M = M2, ML GRN43400
IF (Y (M)) 1, 2, 1 GRN43500
1 HN (M) = -(Y (M) + Y (M1) * DLOG (W - Y (M) / Y (M1))) / (Y (M) * Y (M) * Y (M1)) GRN43600
HP (M) = (Y (M) + Y (MM) * DLOG (W - Y (M) / Y (MM))) / (Y (M) * Y (M) * Y (MM)) GRN43700
GOTO 10 GRN43800
2 HN (M) = W / (T * Y (M1) * Y (M1)) GRN43900
HP (M) = -W / (T * Y (MM) * Y (MM)) GRN44000
10 CONTINUE GRN44100
C GRN44200
C --- CALCULATION OF INTEGRALS IN AND IP (N=NEGATIVE, P=POSITIVE). GRN44300
NPP = NP - 1 GRN44400
ZC = .25D0 * (I - W) GRN44500
ZD = .5D0 * (I - W) GRN44600
DO 3 J = 1, NP GRN44700
S (J) = SJ * J GRN44800
D = S (J) GRN44900
Z = IPW * D GRN45000
DJ (J) = W / (D * D * D) GRN45100
CALL INTKO (D, Z, ZH, ZI) GRN45200
3 ZHH (J) = ZH GRN45300
DO 4 J = 1, NPP GRN45400
4 G (J) = ZHH (J + 1) - ZHH (J) GRN45500
C GRN45600
DO 30 M = M2, ML GRN45700
IN (M) = 0 GRN45800
D = Y (M) - Y (M1) GRN45900
Z = IPW * D GRN46000
IF (D.EQ.S (NP)) GOTO 31 GRN46100
DO 32 J = 2, NP GRN46200
N = J GRN46300
IF (D.GT.S (J - 1).AND.D.LE.S (J)) GOTO 33 GRN46400
32 CONTINUE GRN46500
33 IF (Y (M)) 34, 134, 34 GRN46600
34 DO 35 J = N, NP GRN46700
35 DN (J) = W / (S (J) - Y (M)) ** 2 GRN46800
IF (D.EQ.S (N)) GOTO 36 GRN46900
CALL INTKO (D, Z, ZH, ZI) GRN47000
IN (M) = (DN (N) + W / Y (M1) ** 2) * (ZHH (N) - ZH) GRN47100
IF (N.EQ.NP) GOTO 31 GRN47200
36 DO 37 J = N, NPP GRN47300
37 IN (M) = IN (M) + (DN (J + 1) + DN (J)) * G (J) GRN47400
31 IF (Y (M).EQ.O) GOTO 131 GRN47500
IN (M) = (ZUL (M) - ZKOL (M) / Y (M1) + ZC * IN (M)) / Y (M) GRN47600
GOTO 30 GRN47700
134 IF (D.EQ.S (N)) GOTO 136 GRN47800

```

```

CALL INTKO(D,Z,ZH,ZI)
IN(M) = (D3(N) + W/(D*D*D)) * (ZHH(N) - ZH)
136 IF(N.EQ.NP) GOTO 131
DO 137 J = N,NPP
137 IN(M) = IN(M) + (D3(J+1)+D3(J)) * G(J)
131 IN(M) = ZKOL(M)/(D*D) + ZD*IN(M)
30 CONTINUE
C
DO 50 H = M2,ML
IP(M) = 0
D = Y(MM) - Y(M)
Z = IPW*D
IF(D.GE.S(NP)) GOTO 51
DO 52 J = 2,NP
N = J
IF(D.GT.S(J-1).AND.D.LE.S(J)) GOTO 53
52 CONTINUE
53 IF(Y(M)) 54,154,54
54 DO 55 J = N,NP
55 DP(J) = W/(S(J)+Y(M))**2
IF(D.EQ.S(N)) GOTO 56
CALL INTKO(D,Z,ZH,ZI)
IP(M) = (DP(N)+W/Y(MM)**2) * (ZHH(N) - ZH)
56 IF(N.EQ.NP) GOTO 51
DO 57 J = N,NPP
57 IP(M) = IP(M) + (DP(J+1)+DP(J)) * G(J)
51 IF(Y(M).EQ.O) GOTO 151
IP(M) = (ZUR(M)+ZKOR(M)/Y(MM) + ZC*IP(M))/Y(M)
GOTO 50
154 IF(D.EQ.S(N)) GOTO 156
CALL INTKO(D,Z,ZH,ZI)
IP(M) = (D3(N) + W/(D*D*D)) * (ZHH(N) - ZH)
156 IF(N.EQ.NP) GOTO 151
DO 157 J = N,NPP
157 IP(M) = IP(M) + (D3(J+1)+D3(J)) * G(J)
151 IP(M) = -ZKOR(M)/(D*D) - ZD*IP(M)
50 CONTINUE
C
C --- RE-EVALUATION OF COEFFICIENTS Q AND R TO INCLUDE NEW BOUNDARY
C CONDITIONS.
SN = (Y(M2) - Y(M1)) / (Y(M2) - T*Y(M1))
SP = (Y(MM) - Y(ML)) / (T*Y(MM) - Y(ML))
TN = Y(M1) / (T*Y(M1) - Y(M2))
TP = Y(MM) / (T*Y(MM) - Y(ML))
C
DO 20 H = M2,ML
QQ(M,M2) = QQ(M,M2) + TN*(QQ(M,M1) - Y(M1)*HN(M))
QQ(M,M1) = QQ(M,M1)*SN + TN*Y(M1)*HN(M)
QQ(M,ML) = QQ(M,ML) + TP*(QQ(M,MM) - Y(MM)*HP(M))
20 QQ(M,MM) = QQ(M,MM)*SP + TP*Y(MM)*HP(M)
C
DO 60 H = M2,ML
ZR(M,M2) = ZR(M,M2) + TN*(ZR(M,M1) - ZUL(M) + Y(M1)*IN(M))
ZR(M,M1) = ZUL(M) + SN*(ZR(M,M1) - ZUL(M)) - Y(M1)*TN*IN(M)
ZR(M,ML) = ZR(M,ML) + TP*(ZR(M,MM) - ZUR(M) + Y(MM)*IP(M))
60 ZR(M,MM) = ZUR(M) + SP*(ZR(M,MM) - ZUR(M)) - Y(MM)*TP*IP(M)
C
RETURN
END
C

```

GRN47900  
GRN48000  
GRN48100  
GRN48200  
GRN48300  
GRN48400  
GRN48500  
GRN48600  
GRN48700  
GRN48800  
GRN48900  
GRN49000  
GRN49100  
GRN49200  
GRN49300  
GRN49400  
GRN49500  
GRN49600  
GRN49700  
GRN49800  
GRN49900  
GRN50000  
GRN50100  
GRN50200  
GRN50300  
GRN50400  
GRN50500  
GRN50600  
GRN50700  
GRN50800  
GRN50900  
GRN51000  
GRN51100  
GRN51200  
GRN51300  
GRN51400  
GRN51500  
GRN51600  
GRN51700  
GRN51800  
GRN51900  
GRN52000  
GRN52100  
GRN52200  
GRN52300  
GRN52400  
GRN52500  
GRN52600  
GRN52700  
GRN52800  
GRN52900  
GRN53000  
GRN53100  
GRN53200  
GRN53300  
GRN53400  
GRN53500  
GRN53600  
GRN53700  
GRN53800

```

C----- BPOL -----GRN53900
C --- CALCULATION OF B-POLARIZATION FIELDS. (SEE SECTION 4.3) GRN54000
C GRN54100
SUBROUTINE BPOL GRN54200
  IMPLICIT COMPLEX*16 (E,F,G,I,X,Y,Z), REAL*8 (A-D,K,O-H) GRN54300
  REAL*8 Y GRN54400
  COMMON/A0/ IA,IB,IC,ROOT2,PID2,PID4,PID8,D2,DB,SJ,NP,NN,NDIMA,NRHS GRN54500
  COMMON/A1/ Y(75),BIC(75),KKK(75),X(75),FP(75),FP(75),GG(75) GRN54600
  COMMON/A2/ DEL,SLG,DFREQ,OMEG,I,IPW,O,K,P,PI,M1,MM,M2,ML,M3,MK,JER GRN54700
  COMMON/A3/ ZR(75,75),ZS(75,75),Z2(75,75) GRN54800
  COMMON/A5/ A(75),B(75),C(75),P(75),Q(75),R(75),AA(75),KK(75) GRN54900
  COMMON/WS/ ZA(73,73),ZB(73) GRN55000
C GRN55100
  XL = W/(W+IPW*KKK(M1)) GRN55200
  XR = W/(W+1PW*KKK(MM)) GRN55300
  YRR = XR-XL GRN55400
  FL = -.500*IPW*XL GRN55500
  FR = -.500*IPW*XR GRN55600
  FRR = FR - FL GRN55700
  ZC = T*PI*I GRN55800
C GRN55900
  DO 10 M = M2,ML GRN56000
  L = M - M1 GRN56100
  DO 20 J = M2,ML GRN56200
  N = J - M1 GRN56300
  20 ZA(L,N) = ZR(M,J) + ZS(M,J) GRN56400
  ZL(L,L) = ZA(L,L) + ZC*KKK(M) GRN56500
  10 ZB(L) = ZC*(KKK(M1)-KKK(M))*FL - (ZR(M,MM)+ZS(M,MM))*FRR GRN56600
C GRN56700
  CALL LINSYS(JER,LHS(ZA,'COMPLEX',NN,NDIMA),PRECIS('DOUBLE'), GRN56800
  1 RHS(ZB,NN,NRHS)) GRN56900
  DO 40 M = M2,ML GRN57000
  40 FF(M) = ZB(M-M1) GRN57100
  FF(M1) = 0 GRN57200
  FF(MM) = FRR GRN57300
C GRN57400
  DO 30 M = M2,ML GRN57500
  30 X(M) = T*KKK(M)*FF(M) + IPW*(KKK(M1)-KKK(M))*XL GRN57600
  X(M1) = 0 GRN57700
  X(MM) = YRR GRN57800
C GRN57900
  DO 60 M = M1,ML GRN58000
  60 GG(M) = -.500*(X(M+1)-X(M))*AA(M+1) GRN58100
  GG(MM) = 0 GRN58200
C GRN58300
  DO 70 J = M1,MM GRN58400
  X(J) = X(J) + XL GRN58500
  70 FF(J) = FF(J) + FL GRN58600
C GRN58700
  RETURN GRN58800
  END GRN58900
C GRN59000

```

```

C----- EPOL -----GRN59100
C --- CALCULATION OF E-POLARIZATION FIELDS. (SEE SECTION 4.2) GRN59200
C GRN59300
C SUBROUTINE EPOL(JCOR) GRN59400
  IMPLICIT COMPLEX*16 (E,F,G,I,X,Y,Z), REAL*8 (A-D,K,O-W) GRN59500
  REAL*8 Y GRN59600
  COMMON/A0/ IA,IB,IC,ROOTZ,PID2,PID4,PID8,D2,D8,SJ,NP,NN,NDIMA,NRHS GRN59700
  COMMON/A1/ Y(75),D1C(75),KKK(75), E(75),YM(75),YP(75),ZZ(75) GRN59800
  COMMON/A2/ DEL,SIG,DFREQ,OMEG,I,IPW,O,W,T,PI,M1,MM,M2,ML,M3,MK,JER GRN59900
  COMMON/A3/ ZR(75,75),ZS(75,75),QQ(75,75) GRN60000
  COMMON/A4/ SN,TN,SP,TP GRN60100
  COMMON/A5/ A(75),B(75),C(75),P(75),Q(75),R(75),AA(75),KK(75) GRN60200
  COMMON/WS/ ZA(73,73),ZB(73) GRN60300
C GRN60400
  ZC = I*T*PI GRN60500
  ZE = I/PI GRN60600
  EL = (IPW/T)/(W+IPW*KKK(M1)) GRN60700
  ER = (IPW/T)/(W+IPW*KKK(MM)) GRN60800
  YPL = (W-I)*EL GRN60900
  ERR = ER - EL GRN61000
C GRN61100
  DO 10 M = M2,ML GRN61200
  L = M - M1 GRN61300
  DO 20 J = M2,ML GRN61400
  N = J - M1 GRN61500
  20 ZA(L,N) = ZR(M,J) + QQ(M,J) GRN61600
  ZA(L,L) = ZA(L,L) + ZC*KKK(M) GRN61700
  10 ZB(L) = ZC*(KKK(M1)-KKK(M))*EL - (ZR(M,MM)+QQ(M,MM))*ERR GRN61800
C GRN61900
  CALL LINSYS(JER,LHS(ZA,'COMPLEX',NN,NDIMA),PRECIS('DOUBLE'),
  1 RHS(ZB,NN,NRHS)) GRN62000
  DO 40 M = M2,ML GRN62100
  40 E(M) = ZB(M-M1) GRN62200
  E(M1) = 0 GRN62300
  E(MM) = ERR GRN62400
  IF(JCOR.NE.1) GOTO 30 GRN62500
  E(M1) = TN*E(M2) GRN62600
  E(MM) = TP*E(ML) + SP*ERR GRN62700
C GRN62800
  30 DO 50 M = M2,ML GRN62900
  ZC = ZR(M,MM)*ERR GRN63000
  ZK = QQ(M,MM)*ERR GRN63100
  DO 60 J = M2,ML GRN63200
  ZC = ZC + ZR(M,J)*E(J) GRN63300
  60 ZK = ZK + QQ(M,J)*E(J) GRN63400
  YM(M) = ZK*ZE GRN63500
  50 YP(M) = -ZC*ZE GRN63600
C GRN63700
  DO 70 M = M1,ML GRN63800
  70 ZZ(M) = -I*AA(M+1)*(E(M+1)-E(M)) GRN63900
C GRN64000
  YH(M1) = 0 GRN64100
  YH(MM) = 0 GRN64200
  YP(M1) = 0 GRN64300
  YP(MM) = (W-I)*ERR GRN64400
C GRN64500
  DO 80 J = M1,MM GRN64600
  E(J) = E(J) + EL GRN64700
  YH(J) = YH(J) + W GRN64800
  80 YP(J) = YP(J) + YPL GRN64900
  RETURN GRN65000
  END GRN65100
  GRN65200

```

```

C ----- RESULT ----- GRN65300
C --- PRINT OUT OF OPTIONS AND FIELD VALUES. GRN65400
C GRN65500
C GRN65600
SUBROUTINE RESULT(JP,JHP,JEP,JC,JCP,JT,JN,JDIM,JM,JCOR) GRN65700
IMPLICIT COMPLEX*16(E,F,G,I,X,Y,Z),COMPLEX(C),REAL*8(A,D,K,O-W) GRN65800
COMMON/A1/ S(75),DIC(75),KKK(75),XX(75),YY(75),YP(75),ZZ(75) GRN65900
COMMON/A2/ DEL,SIG,DPREQ,OMEG,I,IPW,O,W,T,PI,M1,MM,M2,ML,M3,HK,JERGRN66000
COMMON/WS/ CX(75),CY(75),CP(75),CZ(75),H(75),HM(75),HIC(75),HK(75) GRN66100
5 FORMAT(' ',I5,3E15.5) GRN66200
6 FORMAT('1'//3X,'ERROR',3X,'FREQUENCY',8X,'OMEGA',10X,'SIGMA',10X, GRN66300
1 'DELTA',7X,'HP',4X,'EP',4X,'JC',3X,'JCF',4X, GRN66400
1 'JT',4X,'JN',3X,'JDIM',3X,'JM',3X,'JCOR'//) GRN66500
7 FORMAT('0',I5,4D15.5,9I6) GRN66600
8 FORMAT('1'//5X,'J',8X,'GRID',10X,'ICOND',12X,'KKK'//) GRN66700
9 FORMAT(I3,F10.3,2E14.5,6E13.4,F10.3) GRN66800
10 FORMAT('1'//2X,'M',6X,'Y(J)',15X,'X',26X,'P',51X,'G',15X, GRN66900
1 'Y(J+1/2)'//) GRN67000
11 FORMAT('1'//2X,'M',6X,'Y(J)',6X,'MOD X',8X,'PHASE X',7X,'MOD P', GRN67100
1 7X,'PHASE P',32X,'MOD G',8X,'PHASE G',6X,'Y(J+1/2)'//) GRN67200
12 FORMAT('1'//2X,'M',5X,'Y(J)',15X,'E',26X,'Y-',24X,'Y+',25X,'Z', GRN67300
1 14X,'Y(J+1/2)'//) GRN67400
13 FORMAT('1'//2X,'M',5X,'Y(J)',6X,'MOD E',9X,'PHASE E',7X,'MOD Y-', GRN67500
1 6X,'PHASE Y-',6X,'MOD Y+',6X,'PHASE Y+',6X,'MOD Z',7X, GRN67600
1 'PHASE Z',6X,'Y(J+1/2)'//) GRN67700
14 FORMAT(11A4,2I2) GRN67800
15 FORMAT(I2,2I4,2D15.5,2A8,6A4) GRN67900
C GRN68000
HSCALE = DEL*1.E-3 GRN68100
DO 1 J = M1,MM GRN68200
HIC(J) = DIC(J) GRN68300
HK(J) = KKK(J) GRN68400
H(J) = S(J) GRN68500
CX(J) = XX(J) GRN68600
CY(J) = YY(J) GRN68700
CP(J) = YP(J) GRN68800
1 CZ(J) = ZZ(J) GRN68900
IP(JDIM.NE.0) GOTO 3 GRN69000
DO 2 J = M1,MM GRN69100
2 H(J) = H(J)*HSCALE GRN69200
3 HM(MM) = 0 GRN69300
DO 4 J = M1,ML GRN69400
4 HM(J) = .5 * (H(J+1)+H(J)) GRN69500
WRITE(6,6) GRN69600
WRITE(6,7) JER,DPREQ,OMEG,SIG,DEL,JHP,JEP,JC,JCP,JT,JN,JDIM,JM, GRN69700
1 JCOR GRN69800
WRITE(6,8) GRN69900
WRITE(6,5) (J,H(J),HIC(J),HK(J),J=M1,MM) GRN70000
IF(JP.EQ.1) WRITE(6,10) GRN70100
IF(JP.EQ.2) WRITE(6,12) GRN70200
WRITE(6,9) (J,H(J),CX(J),CY(J),CP(J),CZ(J),HM(J),J=M1,MM) GRN70300
IF(JC.EQ.1) WRITE(7,15) JP,M1,MM,DPREQ,SIG,OMEG,DEL GRN70400
IF(JC.EQ.1) WRITE(7,14) (H(J),HM(J),HIC(J),CX(J),CY(J),CP(J), GRN70500
1 CZ(J),JP,J,J=M1,MM) GRN70600
CALL MODULO(CX,CX) GRN70700
CALL MODULO(CY,CY) GRN70800
CALL MODULO(CP,CP) GRN70900
CALL MODULO(CZ,CZ) GRN71000
IF(JP.EQ.1) WRITE(6,11) GRN71100
IF(JP.EQ.2) WRITE(6,13) GRN71200
WRITE(6,9) (J,H(J),CX(J),CY(J),CP(J),CZ(J),HM(J),J=M1,MM) GRN71300
IF(JC.EQ.1) WRITE(7,14) (H(J),HM(J),HIC(J),CX(J),CY(J),CP(J), GRN71400

```

1	CZ(J),JP,J,M1,MM)	GRN71500
	RETURN	GRN71600
	END	GRN71700
C		GRN71800
C	----- MODULO -----	GRN71900
C	--- CALCULATION OF MODULUS AND PHASE OF FIELDS.	GRN72000
C		GRN72100
	SUBROUTINE MODULO (CRI,CMP)	GRN72200
	REAL CABS,MOD	GRN72300
	COMPLEX CRI(75),CMP(75),I	GRN72400
	COMMON/A2/ A(24),M1,MM	GRN72500
C		GRN72600
	O = 0.	GRN72700
	I = (0.,1.)	GRN72800
	DO 1 M = M1,MM	GRN72900
	R = REAL(CRI(M))	GRN73000
	AI = AIMAG(CRI(M))	GRN73100
	MOD = CABS(CRI(M))	GRN73200
	PHASE = 0	GRN73300
	IF(R.NE.O.AND.AI.NE.O) PHASE = ATAN2(AI,R)	GRN73400
1	CMP(M) = MOD + I*PHASE	GRN73500
	RETURN	GRN73600
	END	GRN73700



PARTIAL COPYRIGHT LICENSE

I hereby grant the right to lend my thesis (the title of which is shown below) to users of the University of Victoria Library, and to make single copies only for such users or in response to a request from the library of any other university, or similar institution, on its behalf or for one of its users. I further agree that permission for extensive copying of this thesis for scholarly purposes may be granted by me or a member of the University designated by me. It is understood that copying or publication of this thesis for financial gain shall not be allowed without my written permission.

Title of Thesis:

The Two-Dimensional Theory of Electromagnetic Induction  
in Thin Sheets with Applications to the Earth.

Author



Signature

Victor Richard Green

April, 1978